ENDOTHELIAL FUNCTION RESPONSES TO ALTERED BLOOD FLOW

PERIPHERAL ARTERY ENDOTHELIAL FUNCTION RESPONSES TO ALTERED BLOOD FLOW IN HUMANS

By JEM CHENG, Hon.B.Sc.Kin

A Thesis Submitted to the School of Graduate Studies in Partial Fulfillment of the Requirements for the Degree Master of Science in Kinesiology

McMaster University MASTER OF SCIENCE (2017)

Hamilton, Ontario (Kinesiology)

TITLE: Peripheral artery endothelial function responses to altered blood flow in humans

AUTHOR: Jem Cheng, Hon.B.Sc.Kin (McMaster University)

SUPERVISOR: Professor Maureen MacDonald

NUMBER OF PAGES: xii, 186

LAY ABSTRACT

It has been well established that the pattern of blood flow can impact arterial function, but the nuances of this relationship remain unclear. Through the use of heating, cuff compression, and exercise, this study sought to determine the optimal shear stress pattern to see beneficial changes in arterial function in the arm of young healthy males. Our results show many real life interventions alter not only the shear stress pattern in the artery, but also involve other systems like the brain and muscle that are crucial to maintaining the body's physiological balance. It is clear that arterial function is regulated through a variety of different mechanisms, and that the changes we observe will depend on the parameters (e.g. duration, intensity, timing of assessment) of the applied stimulus. More specifically, isolating study designs should be constructed to determine the individual contributions of different human body systems to the arterial regulatory response.

ABSTRACT

Endothelial function is influenced by a variety of factors, including shear stress direction and magnitude. Whereas improvements in endothelial function have mostly been attributed to increased anterograde flow, the results of many interventional models in humans suggest that enhancing blood flow in both anterograde and retrograde directions to create a high shear stress oscillatory stimulus may be optimal for improving endothelial function. Well-controlled studies are necessary to further this theory. The purposes of this study were to determine the brachial artery acute shear stress and endothelial function responses to (1) passive heat stress (HEAT), (2) ECG-gated cuff compressions (CUFF), and (3) ECG-gated rhythmic handgrip exercise (HGEX); and (4) to determine if there is a relationship between the degree of shear stress oscillation and endothelial function, regardless of the stimulus applied. We hypothesized that (1) HEAT would increase anterograde shear stress and decrease retrograde shear stress, leading to an unpredictable change in endothelial function; (2) CUFF would increase both anterograde and retrograde shear stress, leading to an increase in endothelial function; (3) HGEX would increase anterograde and retrograde shear stress and exercise metabolites, leading to an increase in endothelial function; and (4) the change in oscillatory shear index would be positively associated with the change in flow-mediated dilation, such that an increment increase in the degree of shear stress oscillation would be accompanied by a proportional improvement in endothelial function.

In separate visits, 10 young healthy males (22±3 years) underwent 10 minutes of unilateral HEAT, CUFF, or HGEX on the left arm (EXP), while the right arm served as a

within-subject time control (CON). Non-invasive finger plethysmography was used to measure heart rate (HR) and blood pressure (BP) throughout the testing sessions. Ultrasonography was used to obtain measures of blood velocity and arterial diameter from the brachial artery of both limbs throughout the interventions. Anterograde and retrograde shear stress (SS) and oscillatory shear index (OSI) were calculated at baseline and during each intervention to assess the blood flow pattern changes. Endothelial function was assessed before and after each intervention, in both limbs simultaneously using a flow-mediated dilation (FMD) test. HEAT increased HR during the intervention ($P < 0.05$), mean BP and diastolic BP after the intervention ($P < 0.05$), anterograde SS in EXP (rest: 15.2 ± 2.9 *vs.* HEAT: 29.8 ± 8.5 dynes/cm^2, $P < 0.05$), and FMD% in both limbs ($P = 0.000$). CUFF did not change HR or BP, increased anterograde (rest: 17.9 ± 4.1 *vs.* CUFF: 43.0 ± 12.4 dynes/cm^2, $P < 0.05$) and retrograde (rest: -3.1 ± 2.5 *vs.* CUFF: -22.7 ± 6.0 dynes/cm^2, $P < 0.05$) SS in EXP, but did not change FMD% in either limb ($P = 0.248$). HGEX increased HR during the intervention ($P < 0.05$), mean BP during and after the intervention ($P < 0.05$), anterograde SS in EXP (rest: 18.7 ± 5.9 *vs.* HGEX: 56.4 ± 11.5 dynes/cm^2, $P < 0.05$), and FMD% in both limbs ($P = 0.001$). These findings suggest that an anterograde-dominant shear stress stimulus may be effective at improving endothelial function, but the confounding effect of sympathetic nervous system activation may play a more dominant role in the acute control response for shorter duration interventions such as the ones explored in this study.

ACKNOWLEDGEMENTS

This thesis would not have been possible without the support and guidance of many individuals who have made my M.Sc. journey so special. I would like to thank my supervisor Dr. Maureen MacDonald for always being an excellent example of what a scientist should be. In everything you do, you encourage, support, and guide simply because you want people to find what makes them happy. I have always felt that your philosophy towards research is rich, genuine, and purely fueled by curiosity. Thank you for endless opportunities for growth under your supervision. I know that I have become a better everything (writer, communicator, colleague, human being) since working with you. I would like to thank my committee members, Dr. Stuart Phillips and Dr. Gianni Parise, for their incredibly helpful insight, particularly during the study design and interpretation process. I am incredibly humbled and honoured to be able to learn and grow as a scientist from the best of the best.

I am also very grateful to have met such amazing colleagues from the Vascular Dynamics Lab and Kinesiology Graduate Body that have made this experience so memorable. In particular, I would like to thank lab mates Jason, Ninette, Nicole, Patrick, Stacey, Natalie, Daria, Vanessa, and Emily for teaching, supporting, and guiding me always. You are the only people I know that I can make artery jokes with, and that means a lot to me. Thank you Sara for always being willing to die with me through the 200 walking lunges at Outdoor Bootcamp, Skelly for supporting me as a fellow anti-morning person, Beth for all the appropriately-named baked goods you bring seemingly daily, and Jess for always entertaining me with your not so smart S.M.A.R.T goals. To my officemates Kirsten, Athan, and Sean: somehow you always understood when it was time to work and when it was time for taco lunch days and for that I will always be grateful. It is not easy to achieve that balance! The office was such a joy to be around because of you three. Thank you to the rest of the EMRG group, my lab siblings, for your friendship and general nerdiness.

Thank you Dam – you have helped me on many occasions with my tech naïveté, but most recently, thank you for fixing my computer 2 days before my thesis submission deadline when Microsoft Word refused to open any of my documents. Thank you Greg for helping me rig up the cuff compression machine for my study. I have to confess that, despite the cool diagram you drew, I still don't know how electrical resistance works.

Thank you to my family for accepting my "job" even though you still don't understand why you need to exercise when "your great grandmother lived to be 101 years old and she smoked every day." You are the reason cardiovascular disease is still the leading cause of death today, but I love you anyways.

Finally, of course, thank you Jason. Three years ago you showed me how fun research could be and, at the risk of sounding overly dramatic, it changed my life! You showed me what it was like to be truly, deeply, passionately curious about something and always pushed me to be better. You keep me grounded in what research is really about – not the awards and recognitions, but the joy of simply figuring something out that once didn't make sense. I owe a lot of the scientist I am today to you. Thank you for everything.

TABLE OF CONTENTS

LIST OF APPENDICES

LIST OF TABLES AND FIGURES

TABLES

FIGURES

LIST OF ABBREVIATIONS AND SYMBOLS

μ	Blood viscosity
ρ	Blood density
Akt	Protein kinase B
AMPK	AMP-activated protein kinase
BF	Blood flow
BH_4	Tetrahydrobiopterin
CAD	Coronary artery disease
cGMP	Cyclic guanosine monophosphate
CO	Cardiac output
CVD	Cardiovascular disease
D	Artery diameter
DBP	Diastolic blood pressure
ECG	Electrocardiography
ECP	External counterpulsation
eNOS	Endothelial nitric oxide synthase
FMD	Flow-mediated dilation
FMD%	Relative flow-mediated dilation
GC	Guanylate cyclase
HR	Heart rate
I-CAM1	Intercellular adhesion molecule 1
L-NMMA	L-N^G-monomethyl arginine

MAP	Mean arterial pressure
NFκB	Nuclear factor kappa-light-chain-enhancer of activated B cells
NO	Nitric oxide
O_2	Molecular oxygen
O_2^-	Superoxide
$ONOO^-$	Peroxynitrite
OSI	Oscillatory shear index
p65	Transcription factor p65, subunit of NFκB
Re	Reynolds number
ROS	Reactive oxygen species
SBP	Systolic blood pressure
SR	Shear rate
SS	Shear stress
SV	Stroke volume
V	Blood velocity
V-CAM1	Vascular cell adhesion protein 1

CHAPTER 1

Literature Review

1.1 Introduction

Cardiovascular disease (CVD), a broad term used to describe disorders of the heart and blood vessels, has remained the leading cause of death for the last 15 years (63). For although traditional risk factors such as blood lipids, insulin resistance, and blood pressure are recognized as modifiable targets for interventions aiming to reduce CVD (e.g. exercise training), it has become clear that these variables do not explain all of the observed cardiovascular risk reduction. In fact, approximately 40% of the risk reduction is attributable to changes in other, lesser known variables that contribute significantly to the incidence and progression of CVD (40). Endothelial function is a novel and emerging risk factor that refers to the ability of the artery to produce the dilatory or constrictive response necessary to maintain vascular homeostasis (66). Nitric oxide (NO) released by the endothelial cells of arteries deters the accumulation of molecules and particles that propagate the formation of atherosclerotic plaque; and it is the bioavailability of this molecule that is largely responsible for the functional capacity of the artery (66). Endothelial function is most commonly assessed through a flow-mediated dilation (FMD) test – an outcome measure that has been shown to independently predict the risk of future CVD (18, 85). Despite broad leaps in vascular research in recent years, the regulation of endothelial function remains poorly understood, while the morbidity and mortality burden of CVD continues to build (63). Therefore, it is imperative to continue investigating the

mechanisms by which endothelial function is regulated, so that this basic science knowledge can positively inform clinical practice.

1.2 Arterial anatomy and physiology

Arteries are blood vessels that deliver blood away from the heart. The arterial wall is made up of three distinct layers which are, from superficial to deep: (1) the tunica adventitia, which contains elastin, collagen, nerves, and blood vessels; (2) the tunica media, which contains vascular smooth muscle cells, elastin, and collagen; and (3) the tunica intima, which contains endothelial cells attached to a basement membrane that lines the inner wall. The arterial lumen is the space within the tube structure that allows the artery to serve as a conduit for blood (82).

The arterial system transitions between three different types of arteries to optimize blood delivery to all tissues of the body through creation of a pressure gradient. Elastic arteries (e.g., aorta, iliac, carotid) are buffering reservoirs that are large and centrally located, with thick walls and a high proportion of elastic fibres to allow for radial stretch and recoil in response to the high pressures of blood ejected from the heart. Muscular arteries (e.g., brachial, femoral) are medium-sized arteries that branch into the various regions of the body. Because these arteries contain relatively more smooth muscle, they possess a greater vasoconstrictive and vasodilatory capacity for local control of blood flow. Arterioles are the smallest and thinnest arteries, and primarily serve to resist or slow down blood flow as red blood cells move into the single cell-thick capillaries and to their end organ targets (82).

Although seemingly simple in structure, the scope of artery function is vast and complex, and includes the regulation of vascular tone, cellular adhesion, thromboresistance, smooth muscle cell proliferation, and vessel wall inflammation (27, 98). These functions are key to maintaining the balance between atheroprotection and atherogenesis. One of the most basic yet essential functions of the arterial system is to manage the distribution of blood flow to the entire body by making subtle changes to the degree of vasoconstriction and vasodilation in different vascular beds (21). This process of regulation of vascular tone through constriction and relaxation of vascular smooth muscle, facilitated by the function of the endothelial cells, gives rise to a term now known as endothelial function (66).

1.3 Control of Arterial Function

1.3.1 Shear stress-mediated arterial vasodilation

Shear stress-mediated arterial vasodilation is a key principle underlying the concept of endothelial function. In 1980, Furchgott & Zawadzki had just uncovered the importance of a specific "endothelial-derived relaxing factor" for arterial vasodilation. Based on their experiments, they postulated that the binding of acetylcholine to muscarinic receptors on endothelial cells triggered the release of a diffusible, labile substance ("endothelial-derived relaxing factor") that caused the artery to expand (33). This substance, later identified as nitric oxide, has been shown to facilitate arterial vasodilation through relaxation of smooth muscle cells in the tunica media (69). In

addition, NO plays a role in preventing platelet adhesion and aggregation, leukocyte and lipoprotein entry, and eventual thrombus formation in the arterial wall (98).

Shear stress (SS) is the force produced tangential to the fluid-wall interface, and the stimulus through which blood flow is able to alter endothelial function (2, 36, 70, 74, 75, 91). It has since been discovered that endothelial cells respond to shear stress by altering the morphology of its stress fibers to trigger the production of vasodilators or vasoconstrictors (32). Most research groups report shear rate in s^{-1} (SR = 8*V/D) – despite having to yield to the four major assumptions of Poiseuille's equation – simply due to ease of calculation (1). SR is widely accepted as a surrogate measure of vascular shear stress. Alternatively, shear stress in dynes/cm^2 (SS = 2μV/D) can also more precisely be determined through a calculation that accounts for the non-Newtonian fluid properties of blood (71). In the equations above, V = blood velocity, D = arterial diameter, and μ = blood viscosity.

Work in this area, beginning with *in vitro* experiments by Pohl *et al* (1986) in canines, has shown that the concept of a co-dependent relationship between shear stress and endothelial function is one that has only been strengthened with time and experimentation. Most recently, Tinken *et al* (2010) demonstrated that endothelial function is resistant to change in response to an exercise training intervention in the absence of corresponding changes in shear stress. In this study, investigators examined the effects of 6 weeks of bilateral handgrip exercise training on brachial artery endothelial function via FMD. In order to control for changes in shear rate, one limb was subjected to subsystolic cuff inflation to 60 mmHg. At the end of the training period, they observed an

increase in relative flow-mediated dilation in the non-cuffed limb, while no change was evident in the cuffed limb (91). These findings suggest, as is corroborated by many previous studies, that shear stress and the resulting NO produced is required to trigger vascular remodeling pathways that stimulate improvements in endothelial function. Endothelial function depends largely on the ability of the artery to continuously produce NO through shear-mediated mechanisms to prevent atherogenesis. Both up- and down-regulation of NO signaling pathways result in the range of endothelial function observed in humans *in vivo* (95).

1.3.2 Endothelial function and dysfunction

The contrast between endothelial function and dysfunction can be thought of as a balance between endothelial quiescent and activated phenotypes. In normal, healthy, vascular homeostasis, endothelial cells produce vasodilators (e.g., nitric oxide, endothelium-derived hyperpolarizing factor, prostacyclin) and vasoconstrictors (e.g., endothelin-1, prostanoids, angiotensin conversion enzyme) that effectively regulate vascular tone (11, 33, 56, 61, 80). Nitric oxide is the most important of these vasoactive substances, as its availability largely dictates the functional capacity of the endothelium. Production of NO requires the presence of substrate L-arginine, the co-factor tetrahydrobiopterin (BH_4), and the enzyme endothelial NO synthase (eNOS) (31). A reaction involving these components converts molecular oxygen (O_2) to NO, which subsequently diffuses into the smooth muscle layer where it activates guanylate cyclase (GC) to cause an increase in the formation of cyclic guanosine monophosphate (cGMP).

Through cGMP-mediated pathways, calcium ions become sequestered, smooth muscle cells relax, and the artery expands (66, 77). However, more importantly, continuous NO production maintains a state of *endothelial quiescence* through s-nitrosylation of the cysteine residues of NFκB, cell cycle proteins, oxidative phosphorylation machinery in the mitochondria, and various tissue factors (34, 83). By doing so, harmful ROS-producing pathways are effectively silenced.

In a dysfunctional state, NO signaling is impaired primarily by reduced availability of BH_4. BH_4 plays a vital role in stabilizing eNOS in its dimeric form, allowing the reduction of molecular oxygen to be coupled with the oxidation of L-arginine to produce NO (81). Without BH_4, eNOS monomerizes and "uncoupling" occurs, ultimately resulting in the generation of superoxide (O_2^-) instead of NO from O_2 (81). The subsequent binding of O_2^- to remaining NO further reduces NO and BH_4 bioavailability, and creates a very potent reactive oxygen species (ROS) called peroxynitrite ($ONOO^-$) (12, 25). $ONOO^-$ replaces NO in binding to the cysteine residues of NFκB and other downstream proteins mentioned above, resulting in a state of *endothelial activation* (27, 31, 79). Since these proteins are involved in ROS production, propagation of these pathways increases oxidative reactions and encourages an inflammatory response. If transient, this process is an appropriate defense mechanism against biological damage or invaders; however, if prolonged, it can become a toxic cycle that exhausts the ROS-buffering capacity of cells, resulting in endothelial cell senescence and detachment into circulation (104). Once the endothelium has been damaged, arteries become vulnerable to infiltration of lipoprotein particles that, in turn, initiate the

atherosclerotic process (35). As with most other health indicators, endothelial function is optimal in those who are young and healthy, and deteriorates with aging and disease (66). Indeed, many highly prevalent clinical conditions such as hypercholesterolemia, hypertension, type II diabetes, and obesity, have some origin in vascular homeostatic NO-ROS dysregulation and therefore endothelial dysfunction (17). The pervasiveness of diseases with an endothelial dysfunction etiology further highlights the importance of understanding the best ways to promote endothelial quiescence (i.e. increased NO signaling) and prevent endothelial activation (i.e. decreased NO signaling).

1.3.3 Assessment of endothelial function

The aim of most common and widely used methods of assessing endothelial function in humans is to evaluate the ability of an artery to dilate in response to pharmacologically- or physiologically-stimulated NO release. The brachial artery is the most common site of endothelial function assessment because of accessibility and ease of measurement. However, assessments can also be performed in other arterial segments, with varying degrees of invasiveness depending on the type of test employed.

1.3.3.1 Cardiac catheterization

The earliest investigations of endothelial function involved a catheter inserted into the coronary circulation and infusion of vasoactive substances such as acetylcholine or L-NMMA. The resulting change in artery diameter was quantified using coronary angiography and used to indicate the functional capacity of the artery, which can range

from optimal dilation in healthy endothelium to either sub-optimal dilation or constriction in dysfunctional endothelium (23, 57). Although cardiac catheterization is a direct and well-controlled assessment, this procedure is invasive and, therefore, extremely difficult to repeat or reproduce. Additionally, assessment of the coronary circulation does not reflect the systemic origin and development of endothelial dysfunction (27).

1.3.3.2 Venous occlusion plethysmography

Venous occlusion plethysmography, while employing a method similar to but less invasive than arterial cannulation and drug infusion, allows for assessment of endothelial function in a more peripheral region, by measuring changes in blood volume after occlusion. In this technique, pneumatic cuffs are placed around the upper arm (40 mmHg) and wrist (220 mmHg) to allow arterial inflow but block venous outflow in the forearm during measurement. Mercury-in-silastic strain gauges wrapped around the forearm act as resistors to determine changes in forearm blood volume through detection of changes in electrical resistance of the gauge (48). In this case, elevated forearm blood volume corresponds to an increase in arterial diameter and improved endothelial function (27). Although less so when compared to cardiac catheterization, the sensitive technical requirements of this technique still makes implementation in larger studies difficult (27).

1.3.3.3 Flow-mediated dilation

The flow-mediated dilation test conducted using ultrasonography is the reference standard assessment of endothelial function because it is non-invasive, repeatable,

reproducible, with standardized methodology to be able to implement across different laboratories (27). This technique, most commonly performed on blood vessels in the arm, makes use of a standard reactive hyperemia response that occurs following a brief period of ischemia to evaluate the endothelium's innate ability to release NO in response to elevated shear stress. After collecting a 30-second baseline image of the brachial artery to determine resting artery diameter, a pneumatic cuff wrapped around the forearm is inflated to a suprasystolic pressure (200 mmHg) to occlude blood flow to the hand. Following 5 minutes of ischemia, the cuff is released and images are collected for an additional 3 minutes to capture maximum arterial dilation (18, 85). Alternative methods manipulating shear rate have been also been developed to elicit more controlled hyperemic responses (65, 75, 76). To standardize the baseline and peak shear rate generated during an FMD test, a pneumatic piston can be placed over the brachial artery region to compress the artery until a target blood velocity, and consequently, shear rate (e.g. 8 s^{-1}) is achieved. Heated air (42-45 °C) is then circulated through a sealed box surrounding the forearm for 30 minutes, followed by piston release to allow for the natural elevation in shear rate (e.g. 50 s^{-1}) that occurs with this stimulus to transpire (75). As with the cuff occlusion method of FMD assessment, artery diameter is tracked post-ischemia to determine maximum vasodilation. To mimic the type of flow and shear perturbations experienced day-to-day, handgrip exercise can also be used to produce a fluctuating shear rate stimulus. Shorter duration bouts (5-10 minutes) of isotonic exercise (1-sec contraction:2-sec relaxation, 2-sec contraction:3-sec relaxation) create both high and low shear stresses within the artery that result in a measurable dilatory response (7, 8,

65, 76). In all cases, FMD is most commonly expressed as a percentage (FMD%), with the absolute dilation assessed relative to the baseline diameter.

1.3.3.4 Pulse wave analysis (PWA), pulse contour analysis (PCA), and pulse amplitude tonometry (PAT)

Alternative methods for the assessment of endothelial function are based on assessment of reductions in arterial stiffness as indicators of improved endothelial function. The arterial waveform is sensitive to changes in both pressure and wave reflection, which both provide information about the stiffness of an artery. Pulse wave analysis, pulse contour analysis, and pulse amplitude tonometry have been used to evaluate the central arterial waveform for changes in augmentation index, reflection index, and pulse amplitude, respectively, in response to salbutamol administration (62, 102). The β2 agonist salbutamol is known to reduce arterial stiffness in a NO-dependent manner, without a corresponding reduction in blood pressure (47). Although some of these methods have been validated as measures of NO bioavailability, further work is required in a wider range of ages and disease states to clarify their relationship with other more well-established measures of endothelial function (27).

1.4 Blood Flow Pattern as a Moderator of Endothelial Function

In the last three decades, much research in the area of vascular regulation has employed stimulus-response research designs in order to elucidate the control mechanisms regulating arterial function. The pulsatile pattern of blood flow in the arterial

tree results in flow that varies in both direction and magnitude throughout the cardiac cycle and in different segments of the arterial system, and consequently, affects the vascular regulatory response through changes in both shear direction and magnitude (43, 100). Blood flow occurs primarily in either the anterograde (away from the heart) or retrograde (towards the heart) directions; however, it can also be characterized as multidirectional, as is the case at bifurcations, branch points, and curved areas.

1.4.1 Anisotropic effects of blood flow on endothelial cells

Experiments in endothelial cell cultures have shown that there are anisotropic effects to changes in flow direction on at least four critical pathways in vascular regulation: (1) NF-κB (p65), which is involved in the inflammatory response; (2) eNOS, which is involved in flow-dependent vasodilation and the suppression of inflammation; (3) Akt and (4) AMP kinase, which are both involved in shear stress-mediated cellular responses (100). In a study by Wang *et al* (2013), investigators built a chamber that allowed for the application of flow at any angle to bovine aortic endothelial cells seeded onto a slide. They observed that higher flow angles (135-180°) that are more parallel to cell axes induced phosphorylation of eNOS and Akt, while lower flow angles (45-90°) that are more perpendicular to cell axes activated NF-kB by phosphorylation of p65. However, these changes only occurred if the cells had been pre-aligned with 24 hours of laminar flow (100). Nonaligned cells did not exhibit any change in the phosphorylation of key targets, highlighting the importance of cell alignment in the directional flow response.

The directional effects of blood flow on endothelial cells remain largely uncontested, as data in cellular research as a whole have yielded very similar findings (19, 55, 106).

1.4.2 Types of blood flow

1.4.2.1 Pulsatile

The pattern of blood flow in humans at rest is referred to as pulsatile: largely anterograde with a small amount of retrograde flow, driven by contraction of the myocardium during systole coupled with the elastic recoil of the arterial wall, respectively (72). Pulsatile blood flow is typically laminar with high shear stress (10-70 dynes/cm^2), occurs in the straight portions of the arterial tree, and is associated with the maintenance of endothelial function through a steady and constant release of NO (20). In a number of cellular experiments in several different endothelial cell types, including bovine aortic and human umbilical vein endothelial cells, pulsatile laminar flow was associated with increased NO release, eNOS mRNA expression, or phosphorylation of eNOS, all of which are indicators of increased NO signaling, and thus, an atheroprotective phenotype (6, 10, 67, 97).

1.4.2.2 Disturbed and Oscillatory

Disturbed blood flow describes all non-uniform, irregular forms of flow, including reciprocating or oscillatory flows. These types of blood flow are characterized by low net anterograde flow and shear stress (<4 dynes/cm^2), and are thought to contribute to impaired NO production, and consequently, endothelial dysfunction (20). Incidentally,

atherosclerotic lesions are known to occur around atypical vascular regions, such as branch points, curvatures, bifurcations, and post-stenotic regions, where these flow patterns are generally found (3, 28). There is also evidence that oscillatory flow not only upregulates the expression of the vasoconstrictors (ET-1) and a myriad of adhesion molecules (i.e., V-CAM1, I-CAM1, E-selectin, THP-1), but also downregulates eNOS expression (19, 106). Off-axis flows appear unable to direct and align cells, which may be necessary for inducing the molecular pathways that help maintain vascular homeostasis (100, 106).

1.4.2.3 Anterograde-dominant

In an anterograde-dominant blood flow pattern, anterograde flow is elevated from the resting state without any change to retrograde blood flow, such that the majority of blood flow is in the forward direction, away from the heart. This type of blood flow has only been described in *in vivo* models, such as passive heat stress, and has been associated with enhanced endothelium-dependent release of NO (52, 53). An increase in anterograde flow is thought to augment the laminar-type flow that exists at rest, therefore enhancing its general effects. Thus, anterograde-dominant blood flow has generally been accepted as the optimal chronic stimulus for improving endothelial function (40, 90).

1.4.2.4 Retrograde-dominant

In a retrograde-dominant blood flow pattern, retrograde flow is elevated from the resting state without any change to anterograde blood flow, such that the majority of

blood flow is in the backward or reverse direction, towards the heart. This term has also been used to describe any fluid flow opposite the physiological direction. Thijssen *et al* (2009) were the first to demonstrate acute impairment of endothelial function in response to a brief period of elevation in retrograde flow and shear stress in an *in vivo* human model. Using sub-systolic cuff occlusion on the upper limb to 50 and 75 mmHg, they showed a dose-dependent increase in the retrograde shear rate and corresponding acute decline in FMD% in the brachial artery. However, evidence from subsequent work may suggest that retrograde hemodynamics may not be inherently detrimental. In two separate studies, Totosy de Zepetnek *et al* (2014, 2015) used a sub-systolic cuff occlusion intervention that was identical to that of Thijssen and colleagues (87) to investigate the effects of retrograde flow in abled-bodied and spinal cord injured men and in both the brachial and superficial femoral arteries. Unlike with the Thijssen study, the intervention elicited increases in both anterograde and retrograde shear rate, while still resulting in acute decreases in FMD% through the superficial femoral artery (93, 94). Thus, the investigators were unable to isolate the component of the blood flow pattern responsible for the endothelial function response. However, particularly in the case of Totosy de Zepetnek *et. al.* (2015), increased retrograde shear rate is unlikely to be responsible for all of the observed decline in FMD since the same blood flow pattern was produced at the brachial artery where no change in FMD% was observed.

1.4.2.5 Oscillatory with High Shear Stress

One type of change in blood flow pattern that has yet to be formally characterized in the literature is one characterized by increases in both anterograde and retrograde blood flow, above that of resting blood flow. Research in high shear stress oscillatory flow is nearly absent in cellular work, and very incomplete in *in vivo* models. In the lone *in vitro* experimental study by Noris *et al* (1995), researchers measured the amount of L-citrulline produced by human umbilical vein endothelial cells after 6 hours of exposure to either oscillating shear stress (sinusoidal variations from 8.2 to 16.6 dynes/cm^2 with a mean of 12.4 dynes/cm^2) or static conditions. They found levels of L-citrulline, a marker of NO synthesis, to be significantly greater in cells that were under oscillating shear stress compared to the static condition (67). Interestingly, this pattern might be the most relevant to vascular exercise physiology research as *in vivo*, high shear stress oscillatory blood flow patterns are elicited at even greater shear stresses by aerobic or cyclic exercise modalities, such as running and cycling, which have generally been associated with improvements in cardiovascular health that may begin with endothelial function (8, 29, 39). However promising, more studies in this area need to be performed to ascertain the role of elevations in this type of blood flow pattern in regulating endothelial function.

1.4.3 In vivo methods of blood flow alteration

1.4.3.1 Passive heat stress

In addition to the environmental context, heating models have been studied for their application as a therapeutic tool (5). Gradual incremental heating, that which the human body experiences in hot weather, is a potent stimulus known to increase

anterograde blood flow and shear stress, and endothelium-dependent vasodilation. This vascular regulatory response results in the increase in blood flow to the surface of the skin required to dissipate heat. There are several thermoregulatory mechanisms, involving both neural and local inputs, by which passive heat stress causes arterial vasodilation. The initial increase in skin temperature is facilitated locally by cutaneous vasoconstrictors and vasodilators. The subsequent increase in skin temperature with accompanying increases in core temperature occurs through the abolishment of vasoconstrictor input and most importantly, accounting for 80-95% of the increase in skin blood flow, the large increase in core temperature is achieved through active vasodilation (52). Several theories have been suggested as to the mechanisms that control active vasodilation, including a proposed link between the sudomotor nerve and the release of nitric oxide. Local nitric oxide release has been shown to be particularly important for the prolonged increase in skin blood flow that occurs with passive heat stress (53, 54, 60). Maximum skin blood flow has been established to occur when skin temperature is elevated to 42 °C for 35-55 minutes (52).

Aside from a heat chamber, which is more commonly used in environmental physiology, water immersion, water-perfused heating suits, and heating blankets have all been used to apply passive heat stress to the body. When applied chronically, heat has been shown to be a potent therapy for improving endothelial function. In a series of studies by Green and colleagues, the effects of 8 weeks (thrice weekly 30-minute sessions) of heat training via ~40-42 °C limb immersion were examined (13, 14, 42, 64). Controls such as cuff occlusion (80-100 mmHg) and temperature clamping were used to

determine the influence of shear rate and temperature, respectively, on the vascular functional response. In all experiments, they found that microvascular and conduit arterial function improved with repetitive exposure to heat, but only when exposed to the associated increase in shear rate (13, 14, 42, 64). Microvascular function also appeared to be attenuated when temperature was fixed at resting state (30 °C) (13). Moreover, heat has been shown to be able to counteract the negative effect of reduced physical activity on popliteal artery endothelial function (84). Teixieira *et al* (2017) recently demonstrated that submerging the foot (up to the ankle) in 42 °C water for 30 minutes, 3 times a day for 5 days can prevent the decline in popliteal artery FMD% associated with reduced physical activity (<5,000 steps/day). They attributed this outcome to the large increases in shear rate in the leg during heating sessions. Unfortunately, the acute effects of heat are less clear. To date, only two studies have been published, both in groups of young healthy individuals. Furthermore, the results from these studies report conflicting findings: improvement (90) and no change (88) in brachial artery FMD in response to a single session of passive heat stress. Interestingly, regardless of localization of heating (e.g. upper or lower limb), passive heat stress is consistent in creating an anterograde-dominant flow profile in the brachial artery (88, 90).

1.4.3.2 External counterpulsation therapy

External counterpulsation (ECP) is a US FDA-approved, non-invasive therapy for patients with coronary artery disease (CAD) and unstable angina that have not been responsive to intensive pharmacological treatment or surgical revascularization (44).

Instrumentation involves the application of three sets of cuffs around the calves, lower thighs, and upper thighs and hips. The therapy uses the ECG signal as a trigger to sequentially inflate the cuffs to a suprasystolic pressure immediately prior to diastole, and then simultaneously deflate the cuffs immediately prior to systole. Strong repeated physical compressions sequenced in a distal to proximal manner are thought to facilitate venous return and cardiac unloading, which stimulate coronary angiogenesis in patients with CAD (4, 15, 44). Many studies have shown the multitude of beneficial effects of ECP, including improvements in exercise capacity, glucose tolerance, and inflammation that are thought to contribute to the overall improvement in cardiovascular health in patients that partake in this therapy. Moreover, Gurovich & Braith (2013) suggest that vascular adaptations may be one of the key mechanisms by which ECP alleviates symptoms. In this study, blood flow and shear stress pattern, as well as the acute flow-mediated dilation response, produced by 45 minutes of ECP was assessed in young, healthy males. Most interestingly, increased retrograde turbulent blood flow through the superficial femoral artery was associated with an improvement in FMD (44). These findings suggest that retrograde flow can be beneficial, and that other factors, such as flow turbulence may also affect the acute and chronic endothelial responses.

ECG-gated repeated cuff compression is a modified version of ECP therapy that has been developed in our lab to allow for the study of mechanistic considerations of similar blood flow patterns. In this intervention, a single pneumatic cuff placed around the forearm inflates and deflates every other heart cycle, triggered in early diastole (approximately 1.1 seconds after the R spike). In the brachial artery, the cuff

compressions create a high shear stress oscillatory blood flow pattern. The effects of this stimulus on endothelial function have not been previously investigated.

1.4.3.3 Physical exercise

Physical exercise of different modalities is known to produce both acute and chronic vascular responses that have been linked to the acute blood flow and shear stress patterns that are generated by the exercise, and are distinctive in their time course and outcomes. The "hormesis" hypothesis describes the phenomenon that improvements in physiological measures in response to repeated application of a stressor can be induced if the stressor temporarily impairs the physiological system (26). In the case of endothelial function, this hypothesis suggests that improvements in FMD% with exercise training are achieved as a result of acute impairments to FMD%. Such challenges to vascular homeostasis allow the artery to adapt to better accommodate the stress of exercise. Therefore, the proposed acute response to exercise is a brief nadir followed by normalization of FMD% that varies slightly based on factors such as exercise duration, exercise intensity, and fitness level (26).

1.4.3.3.1 Aerobic exercise

Exercise modes that are rhythmic tend to produce increases in systolic anterograde flow and shear rate, large increases in diastolic retrograde flow and shear rate and minimal changes to arterial blood pressure (86). These shear and transmural forces, commonly observed in aerobic exercise modalities such as running and cycling, have

been shown to elicit variable FMD responses immediately following exercise that appear to be dependent upon a number of factors including baseline endothelial function, vessel examined, the intensity and duration of the exercise and the time of examination after exercise cessation (26). Specifically, populations with existing endothelial dysfunction generally experience increased FMD acutely after exercise (24, 45), while those with good or optimal vascular health tend to further display variable change in FMD after exercise. High intensity exercise tends to decrease FMD (9, 50), while low to moderate intensity exercise almost always increase FMD post-exercise (22, 45, 46, 49, 68, 90, 96, 105). In addition, high intensity exercise of longer duration appears to exaggerate the nadir phase of the typical response compared to shorter bursts, which seem insufficient to elicit a decrease in FMD (50). Physical fitness has also been shown to attenuate the decrease in FMD following exercise (45). Despite disparities in acute findings, repeated application of this type shear stress stimulus through aerobic exercise training has been shown to improve FMD regardless of vascular health status, but only up to 4 weeks (8, 29, 30, 92, 101, 103). Beyond this point, structural changes typically in the form of increased arterial diameter complete the adaptive response, causing FMD to revert back to pre-training values (89).

1.4.3.3.2 Resistance exercise

Exercise that is resistance-type (i.e. weightlifting) is more closely linked to systolic blood pressure-driven increases in anterograde shear rate with no change in retrograde shear rate (86). This type of shear stress pattern has been linked to decreased

FMD acutely after exercise (37, 38, 51, 73, 99), and no change in FMD assessed at multiple time points throughout and after training (16, 78). Similar to aerobic exercise, trained status appears to have a protective effect in counteracting the decrease and, in some cases, even increasing FMD immediately post-exercise (51, 73, 99). It is worth noting that the literature in this area is very sparse, with few examinations to date on traditional types of resistance exercise such as weightlifting.

1.4.3.3.3 Handgrip exercise

In contrast to most other modes of exercise, which involves movement artifact and cumbersome equipment, handgrip exercise offers a logistically simpler alternative to study exercise *in vivo*. Many handgrip dynamometers can be connected to commercially-available data acquisition units to display and record force production in real time. In the research setting, a wide range of protocols has been used to study the effect of handgrip exercise on arterial function parameters. Although total exercise duration varies, 30 minutes is typical of most protocols. Some interventions employ isometric (squeeze and hold) contractions, while others use rhythmic (squeeze and release) contractions. Rhythmic handgrip exercise can further differ in the timing of not only contractions but rest periods between sequential bouts. Intensity can be absolute, using fixed kilogram loads, or relative, using a percentage of maximal voluntary contraction; and can also be consistent or increase in workload as the exercise bout progresses. Therefore, it should not be surprising that blood flow, shear stress, and endothelial function responses to handgrip exercise are equally variable, depending on protocol (37, 58, 59, 87, 91). Some

protocols increase anterograde shear alone (37, 41), whereas others increase both anterograde and retrograde shear (90, 91). Acute effects on FMD% also range considerably with studies that have demonstrated no change (37), increases (58, 90, 91), and even decreases (37) with a single bout of exercise. What appears to be consistent is that training with handgrip exercise improves FMD% through shear-mediated mechanisms, regardless of protocol (58, 59, 91).

Handgrip exercise is an interesting stimulus in that, depending on how it is performed, it can appear to mimic either aerobic or resistance exercise modes. Gonzales *et al* (2011) showed this phenomenon in their study, wherein participants performed handgrip exercise with fast (0.5 m/s) or slow (0.2 m/s) contractions. The blood flow pattern produced with fast contractions was more oscillatory than that produced with the slow contractions. Furthermore, the anterograde-dominant, slow contraction handgrip exercise protocol was shown to acutely decrease FMD%, while the high shear stress oscillatory fast contraction handgrip exercise protocol did not change FMD% acutely (37).

1.5 Purposes and Hypotheses

Evidently, much regarding the modulating effect of blood flow pattern, particularly in *in vivo* models, remains to be understood. The results from human studies do not always agree with other experimental models, primarily due to the lack of ability to accurately control anterograde and retrograde shear forces, leaving some ambiguity as to the exact role of directional shear in regulating endothelial function. Altogether, the

literature supports the idea that a high shear stress oscillatory blood flow pattern, that is, one that includes increases in both anterograde and retrograde components, may be what is required to improve endothelial function. Non-metabolic stimuli such as passive heat stress and external counterpulsation therapy can be a useful tool to isolate the effects of flow properties alone on endothelial function.

The purposes of this study were to determine the acute shear stress and endothelial function responses in the brachial artery to (1) passive heat stress, (2) ECG-gated cuff compressions, and (3) ECG-gated rhythmic handgrip exercise; and (4) to determine if there is a relationship between the degree of shear stress oscillation and endothelial function, regardless of the stimulus applied. We hypothesized the following: (1) Based on a combination of cell work (100), acute heating interventions (88, 90), and resistance-type exercise models (37), passive heat stress would increase anterograde shear stress and decrease retrograde shear stress, leading to no change in endothelial function; (2) Based on the work in acute aerobic exercise and ECP studies (26, 44), ECG-gated cuff compressions would increase both anterograde and retrograde shear stress, leading to an increase in endothelial function; (3) Based on the work in acute aerobic exercise and some handgrip models (26, 90, 91), ECG-gated rhythmic handgrip exercise would increase anterograde and retrograde shear stress and exercise metabolites, leading to an increase in endothelial function; and (4) the change in oscillatory shear index would be positively associated with the change in flow-mediated dilation, such that an increment increase in the degree of shear stress oscillation would be accompanied by a proportional improvement in endothelial function.

1.6 References

1. **Ade CJ**, **Broxterman RM**, **Wong BJ**, **Barstow TJ**. Anterograde and retrograde blood velocity profiles in the intact human cardiovascular system. *Exp Physiol* 97: 849–60, 2012.
2. **Anderson EA**, **Mark AL**. Flow-Mediated and Reflex Changes in Large Peripheral Artery Tone in Humans. *Circulation* 79: 93–100, 1989.
3. **Asakura T**, **Karino T**. Flow Patterns and Spatial Distribution of Atherosclerotic Lesions in Human Coronary Arteries. *Circ Res* 66: 1045–1066, 1990.
4. **Beck DT**, **Martin JS**, **Casey DP**, **Avery JC**, **Sardina PD**, **Braith RW**. Enhanced external counterpulsation improves endothelial function and exercise capacity in patients with ischaemic left ventricular dysfunction. *Clin Exp Pharmacol Physiol* 41: 628–36, 2014.
5. **Benzon H**, **Raj PP**, **Rathmell JP**, **Wu CL**, **Turk DC**, **Argoff CE**. *Practical Management of Pain 3rd ed.* 2000.
6. **Berk BC**. Atheroprotective signaling mechanisms activated by steady laminar flow in endothelial cells. *Circulation* 117: 1082–1089, 2008.
7. **Betik AC**, **Luckham VB**, **Hughson RL**. Flow-mediated dilation in human brachial artery after different circulatory occlusion conditions. *Am J Physiol Hear Circ Physiol* 286: H442–H448, 2004.
8. **Birk G**, **Dawson E**, **Atkinson C**, **Haynes A**, **Cable N**, **Thijssen D**, **Green D**. Brachial artery adaptation to lower limb exercise training: role of shear stress. *J Appl Physiol* 112: 1653–1658, 2012.

9. **Birk GK**, **Dawson EA**, **Batterham AM**, **Atkinson G**, **Cable T**, **Thijssen DHJ**, **Green DJ**. Effects of exercise intensity on flow mediated dilation in healthy humans. *Int J Sports Med* 34: 409–414, 2013.

10. **Buga GM**, **Gold ME**, **Fukuto JM**, **Ignarro LJ**. Shear stress-induced release of nitric oxide from endothelial cells grown on beads. *Hypertension* 17: 187–193, 1991.

11. **Busse R**, **Edwards G**, **Félétou M**, **Fleming I**, **Vanhoutte PM**, **Weston AH**. EDHF: bringing the concepts together. *TRENDS Pharmacol Sci* 23: 374–380, 2002.

12. **Cai H**, **Harrison DG**. Endothelial Dysfunction in Cardiovascular Diseases: The Role of Oxidant Stress. *Circ Res* 87: 840–844, 2000.

13. **Carter HH**, **Spence AL**, **Atkinson CL**, **Pugh CJA**, **Cable NT**, **Thijssen DHJ**, **Naylor LH**, **Green DJ**. Distinct effects of blood flow and temperature on cutaneous microvascular adaptation. *Med Sci Sport Exer* 46: 2113–2121, 2014.

14. **Carter HH**, **Spence AL**, **Atkinson CL**, **Pugh CJA**, **Naylor LH**, **Green DJ**. Repeated core temperature elevation induces conduit artery adaptation in humans. *Eur J Appl Physiol* 114: 859–865, 2014.

15. **Casey DP**, **Beck DT**, **Nichols WW**, **Conti CR**, **Choi CY**, **Khuddus MA**, **Braith RW**. Effects of enhanced external counterpulsation on arterial stiffness and myocardial oxygen demand in patients with chronic angina pectoris. *Am J Cardiol* 107: 1466–1472, 2011.

16. **Casey DP**, **Pierce GL**, **Howe KS**, **Mering MC**, **Braith RW**. Effect of resistance training on arterial wave reflection and brachial artery reactivity in normotensive

postmenopausal women. *Eur J Appl Physiol* 100: 403–408, 2007.

17. **Celermajer DS**, **Sorensen KE**, **Bull C**, **Robinson J**, **Deanfield JE**. Endothelium-Dependent Dilation in the Systemic Arteries of Asymptomatic Subjects Relates to Coronary Risk Factors and Their Interaction. *J Am Coll Cardiol* 24: 1468–1474, 1993.

18. **Celermajer DS**, **Sorensen KE**, **Gooch VM**, **Spiegelhalter DJ**, **Miller OI**, **Sullivan ID**, **Lloyd JK**, **Deanfield JE**. Non-invasive detection of endothelial dysfunction in children and adults at risk of atherosclerosis. *Lancet* 340: 1111–1115, 1992.

19. **Chappell DC**, **Varner SE**, **Nerem RM**, **Medford RM**, **Alexander RW**. Oscillatory Shear Stress Stimulates Adhesion Molecule Expression in Cultured Human Endothelium. *Circ Res* 82: 532–539, 1998.

20. **Chiu J-J**, **Chien S**. Effects of disturbed flow on vascular endothelium: pathophysiological basis and clinical perspectives. *Physiol Rev* 91: 327–387, 2011.

21. **Corson MA**, **James NL**, **Latta SE**, **Nerem RM**, **Berk BC**, **Harrison DG**. Phosphorylation of Endothelial Nitric Oxide Synthase in Response to Fluid Shear Stress. *Circ Res* 79: 984–991, 1996.

22. **Cosio-Lima LM**, **Thompson PD**, **Reynolds KL**, **Headley SA**, **Winter CR**, **Manos T**, **Lagasse MA**, **Todorovich JR**, **Germain M**. The acute effect of aerobic exercise on brachial artery endothelial function in renal transplant recipients. *Prev Cardiol* 9: 211–214, 2006.

23. **Cox DA**, **Vita JA**, **Treasure CB**, **Fish RD**, **Alexander RW**, **Ganz P**, **Selwyn AP**.

Atherosclerosis Impairs Flow-Mediated Dilation of Coronary Arteries in Humans. *Circulation* 80: 458–465, 1989.

24. **Currie KD**, **McKelvie RS**, **MacDonald MJ**. Flow-mediated dilation is acutely improved after high-intensity interval exercise. *Med Sci Sports Exerc* 44: 2057–2064, 2012.

25. **Darley-Usmar V**, **Wiseman H**, **Halliwell B**. Nitric oxide and oxygen radicals: a question of balance. *FEBS Lett* 369: 131–135, 1995.

26. **Dawson EA**, **Green DJ**, **Cable NT**, **Thijssen DHJ**. Effects of acute exercise on flow-mediated dilatation in healthy humans. *J Appl Physiol* 115: 1589–98, 2013.

27. **Deanfield JE**, **Halcox JP**, **Rabelink TJ**. Endothelial function and dysfunction: Testing and clinical relevance. *Circulation* 115: 1285–1295, 2007.

28. **DeBakey M**, **Lawrie G**, **Glaeser D**. Patterns of atherosclerosis and their surgical significance. *Ann Surg* 201: 115–131, 1985.

29. **DeSouza CA**, **Shapiro LF**, **Clevenger CM**, **Dinenno FA**, **Monahan KD**, **Tanaka H**, **Seals DR**. Regular Aerobic Exercise Prevents and Restores Age-Related Declines in Endothelium-Dependent Vasodilation in Healthy Men. *Circulation* 102: 1351–1357, 2000.

30. **Edwards DG**, **Schofield RS**, **Lennon SL**, **Pierce GL**, **Nichols WW**, **Braith RW**. Effect of exercise training on endothelial function in men with coronary artery disease. *Am J Cardiol* 93: 617–20, 2004.

31. **Förstermann U**, **Münzel T**. Endothelial Nitric Oxide Synthase in Vascular Disease: From Marvel to Menace. *Circulation* 113: 1708–1714, 2006.

32. **Franke R**, **Gräfe M**, **Schnittler H**, **Seiffge D**, **Mittermayer C**, **Drenckhahn D**. Induction of human vascular endothelial stress fibres by fluid shear stress. *Nature* 307: 648–649, 1984.

33. **Furchgott RF**, **Zawadzki J V**. The obligatory role of endothelial cells in the relaxation of arterial smooth muscle by acetylcholine. *Nature* 288: 373–376, 1980.

34. **Ghosh S**, **Karin M**. Missing Pieces in the NF-κB Puzzle. *Cell* 109: S81–S96, 2002.

35. **Gimbrone MA**, **García-Cardeña G**. Endothelial Cell Dysfunction and the Pathobiology of Atherosclerosis. *Circ Res* 118: 620–636, 2016.

36. **Gnasso A**, **Carallo C**, **Irace C**, **Franceschi MS De**, **Luigi P**, **Motti C**, **Cortese C**. Association between wall shear stress and flow-mediated vasodilation in healthy men. *Atherosclerosis* 156: 171–176, 2001.

37. **Gonzales JU**, **Thompson BC**, **Thistlethwaite JR**, **Scheuermann BW**. Association between exercise hemodynamics and changes in local vascular function following acute exercise. *Appl Physiol Nutr Metab* 36: 137–144, 2011.

38. **Gori T**, **Grotti S**, **Dragoni S**, **Lisi M**, **Di Stolfo G**, **Sonnati S**, **Fineschi M**, **Parker JD**. Assessment of vascular function: flow-mediated constriction complements the information of flow-mediated dilatation. *Heart* 96: 141–147, 2010.

39. **Green D**, **Cheetham C**, **Mavaddat L**, **Watts K**, **Best M**, **Taylor R**, **O'Driscoll G**. Effect of lower limb exercise on forearm vascular function: contribution of nitric oxide. *Am J Physiol Heart Circ Physiol* 283: H899–H907, 2002.

40. **Green DJ**. Exercise training as vascular medicine: direct impacts on the

vasculature in humans. *Exerc Sport Sci Rev* 37: 196–202, 2009.

41. **Green DJ**, **Bilsborough W**, **Naylor LH**, **Reed C**, **Wright J**, **O'Driscoll G**, **Walsh JH**. Comparison of forearm blood flow responses to incremental handgrip and cycle ergometer exercise: relative contribution of nitric oxide. *J Physiol* 5622: 617–628, 2005.

42. **Green DJ**, **Carter HH**, **Fitzsimons MG**, **Cable NT**, **Thijssen DHJ**, **Naylor LH**. Obligatory role of hyperaemia and shear stress in microvascular adaptation to repeated heating in humans. *J Physiol* 588: 1571–1577, 2010.

43. **Gurovich AN**, **Braith RW**. Analysis of both pulsatile and streamline blood flow patterns during aerobic and resistance exercise. *Eur J Appl Physiol* 112: 3755–3764, 2012.

44. **Gurovich AN**, **Braith RW**. Enhanced external counterpulsation creates acute blood flow patterns responsible for improved flow-mediated dilation in humans. *Hypertens Res* 36: 1–9, 2013.

45. **Harris RA**, **Padilla J**, **Hanlon KP**, **Rink LD**, **Wallace JP**. The flow-mediated dilation response to acute exercise in overweight active and inactive men. *Obesity* 16: 578–584, 2008.

46. **Harvey PJ**, **Picton PE**, **Su WS**, **Morris BL**, **Notarius CF**, **Floras JS**. Exercise as an alternative to oral estrogen for amelioration of endothelial dysfunction in postmenopausal women. *Am Heart J* 149: 291–297, 2005.

47. **Hayward CS**, **Kraidly M**, **Webb CM**, **Collins P**. Assessment of Endothelial Function Using Peripheral Waveform Analysis: A Clinical Application. *J Am Coll*

Cardiol 40: 521–528, 2002.

48. **Joannides R**, **Bellien J**, **Thuillez C**. Clinical methods for the evaluation of endothelial function – a focus on resistance arteries. *Fundam Clin Pharmacol* 20: 311–320, 2006.

49. **Johnson BD**, **Mather KJ**, **Newcomer SC**, **Mickleborough TD**, **Wallace JP**. Brachial Artery Flow-mediated Dilation Following Exercise with Augmented Oscillatory and Retrograde Shear Rate. *Cardiovasc Ultrasound* 10: 34, 2012.

50. **Johnson BD**, **Padilla J**, **Wallace JP**. The exercise dose affects oxidative stress and brachial artery flow-mediated dilation in trained men. *Eur J Appl Physiol* 112: 33–42, 2012.

51. **Jurva JW**, **Phillips SA**, **Syed AQ**, **Syed AY**, **Pitt S**, **Weaver A**, **Gutterman DD**. The Effect of Exertional Hypertension Evoked by Weight Lifting on Vascular Endothelial Function. *J Am Coll Cardiol* 48: 588–589, 2006.

52. **Kellogg DL**. In vivo mechanisms of cutaneous vasodilation and vasoconstriction in humans during thermoregulatory challenges. *J Appl Physiol* 100: 1709–1718, 2006.

53. **Kellogg DL**, **Crandall CG**, **Liu Y**, **Charkoudian N**, **Johnson JM**. Nitric oxide and cutaneous active vasodilation during heat stress in humans. *J Appl Physiol* 85: 824–829, 1998.

54. **Kellogg DL**, **Liu Y**, **Kosiba IF**, **O'Donnell D**. Role of nitric oxide in the vascular effects of local warming of the skin in humans. *J Appl Physiol* 86: 1185–1190, 1999.

55. **De Keulenaer GW**, **Chappell DC**, **Ishizaka N**, **Nerem RM**, **Alexander RW**, **Griendling KK**. Oscillatory and Steady Laminar Shear Stress Differentially Affect Human Endothelial Redox State : Role of a Superoxide-Producing NADH Oxidase. *Circ Res* 82: 1094–1101, 1998.

56. **Kinlay S**, **Behrendt D**, **Wainstein M**, **Beltrame J**, **Fang JC**, **Creager MA**, **Selwyn AP**, **Ganz P**. Role of Endothelin-1 in the Active Constriction of Human Atherosclerotic Coronary Arteries. *Circulation* 104: 1114–1118, 2001.

57. **Ludmer PL**, **Selwyn AP**, **Shook TL**, **Wayne RR**, **Mudge GH**, **Alexander RW**, **Ganz P**. Paradoxical Vasoconstriction Induced by Acetylcholine in Atherosclerotic Coronary Arteries. *N Engl J Med* 315: 1046–1051, 1986.

58. **McGowan CL**, **Levy a S**, **Millar PJ**, **Guzman JC**, **Morillo C a**, **McCartney N**, **Macdonald MJ**. Acute vascular responses to isometric handgrip exercise and effects of training in persons medicated for hypertension. *Am J Physiol Hear Circ Physiol* 291: H1797-802, 2006.

59. **McGowan CL**, **Visocchi A**, **Faulkner M**, **Verduyn R**, **Rakobowchuk M**, **Levy AS**, **McCartney N**, **MacDonald MJ**. Isometric handgrip training improves local flow-mediated dilation in medicated hypertensives. *Eur J Appl Physiol* 99: 227–234, 2007.

60. **Minson CT**, **Berry LT**, **Joyner MJ**. Nitric oxide and neurally mediated regulation of skin blood flow during local heating. *J Appl Physiol* 91: 1619–1626, 2001.

61. **Moncada S**, **Higgs E**, **Vane J**. Human arterial and venous tissues generate prostacyclin (prostaglandin x), a potent inhibitor of platelet aggregation. *Lancet* 1:

18–20, 1977.

62. **Naka KK**, **Tweddel AC**, **Doshi SN**, **Goodfellow J**, **Henderson AH**. Flow-mediated changes in pulse wave velocity: a new clinical measure of endothelial function. *Eur Heart J* 27: 302–309, 2006.

63. **Nascimento BR**, **Brant LCC**, **Moraes DN**, **Ribeiro ALP**. Global health and cardiovascular disease. *Heart* 100: 1743–1749, 2014.

64. **Naylor LH**, **Carter H**, **FitzSimons MG**, **Cable NT**, **Thijssen DHJ**, **Green DJ**. Repeated increases in blood flow, independent of exercise, enhance conduit artery vasodilator function in humans. *Am J Physiol Heart Circ Physiol* 300: H664–H669, 2011.

65. **Naylor LH**, **Weisbrod CJ**, **O'Driscoll G**, **Green DJ**. Measuring peripheral resistance and conduit arterial structure in humans using Doppler ultrasound. *J Appl Physiol* 98: 2311–2315, 2005.

66. **Nichols WW**, **O'Rourke MF**. *McDonald's Blood Flow in Arteries: Theoretical, Experimental and Clinical Principles*. 2005.

67. **Noris M**, **Morigi M**, **Donadelli R**, **Aiello S**, **Foppolo M**, **Todeschini M**, **Orisio S**, **Remuzzi G**, **Remuzzi A**. Nitric Oxide Synthesis by Cultured Endothelial Cells Is Modulated by Flow Conditions. *Circ Res* 76: 536–543, 1995.

68. **Padilla J**, **Harris RA**, **Fly AD**, **Rink LD**, **Wallace JP**. The effect of acute exercise on endothelial function following a high-fat meal. *Eur J Appl Physiol* 98: 256–262, 2006.

69. **Palmer RMJ**, **Ferrige AG**, **Moncada S**. Nitric oxide release accounts for the

biological activity of endothelium-derived relaxing factor. *Nature* 327: 524–526, 1987.

70. **Paniagua OA**, **Bryant MB**, **Panza JA**. Role of Endothelial Nitric Oxide in Shear Stress-Induced Vasodilation of Human Microvasculature. *Circulation* 103: 1752–1758, 2001.

71. **Papaioannou TG**, **Stefanadis C**. Vascular Wall Shear Stress: Basic Principles and Methods. *Hell J Cardiol* 46: 9–15, 2005.

72. **Peterson LH**. The Dynamics of Pulsatile Blood Flow. *Circ Res* 2: 127–139, 1954.

73. **Phillips S a**, **Das E**, **Wang J**, **Pritchard K**, **Gutterman DD**. Resistance and aerobic exercise protects against acute endothelial impairment induced by a single exposure to hypertension during exertion. *J Appl Physiol* 110: 1013–20, 2011.

74. **Pohl U**, **Holtz J**, **Busse R**, **Bassenge E**. Crucial Role of Endothelium in the Vasodilator Response to Increased Flow in Vivo. *Hypertension* 8: 37–44, 1986.

75. **Pyke KE**, **Dwyer EM**, **Tschakovsky ME**. Impact of controlling shear rate on flow-mediated dilation responses in the brachial artery of humans. *J Appl Physiol* 97: 499–508, 2004.

76. **Pyke KE**, **Poitras V**, **Tschakovsky ME**. Brachial artery flow-mediated dilation during handgrip exercise: evidence for endothelial transduction of the mean shear stimulus. *Am J Physiol Hear Circ Physiol* 294: H2669–H2679, 2008.

77. **Quyyumi AA**. Endothelial Function in Health and Disease: New Insights into the Genesis of Cardiovascular Disease. *Am J Med* 105: 32S–39S, 1998.

78. **Rakobowchuk M**, **Mcgowan CL**, **de Groot PC**, **Hartman JW**, **Phillips SM**,

MacDonald MJ. Endothelial function of young healthy males following whole body resistance training. *J Appl Physiol* 98: 2185–2190, 2005.

79. **Rhee SG**. H2O2, a Necessary Evil for Cell Signaling. *Science (80-)* 312: 1882–1883, 2006.

80. **Saye JA**, **Singer HA**, **Peach MJ**. Role of Endothelium in Conversion of Angiotensin I to Angiotensin II in Rabbit Aorta. *Hypertension* 6: 216–221, 1984.

81. **Schmidt TS**, **Alp NJ**. Mechanisms for the role of tetrahydrobiopterin in endothelial function and vascular disease. *Clin Sci* 113: 47–63, 2007.

82. **Seeley R**, **VanPutte C**, **Regan J**, **Russo A**. *Seeley's Anatomy & Physiology*. 2011.

83. **Stamler JS**, **Lamas S**, **Fang FC**. Nitrosylation: The Prototypic Redox-Based Signaling Mechanism. *Cell* 106: 675–683, 2001.

84. **Teixeira AL**, **Padilla J**, **Vianna LC**. Impaired popliteal artery flow-mediated dilation caused by reduced daily physical activity is prevented by increased shear stress. *J Appl Physiol* (2017). doi: 10.1152/japplphysiol.00001.2017.

85. **Thijssen DHJ**, **Black M a**, **Pyke KE**, **Padilla J**, **Atkinson G**, **Harris R a**, **Parker B**, **Widlansky ME**, **Tschakovsky ME**, **Green DJ**. Assessment of flow-mediated dilation in humans: a methodological and physiological guideline. *Am J Physiol Heart Circ Physiol* 300: H2–H12, 2011.

86. **Thijssen DHJ**, **Dawson EA**, **Black MA**, **Hopman MTE**, **Cable NT**, **Green DJ**. Brachial artery blood flow responses to different modalities of lower limb exercise. *Med Sci Sports Exerc* 41: 1072–1079, 2009.

87. **Thijssen DHJ**, **Dawson EA**, **Tinken TM**, **Cable NT**, **Green DJ**. Retrograde Flow

and Shear Rate Acutely Impair Endothelial Function in Humans. *Hypertension* 53: 986–992, 2009.

88. **Thomas KN**, **Rij AM van**, **Lucas SJE**, **Gray AR**, **Cotter JD**. Substantive hemodynamic and thermal strain upon completing lower-limb hot-water immersion; comparisons with treadmill running. *Temperature* 8940, 2016.

89. **Tinken TM**, **Thijssen DH**, **Black MA**, **Cable NT**, **Green DJ**. Time course of change in vasodilator function and capacity in response to exercise training in humans. *J Physiol* 586: 5003–5012, 2008.

90. **Tinken TM**, **Thijssen DHJ**, **Hopkins N**, **Black MA**, **Dawson EA**, **Minson CT**, **Newcomer SC**, **Laughlin MH**, **Cable NT**, **Green DJ**. Impact of shear rate modulation on vascular function in humans. *Hypertension* 54: 278–285, 2009.

91. **Tinken TM**, **Thijssen DHJ**, **Hopkins N**, **Dawson EA**, **Cable NT**, **Green DJ**. Shear stress mediates endothelial adaptations to exercise training in humans. *Hypertension* 55: 312–318, 2010.

92. **Tjønna AE**, **Lee SJ**, **Rognmo Ø**, **Stølen TO**, **Bye A**, **Haram PM**, **Loennechen JP**, **Al-Share QY**, **Skogvoll E**, **Slørdahl SA**, **Kemi OJ**, **Najjar SM**, **Wisløff U**. Aerobic interval training versus continuous moderate exercise as a treatment for the metabolic syndrome: A pilot study. *Circulation* 118: 346–354, 2008.

93. **Totosy de Zepetnek JO**, **Ditor DS**, **Au JS**, **Macdonald MJ**. Impact of shear rate pattern on upper and lower limb conduit artery endothelial function in both spinal cord-injured and able-bodied men. *Exp Physiol Exp Physiol Exp Physiol* 1001010: 1107–1117, 2015.

94. **Totosy de Zepetnek JO**, **Jermey TL**, **MacDonald MJ**. Superficial femoral artery endothelial responses to a short-term altered shear rate intervention in healthy men. *PLoS One* 9: e113407, 2014.

95. **Tousoulis D**, **Kampoli A-M**, **Tentolouris Nikolaos Papageorgiou C**, **Stefanadis C**. The role of nitric oxide on endothelial function. *Curr Vasc Pharmacol* 10: 4–18, 2012.

96. **Tyldum GA**, **Schjerve IE**, **Tjønna AE**, **Kirkeby-Garstad I**, **Stølen TO**, **Richardson RS**, **Wisløff U**. Endothelial Dysfunction Induced by Post-Prandial Lipemia. Complete Protection Afforded by High-Intensity Aerobic Interval Exercise. *J Am Coll Cardiol* 53: 200–206, 2009.

97. **Uematsu M**, **Ohara Y**, **Navas JP**, **Nishida K**, **Murphy TJ**, **Alexander RW**, **Nerem RM**, **Harrison DG**. Regulation of endothelial cell nitric oxide synthase mRNA expression by shear stress. *Am J Physiol Cell Physiol* 269: C1371–C1378, 1995.

98. **Vane JR**, **Änggard EE**, **Botting RM**. Regulatory Functions of the Vascular Endothelium. *N Engl J Med* 323: 27–36, 1990.

99. **Varady KA**, **Bhutani S**, **Church EC**, **Phillips SA**. Adipokine responses to acute resistance exercise in trained and untrained men. *Med Sci Sports Exerc* 42: 456–462, 2010.

100. **Wang C**, **Baker BM**, **Chen CS**, **Schwartz MA**. Endothelial cell sensing of flow direction. *Arterioscler Thromb Vasc Biol* 33: 2130–2136, 2013.

101. **Watts K**, **Beye P**, **Siafarikas A**, **O'Driscoll GG**, **Jones TW**, **Davis EA**, **Green**

DJ. Effects of exercise training on vascular function in obese children. *J Pediatr* 146: 296; author reply 296-7, 2005.

102. **Wilkinson IB**, **Hall IR**, **Maccallum H**, **Mackenzie IS**, **Mceniery CM**, **Arend BJ Van Der**, **Shu Y**, **Mackay LS**, **Webb DJ**, **Cockcroft JR**. Pulse-Wave Analysis: Clinical Evaluation of a Noninvasive, Widely Applicable Method for Assessing Endothelial Function. *Arter Thromb Vasc Biol* 22: 147–152, 2002.

103. **Wisløff U**, **Støylen A**, **Loennechen JP**, **Bruvold M**, **Rognmo Ø**, **Haram PM**, **Tjønna AE**, **Helgerud J**, **Slørdahl SA**, **Lee SJ**, **Videm V**, **Bye A**, **Smith GL**, **Najjar SM**, **Ellingsen Ø**, **Skjærpe T**. Superior cardiovascular effect of aerobic interval training versus moderate continuous training in heart failure patients: A randomized study. *Circulation* 115: 3086–3094, 2007.

104. **Woywodt A**, **Bahlmann FH**, **Groot K De**, **Haller H**, **Haubitz M**. Circulating endothelial cells: life, death, detachment and repair of the endothelial cell layer. *Nephrol Dial Transpl* 17: 1728–1730, 2002.

105. **Zhu W**, **Zeng J**, **Yin J**, **Zhang F**, **Wu H**, **Yan S**, **Wang S**. Both flow-mediated vasodilation procedures and acute exercise improve endothelial function in obese young men. *Eur J Appl Physiol* 108: 727–732, 2010.

106. **Ziegler T**, **Bouzourene K**, **Harrison VJ**, **Brunner HR**, **Hayoz D**. Influence of Oscillatory and Unidirectional Flow Environments on the Expression of Endothelin and Nitric Oxide Synthase in Cultured Endothelial Cells. *Arterioscler Thromb Vasc Biol* 18: 686–692, 1998.

CHAPTER TWO

Peripheral artery endothelial function responses to altered blood flow in humans

2.1 Introduction

Structural and functional changes to peripheral arteries in humans can be stimulated through the cumulative effects of blood flow-mediated fluctuations in shear stress against the arterial wall (2, 4, 30). Through mechanotransduction, these forces at the fluid-wall interface are detected by endothelial cells, which have the ability to trigger molecular signaling pathways that are either atheroprotective or atherogenic (19, 22, 31). The propagation of these pathways is the chief regulator of endothelial function, an emerging indicator of arterial health and a functional measure of the capacity of the artery to continuously produce vasoactive substances in order to maintain vascular homeostasis (26). In a dysfunctional state, an imbalance of vasodilators and vasoconstrictors produced by endothelial cells, over time, results in the creation of a pro-inflammatory environment that negatively impacts arterial health (8).

Endothelial function is influenced by a variety of factors, including blood flow direction and magnitude. In the last decade, research in this area strongly suggests that anterograde flow (i.e. forward, away from the heart) is beneficial, while retrograde flow (i.e. backward, towards the heart) is detrimental, to arterial function. Although this theory is well-supported by highly controlled *in vitro* experiments in endothelial cell cultures (34), the findings and conclusions from many *in vivo* studies in humans are not as well aligned or consistent (27, 29). For instance, exercise models have been used extensively in stimulus-response research designs to examine this type of research question.

Generally, moderate intensity aerobic-type exercise modes (e.g. running, cycling), which produce high shear stress increases in both anterograde and retrograde directions have been associated with acute improvements in endothelial function (7, 14, 29, 30); while resistance-type exercise modes (e.g. leg kicking), which produce mainly systolic blood pressure-driven increases in anterograde shear stress have been associated with acute decrements in endothelial function (12, 27). However, the additional confounding metabolic influence present with the examination of exercise induced changes in blood flow patterns makes it difficult to interpret these results as specifically linked to changes in the direction or magnitude of the blood flow. There is clearly a need for controlled, stimulus-response *in vivo* study designs in humans to better isolate the effects of changes in blood flow direction and other flow properties on endothelial function.

The purposes of this study were to determine the brachial artery acute shear stress and endothelial function responses to (1) passive heat stress (HEAT), (2) ECG-gated cuff compressions (CUFF), and (3) ECG-gated rhythmic handgrip exercise (HGEX); and (4) to determine if there is a relationship between the degree of shear stress oscillation and endothelial function, regardless of the stimulus applied. Guided by the theory that degree of shear stress oscillation, rather than directionality of shear stress, is the main determinant in the acute endothelial function response, we hypothesized the following: (1) Based on a combination of cell work, acute heating interventions, and resistance-type exercise models, HEAT would increase anterograde shear stress and decrease retrograde shear stress, leading to an unpredictable change in endothelial function; (2) Based on the work in acute aerobic exercise and external counterpulsation (ECP) therapy, CUFF would

increase both anterograde and retrograde shear stress, leading to an increase in endothelial function; (3) Based on the work in acute aerobic exercise and some handgrip models, HGEX would increase anterograde and retrograde shear stress and exercise metabolites, leading to an increase in endothelial function; and (4) the change in oscillatory shear index would be positively associated with the change in flow-mediated dilation, such that an increment increase in the degree of shear stress oscillation would be accompanied by a proportional improvement in endothelial function.

2.2 Methods

2.2.1 Participants

Ten young, healthy males (22 ± 3 years old) were recruited from McMaster University. Based on the effects observed in Totosy de Zepetnek *et al* (2015) examining the impact of a shear-altering stimulus (sub-systolic cuff occlusion) in young, healthy males, we anticipated large-sized effects (f = 1.92) for acute changes in relative flow-mediated dilation (FMD%). Four participants were required to have 80% power to detect significant differences of this magnitude, with $\alpha = 0.05$ and use of a two-tailed test. In order to account for potential issues with data quality or subject attrition, 10 participants were recruited. Exclusion criteria included smoking and/or drug use and a history of cardiovascular, musculoskeletal, or metabolic disease.

2.2.2 Study Design and Protocol

This study employed a within-subjects interventional design and involved a total of four visits to the Vascular Dynamics Lab at McMaster University. Interested individuals were invited to the lab for a screening and familiarization visit, wherein the right brachial artery (BA) was scanned to assess image quality, and a BA flow-mediated dilation (FMD) test was performed to ensure participant familiarity during data collection visits. All qualified participants were instructed to refrain from vigorous physical activity > 24 hours, alcohol and caffeine > 6 hours, and food > 4 hours prior to each of the three subsequent visits. A unilateral model was used such that the left side of the body underwent all experimental interventions (EXP) while the right side of the body served as the within-subject time control (CON). In a randomized order, participants underwent three different, unilateral, blood flow-altering interventions (i.e. passive heat stress (HEAT), cuff compressions (CUFF), handgrip exercise (HGEX)) in separate visits.

Upon arrival at the lab for each of these visits, hematocrit was measured in duplicate with a fingertip blood sample. Participants were then asked to lie supine while they were instrumented with three sets of single-lead ECG (Powerlab model ML795, AD Instruments, Colorado Springs, CO, USA) and a non-invasive finger cuff (Finometer MIDI, Finapres Medical Systems, The Netherlands) for continuous heart rate and blood pressure monitoring. Thermistors were also secured to two sites on the anterior skin surface of the forearms for measurement of skin temperature (Omega Precision Fine Wire Thermocouples Part #5SRTC-GG-T-30-72, Stamford, CT, USA; AD Instruments T type pod, Colorado Springs, CO, USA). Following 10 minutes of rest, participants underwent a fixed 10-minute duration of either HEAT, CUFF, or HGEX. Systolic (SBP), diastolic

(DBP), and mean blood pressure (MAP), heart rate (HR), cardiac output (CO), and stroke volume (SV) were assessed beat-to-beat throughout the entire protocol using the Beatscope software (Finapres, Netherlands). Core temperature was measured in triplicate and averaged using a commercially available tympanic thermometer before, during, and after each of the interventions (FirstTemp Genius, Sherwood Medical, St. Louis, MO, USA). BA diameters and blood velocities, blood flow turbulence, endothelial shear stress, and oscillatory shear index were assessed before and during each of the interventions; and FMD% was assessed before and immediately after each of the interventions.

2.2.3 Interventions

1. **Passive heat stress (HEAT):** A commercially-available heating pad (Sunbeam) set to high was wrapped around the left forearm from the elbow to the wrist to heat the region to 42.0 ± 0.8 °C.
2. **ECG-gated cuff compressions (CUFF):** As a modification of external counterpulsation therapy, this intervention involved the repetitive inflation (to 300 mmHg) and deflation of a single cuff wrapped around the left forearm (Hokanson, Bellevue, WA, USA), triggered with a delay of 1.1 seconds following the ECG R spike. With a duty cycle of two heart cycles, inflation and deflation alternatingly occurred every other heart cycle.
3. **ECG-gated rhythmic handgrip exercise at 20% MVC (HGEX):** In order to determine each participant's exercise intensity, while in the supine position but prior to beginning the rest period, participants performed two MVCs with their left hand on

a handgrip dynamometer connected to a commercially-available data acquisition unit (Powerlab model ML795, AD Instruments, Colorado Springs, CO, USA). If the two measurements differed by 5%, a third was performed. All measurements collected were averaged to yield a single MVC value, which was used to determine 20% of MVC. During the intervention, participants were instructed to alternate contraction and relaxation on the handgrip dynamometer in the same duty cycle as the CUFF intervention with visual feedback of force production from our data acquisition software (Labchart).

2.2.4 Outcome Measures

2.2.4.1 Hematocrit

After cleansing the right index finger with an alcohol swab, a lancet was used to prick the outer edge of the finger. Each of the two capillary tubes were then held at a 45° angle against the finger to collect blood until they were approximately two-thirds full. Critoseal was used close off the opposite end of the tube. Tubes were spun to allow for separation of whole blood components, and a manual hematocrit reader (Adams Micro-Hematocrit Reader, ClayAdams, Parsippany, NJ, USA) was used to determine the percentage of red blood cells in the samples.

2.2.4.2 Blood velocity and diameter

BA diameters and blood velocities were assessed before and during (immediately prior to termination of) each of the interventions using 2D Doppler ultrasonography

(Vivid q, GE Medical Systems) with a 12 MHz linear array probe for 30 seconds at 7.7 fps. Images were saved in DICOM format and analyzed off-line using semi-automated edge-tracking software (Arterial Measurement System, Gothenburg, Sweden) to determine arterial diameter. Blood velocity profiles were analyzed on a pixel-based tracking software to determine mean blood velocity (Measurements from Arterial Ultrasound Imaging software, Hedgehog Medical).

2.2.4.3 Blood flow turbulence

Blood flow turbulence, quantified by Reynolds number (Re), was calculated before and during each of the interventions. Re is a dimensionless ratio of blood inertial forces to viscous forces, expressed with the formula: $Re = (V*D*\rho)/\mu$, where V is peak blood flow velocity, D is artery diameter, ρ is blood density, and μ is blood viscosity (13). Blood density was calculated using the equation: $\rho = [1.09Hct + 1.035 \times (1-Hct)]$, where hematocrit is expressed as a fraction; and blood viscosity was calculated using the equation: $\mu = \mu_{plasma} \times \exp(2.31Hct)$, where $\mu_{plasma} = \exp[-5.64 + (1800/(T+ 273))]/SR$, where plasma viscosity is expressed in $10^{-1}Nm^{-2}$ per s, T is temperature expressed in °C, and SR is shear rate is s^{-1} (if <100, SR = 8*V/D; if ≥100, SR = 100). Blood flow was considered laminar when Re < |2000| and turbulent when Re ≥ |2000|.

2.2.4.4 Endothelial shear stress and oscillatory shear index

Endothelial shear stress, the tangential force of blood flow against the arterial wall, was calculated before and during each of the interventions as follows: ESS =

2*μ*V/D, where μ is blood viscosity, V is blood velocity, and D is artery diameter (13). Oscillatory shear index, a measure of the magnitude of shear oscillation or reversal, was calculated using the formula: OSI = |Retrograde SR|/(|Retrograde SR| + |Anterograde SR|), where SR = 8*V/D is shear rate in s^{-1} (20, 32). A value of 0.5 indicates purely oscillatory flow.

2.2.4.5 Flow-mediated dilation

FMD% was calculated for both CON and EXP limbs before and after each of the interventions according to the latest standard guidelines. Duplex ultrasound using a 12 MHz linear probe at 7.7 fps (Vivid q, GE Medical Systems) was used to simultaneously acquire B-mode images and blood velocity measurements at the BA, 5-10 cm proximal to the olecranon process. Prior to the application of the ischemic stimulus, baseline images were collected for a period of 30 seconds. A pneumatic cuff positioned on the distal forearm was inflated to an occlusion pressure of 200 mmHg (minimum 50 mmHg above systolic blood pressure) for 5 minutes, and then subsequently released while images were continuously collected for an additional 3 minutes during reactive hyperemia. Data analysis was similar to that of blood velocity and diameter, described in the subsection above.

2.2.5 Statistical Analysis

Statistical analyses were performed using IBM SPSS Statistics for Macintosh (version 20.0.0; IBM Comp., Armonk, N.Y., USA). Normality was assessed with the

Shapiro-Wilk test, and homogeneity of variance was assessed with Mauchly's test of sphericity. A 2x2 (limb x time) repeated measures ANOVA was used to compare all outcome measures before and during or after each intervention. Tukey's HSD was used as a post-hoc analysis for significant interactions. To examine the relationship between ΔOSI and ΔFMD%, a robust regression was run with the vce(cluster) function on STATA (version 14.2; College Station, TX, USA) to account for a violation of the assumption of independence by adjusting the standard error of the model predictors. For all statistical tests, significance was set at $\alpha = 0.05$.

Use of ratio statistics such as FMD% is appropriate only if the fundamental assumption of unity is satisfied, meaning that the relationship between the numerator and denominator is a straight line through the origin. Otherwise, allometric scaling should be performed to avoid over- or underestimation of FMD% values from arteries of different sizes (1). To confirm that this type of analysis was required for our data set, linear regression analyses were performed to determine the slope and 95% confidence intervals of the relationship between the natural log of peak arterial diameter (lnD_{peak} dependent variable) and baseline arterial diameter (lnD_{base}, independent variable) for each limb (CON and EXP). Allometric scaling was warranted if the unstandardized β coefficient deviated from 1 and/or the 95% CI had an upper limit < 1, indicating that peak arterial diameter did not increase as a constant proportion of baseline arterial diameter. A generalized estimating equations analysis with an exchangeable correlation structure was performed with lnD_{diff} (i.e. $lnD_{peak} - lnD_{base}$) as the dependent variable, time (Pre *vs.* Post) and limb (CON *vs.* EXP) as the within-subject factors, and lnD_{base} as the predictor.

Fisher's LSD test was used as a posthoc for significant interactions. For each intervention, limb- and time-specific estimated means (EM) were back transformed to obtain scaled FMD $[(e^{EM}-1)\times 100]$, and estimated standard errors (SE) were back transformed and used to estimate standard deviations $[((e^{SE}-1)\times 100)\times(\sqrt{n})]$, where *n* is the group sample size.

2.3 Results

Participant characteristics are outlined in **Table 1**. All individuals recruited were young, normal weight, and normotensive. In addition, there were no differences in resting blood pressure and heart rate between visits ($p > 0.05$).

2.3.1 Effect of passive heat stress

HEAT increased HR during the intervention, and MAP and DBP after the intervention ($P < 0.05$) (**Table 2**). Core temperature did not change throughout the intervention. Skin temperature increased with HEAT in EXP (rest: 33.7 ± 0.8 *vs.* HEAT: 42.0 ± 0.8 °C, $P < 0.05$), as expected, but was also different between CON and EXP at rest (32.5 ± 0.9 *vs.* 33.7 ± 0.8 °C, $P < 0.05$). Anterograde blood flow increased (rest: 95.2 ± 30.0 *vs.* HEAT:126.9 ± 42.1 cm^3/min, $P < 0.05$) while retrograde blood flow decreased (rest: -17.4 ± 9.1 *vs.* HEAT: -8.8 ± 5.5 cm^3/min, $P < 0.05$) in EXP, but not CON, with HEAT (**Table 5**). Re increased in anterograde flow (rest: 1358 ± 467 *vs.* HEAT: 2120 ± 678, $P < 0.05$) and decreased in retrograde flow (rest: -241 ± 126 *vs.* HEAT: -144 ± 84, $P < 0.05$) in EXP only; but blood flow was only considered turbulent in the anterograde

direction (**Table 5**). Anterograde shear stress increased with the HEAT condition in EXP (rest: 15.2 ± 2.9 *vs.* HEAT: 29.8 ± 8.5 dynes/cm^2, P < 0.05), with no effect to CON (**Figure 1A**). Meanwhile, scaled FMD% increased in both limbs (P = 0.000) after the intervention, and values from CON were lower than that from EXP (P = 0.000) (**Figure 1A**).

2.3.2 Effect of ECG-gated cuff compressions

CUFF did not change any central hemodynamic measures (**Table 3**). Neither core temperature nor skin temperature changed throughout the intervention. Anterograde (rest: 99.1 ± 44.3 *vs.* CUFF: 168.5 ± 42.8 cm^3/min, P < 0.05) and retrograde (rest: -14.3 ± 6.7 *vs.* CUFF: -90.1 ± 26.1 cm^3/min, P < 0.05) blood flow increased in EXP and not CON with CUFF (**Table 5**). While Re increased in both anterograde (rest: 1434 ± 678 *vs.* CUFF: 2814 ± 626, P < 0.05) and retrograde (rest: -202 ± 100 *vs.* CUFF: -1488 ± 306, P < 0.05) flows in EXP, only that in the anterograde direction became turbulent with the intervention (**Table 5**). CON did not generate any changes in Re with the intervention. Additionally, although flow was considered laminar in both limbs, anterograde Re was greater in EXP compared to the control limb at baseline (rest: 1434 ± 678 *vs.* CUFF: 890 ± 341, P < 0.05) (**Table 5**). CUFF increased anterograde (rest: 17.9 ± 4.1 *vs.* CUFF: 43.0 ± 12.4 dynes/cm^2, P < 0.05) and retrograde (rest: -3.1 ± 2.5 *vs.* CUFF: -22.7 ± 6.0 dynes/cm^2, P < 0.05) shear stress in EXP, with no effect to CON (**Figure 1B**). There was no change in scaled FMD% from pre to post intervention (p = 0.248); however, the values from CON were lower than that from EXP (p = 0.000) (**Figure 1B**).

2.3.3 Effect of ECG-gated rhythmic handgrip exercise

HGEX increased HR during the intervention, and MAP during and after the intervention ($P < 0.05$) (**Table 4**). Core temperature did not change throughout the intervention. Skin temperature increased from rest to during HGEX in EXP (rest: 33.7 ± 1.1 *vs.* HGEX: 34.6 ± 1.3 °C, $P < 0.05$), but was also different between CON and EXP at rest (32.6 ± 1.0 *vs.* 33.7 ± 1.1 °C, $P < 0.05$). Anterograde (rest: 103.5 ± 34.0 *vs.* HGEX: 364.0 ± 111.7 cm^3/min, $P < 0.05$) and retrograde (rest: -16.7 ± 10.0 *vs.* HGEX: -35.5 ± 16.7 cm^3/min, $P < 0.05$) blood flow increased in EXP, but not CON with HGEX (**Table 5**). In only EXP, Re increased in both anterograde (rest: 1498 ± 438 *vs.* HGEX: 5114 ± 1219, $P < 0.05$) and retrograde (rest: -231 ± 117 *vs.* HGEX: -504 ± 236, $P < 0.05$) flows (**Table 5**). Once again, only anterograde blood flow became turbulent with the 10-minute intervention. Anterograde shear stress increased (rest: 18.7 ± 5.9 *vs.* HGEX: 56.4 ± 11.5 dynes/cm^2, $P < 0.05$) while retrograde shear stress remained unchanged in EXP. No changes in shear stress were observed in CON (**Figure 1C**). Scaled FMD% increased from pre to post intervention in both limbs ($P = 0.001$), but values from CON were lower than that from EXP ($P = 0.000$) (**Figure 1C**).

2.3.4 Relationship between OSI and FMD%

Robust regression analysis on the EXP limb data revealed no significant association between ΔOSI (independent variable) and ΔFMD% (dependent variable)

when the interventions were pooled, suggesting that changes in oscillatory shear index are not associated with changes in FMD% ($P = 0.98$) (**Figure 2**).

Table 1. Participant Characteristics

N = 10			**HEAT**	**CUFF**	**HGEX**
Age (yrs)	22 ± 3				
Height (m)	1.78 ± 0.05	SBP (mmHg)	121 ± 10	121 ± 12	120 ± 8
Weight (kg)	82.2 ± 16.3	DBP (mmHg)	65 ± 6	65 ± 8	66 ± 6
BMI (kg/m^2)	25.8 ± 4.5	MAP (mmHg)	86 ± 5	87 ± 8	87 ± 5
MVC (N)	520.6 ± 112.2	HR (bpm)	60 ± 6	62 ± 6	62 ± 8

All values are expressed in mean ± SD. BMI = body mass index; MVC = maximum voluntary contraction; SBP = systolic blood pressure; DBP = diastolic blood pressure; MAP = mean arterial pressure; HR = heart rate.

Table 2. Central Hemodynamics with HEAT

	PRE	DURING	POST	P value
SBP (mmHg)	130 ± 12	136 ± 17	136 ± 9	0.178
DBP (mmHg)	75 ± 7	78 ± 11	80 ± 8	0.015*
MAP (mmHg)	94 ± 9	97 ± 11	100 ± 10	0.015*
HR (bpm)	60 ± 7	64 ± 8	61 ± 5	0.008*
SV (mL)	100.8 ± 17.8	100.6 ± 18.3	103.6 ± 19.1	0.268
CO (L/min)	6.1 ± 1.1	6.5 ± 1.5	6.3 ± 1.4	0.106

All values are expressed in mean ± SD. SBP = systolic blood pressure; DBP = diastolic blood pressure; MAP = mean arterial pressure; HR = heart rate; SV = stroke volume; CO = cardiac output. *Significant main effect of time.

Table 3. Central Hemodynamics with CUFF

	PRE	DURING	POST	P value
SBP (mmHg)	143 ± 22	147 ± 20	147 ± 20	0.460
DBP (mmHg)	85 ± 15	87 ± 13	88 ± 11	0.312
MAP (mmHg)	105 ± 18	107 ± 16	109 ± 14	0.379
HR (bpm)	61 ± 5	62 ± 5	58 ± 5	0.105
SV (mL)	98.4 ± 15.6	97.7 ± 16.4	96.2 ± 14.1	0.547
CO (L/min)	6.1 ± 1.2	6.1 ± 1.1	5.8 ± 0.9	0.391

All values are expressed in mean ± SD. SBP = systolic blood pressure; DBP = diastolic blood pressure; MAP = mean arterial pressure; HR = heart rate; SV = stroke volume; CO = cardiac output.

Table 4. Central Hemodynamics with HGEX

	PRE	DURING	POST	P value
SBP (mmHg)	130 ± 9	135 ± 15	139 ± 10	0.064
DBP (mmHg)	75 ± 5	79 ± 9	80 ± 7	0.106
MAP (mmHg)	93 ± 5	101 ± 10	101 ± 8	0.022*
HR (bpm)	61 ± 7	73 ± 8	65 ± 8	0.003*
SV (mL)	99.3 ± 26.7	97.1 ± 29.8	98.0 ± 25.0	0.678
CO (L/min)	6.1 ± 1.9	7.0 ± 2.3	6.5 ± 1.8	0.097

All values are expressed in mean ± SD. SBP = systolic blood pressure; DBP = diastolic blood pressure; MAP = mean arterial pressure; HR = heart rate; SV = stroke volume; CO = cardiac output. *Significant main effect of time.

Table 5. Blood Flow and Turbulence

	CONTROL		EXPERIMENTAL	
	PRE	DURING	PRE	DURING
HEAT				
BF (cm^3/min)				
Anterograde	80.7 ± 20.5	81.2 ± 28.8	95.2 ± 30.0	126.9 ± 42.1*†
Retrograde	-19.6 ± 11.4	-19.8 ± 8.1	-17.4 ± 9.1	-8.8 ± 5.5*†
Re				
Anterograde	1030 ± 265	1016 ± 436	1358 ± 467	2120 ± 678*†
Retrograde	-246 ± 135	-243 ± 107	-241 ± 126	-144 ± 84*†
CUFF				
BF (cm^3/min)				
Anterograde	70.4 ± 21.9	68.4 ± 20.0	99.1 ± 44.3†	168.5 ± 42.8*†
Retrograde	-13.7 ± 6.8	-16.1 ± 8.5	-14.3 ± 6.7	-90.1 ± 26.1*†
Re				
Anterograde	890 ± 341	760 ± 229	1434 ± 678†	2814 ± 626*†
Retrograde	-173 ± 100	-176 ± 86	-202 ± 100	-1488 ± 306*†
HGEX				
BF (cm^3/min)				
Anterograde	80.8 ± 37.3	88.4 ± 33.3	103.5 ± 34.0	364.0 ± 111.7*†
Retrograde	-19.7 ± 12.7	-15.6 ± 14.2	-16.7 ± 10.0	-35.5 ± 16.7*†
Re				
Anterograde	984 ± 492	1214 ± 410	1498 ± 438	5114 ± 1219*†
Retrograde	-221 ± 125	-207 ± 174	-231 ± 117	-504 ± 236*†

All values are expressed as mean ± SD. BF = blood flow; Re = Reynolds number.
*Different from PRE, †Different from CON

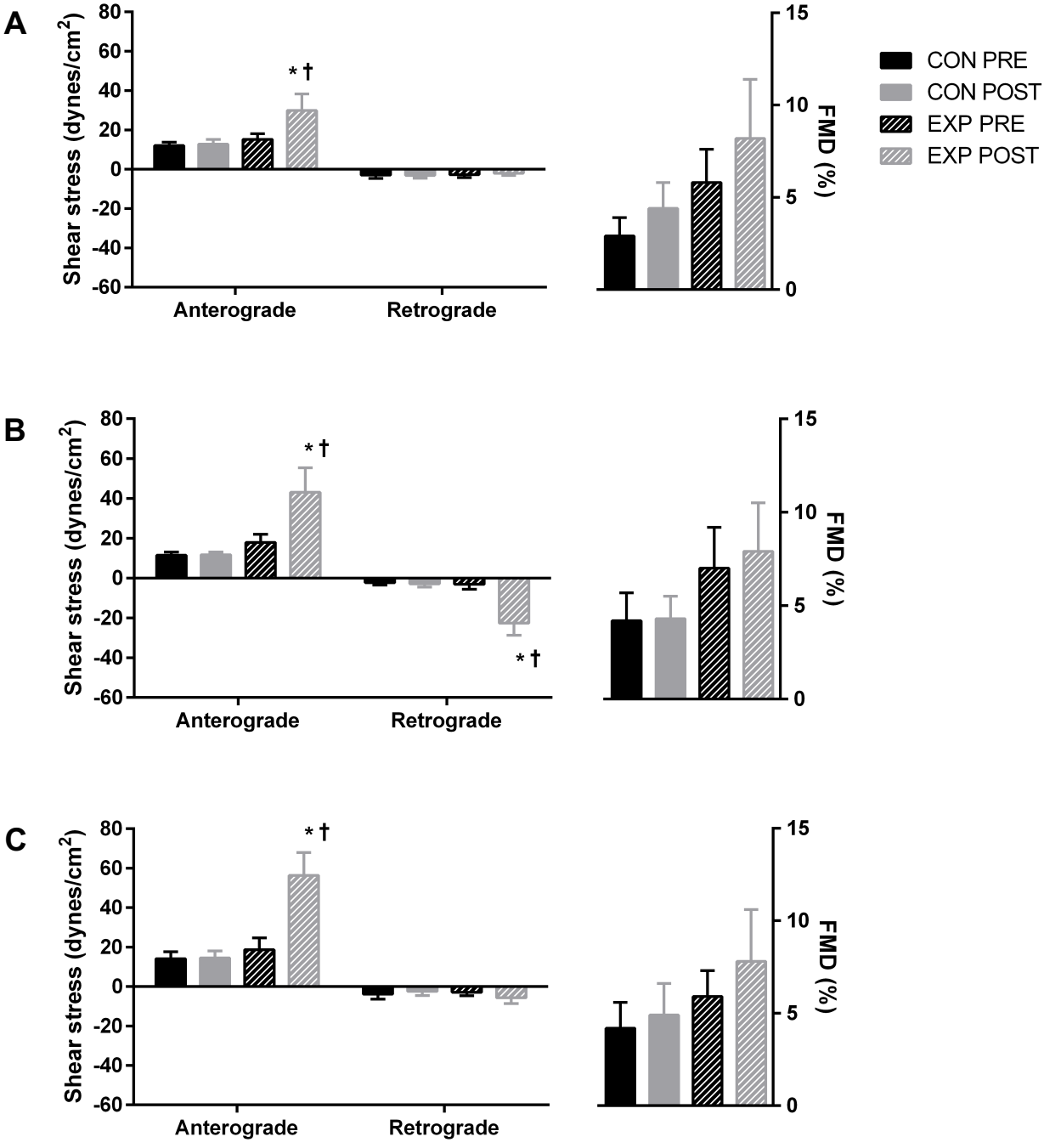

Figure 1. Shear stress and endothelial function responses to (A) HEAT, (B) CUFF, and (C) HGEX. Solid bars represent the control limb (CON), dashed bars represent the experimental limb (EXP); black bars represent the pre-intervention timepoint (PRE), gray bars represent the during or post-intervention timepoint (POST). *Different from PRE, †Different from CON. For FMD%, a main effect of limb was observed in all 3 interventions; whereas a main effect of time was only observed for HEAT and HGEX.

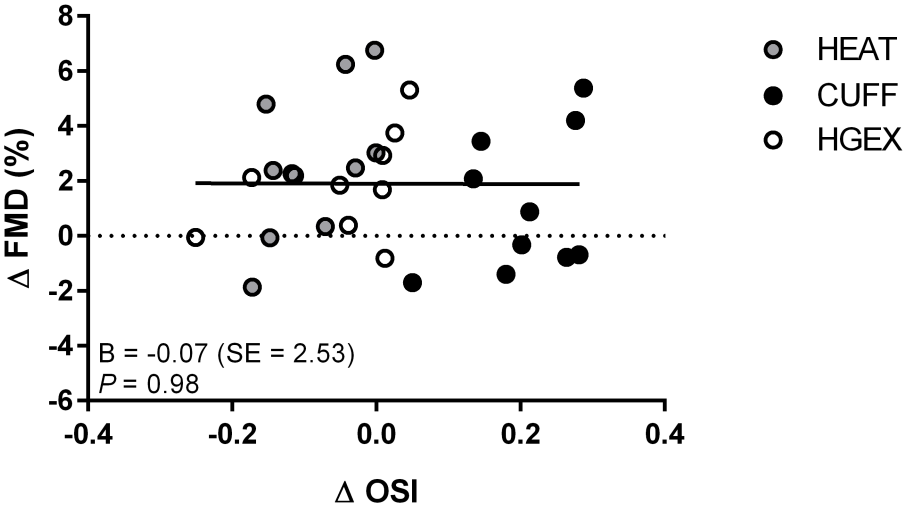

Figure 2. Relationship between the change in oscillatory shear index (ΔOSI) and the change in relative flow-mediated dilation (ΔFMD%) in the pooled data from the EXP limb.

2.4 Discussion

In the current study, we sought to determine the shear stress and endothelial function responses to different stimuli designed to alter blood flow patterns in the BA. The main findings of this study are four-fold: (1) HEAT is an anterograde-dominant shear stress stimulus that acutely improves FMD% locally and systemically; (2) CUFF is a high shear stress oscillatory stimulus that that does not change FMD%; (3) HGEX is an anterograde-dominant shear stress stimulus that acutely improves FMD% locally and systemically; and (4) change in OSI, an index of the oscillatory nature of blood flow, is not associated with change in FMD%. In agreement with the current general consensus, it appears unopposed anterograde shear increases are linked to acute endothelial function increases. However, these results also suggest that although shear stress pattern is an

important determinant of endothelial function, other factors such as stress duration or sympathetic activation, may favour alternate control mechanisms.

In designing our study, we aimed to create controlled shear stress conditions within the artery, wherein anterograde shear magnitude is matched between interventions, to isolate the role of shear direction and pattern on endothelial function. On the whole, our interventions were successful at eliciting the desired shear stress profiles; however, we did not anticipate that any of our interventions would have systemic impacts on the control limb. The HEAT intervention was an anterograde-dominant shear stimulus, approximately doubling the anterograde shear stress through the BA, similar to previous literature (28, 29). We demonstrated that FMD% improves acutely after a single bout of HEAT, which agrees with a previous report (29). The increase in FMD% with heating has often been attributed to elevated anterograde shear rate (29); however, we also observed an FMD% increase in the control limb, which did not experience any changes in shear stress, suggesting that other factors may be involved in the acute FMD% response. Currently, there is no consensus on the regulation of the acute effect of heating on endothelial function as the immediate control mechanisms that take place within the artery are unknown. For instance, a recent study did not observe a change in FMD% despite heating a much greater proportion of body mass. Their protocol should have activated moderate to high skin thermoregulatory mechanisms to maintain homeostasis (28). It should be noted that the heating protocols used in all 3 studies were vastly different: 40 ± 1.0 °C bilateral water immersion for 30 minutes in Tinken *et al* (2009) *vs.* 42 ± 0.4 °C lower limb water immersion for 30 minutes in Thomas *et al* (2016) *vs.* 42 ±

0.8 °C unilateral heating with a heating blanket for 10 minutes in the current study. For the duration and localization of heating in our protocol, it is likely that we only reached the initial phase of the skin blood flow response, which involves only cutaneous vasoconstrictor and vasodilator nerve activity (17, 24). At this stage, the increase in skin blood flow is caused by antidromic neurotransmitter release from sensory afferents that are mediated by temperature-sensitive vanilloid type I receptors (18). Active vasodilator pathways involving the generation and release of NO, which may further enhance vasodilatory capacity, are not involved at this point, supporting the hypothesis that alternative mechanisms are likely responsible for the observed acute increase in FMD% with our protocol. Of the 3 available studies to date, only our study included a within-subject control limb that clarified the systemic effects of a heat intervention. We also observed increases in blood pressure after HEAT that are typically linked to SNS-mediated vasoconstriction and consequent decreased FMD%. Although BA diameter decreased in EXP during the intervention (4.5 ± 0.4 *vs.* 3.9 ± 0.3 cm, $P < 0.05$), it returned to approximate the resting value by the post-intervention time point, suggesting some vasoconstriction but perhaps not enough to affect FMD%. Indeed, the increase rather than decrease in FMD% in the presence of SNS activation contradicts our current understanding of the relationship between these variables and supports an insufficiency hypothesis.

With the CUFF intervention, we were able to achieve our goal of creating a well-controlled high shear stress oscillatory stimulus. That is, CUFF generated increases in both the anterograde and retrograde directions, while FMD%, blood pressure, cardiac

output, heart rate stroke volume, core and skin temperatures remained unchanged. The absolute level of anterograde shear stress in CUFF appeared to be slightly greater than that achieved with HEAT. Compared to ECP therapy, which was our model stimulus, CUFF increased retrograde shear stress at the BA whereas ECP did not (13). Site-specific differences in the normal flow pattern and proximity of the intervention to the measurement site in the CUFF condition are likely responsible for this dissimilarity. As a novel stimulus, it is difficult to hypothesize the reason for the lack of change in FMD%; however, the brief intervention duration of 10 minutes may not have been sufficient to elicit the expected short-term change in endothelial function. Our results clearly demonstrate that a high shear stress oscillatory pattern applied for 10 minutes, without alterations to neural or metabolic state, does not change FMD%.

Our HGEX protocol did not create an oscillatory shear stress pattern, as we expected; rather, it increased anterograde shear stress alone to a level that appeared to be much greater than in HEAT. Although not typically associated with rhythmic exercise, this shear stress pattern has been observed before, in a study comparing the effects of 30 minutes of handgrip exercise with fast or slow contraction velocity on FMD%. Specifically, researchers found that the slow contractions produced an anterograde-dominant hemodynamic stimulus through the brachial artery that reduced FMD%. Despite a similar shear stress pattern to this previous work, we observed an improvement in FMD% in both the control and experimental limbs with a shorter period of exercise. As with HEAT, other factors are likely at play in this particular response, since an improvement in FMD% was observed in the CON limb in which shear stress was

unchanged. Similar to HEAT, MAP was elevated post-intervention, which is typically a trigger for the SNS to increase vasoconstrictor tone and negatively impact endothelial function. In contrast to HEAT, BA diameter increased in EXP (4.4 ± 0.5 *vs.* 4.6 ± 0.4 cm, $P < 0.05$), a finding that is typical as the body works to redirect blood flow from other vascular beds to the working muscle. This key difference may explain the increase in FMD% with HGEX but not with HEAT. HGEX is also the only one of the 3 interventions to increase metabolic demand at the forearm muscle, which may have also influenced the FMD% response. Though the acute vascular effects of physical exercise are not as well established, training improves endothelial function by increasing superoxide dismutase and decreasing NADPH oxidase, both of which act to reduce ROS that tend to interfere with NO bioavailability and action (9). As recommended by the Canadian Physical Activity Guidelines and supported by a recent large population study, accruing physical activity in 10-minute bouts is similarly beneficial as longer sessions for maintaining a healthy CVD risk profile (11). Therefore, the HGEX protocol used in our study may have been a sufficient multi-system stimulus to acutely improve FMD%.

Based on our findings, it may appear that an anterograde-dominant shear stress stimulus (i.e. HEAT, HGEX) improves FMD% both locally and systemically while an oscillatory high shear stress stimulus (i.e. CUFF) does not change FMD%. However, the confounding effect of HR and BP changes in the anterograde-dominant shear interventions precludes us from making a definitive conclusion. Aside from the type of shear pattern produced, HEAT and HGEX increased HR during the interventions, which were no longer significant at the post-intervention FMD assessment timepoint.

Sympathetic nervous system activity is closely linked to endothelial function through common mediators NO, reactive oxygen species (ROS), endothelin-1 (ET-1), and the renin-angiotensin system (RAAS) (3). NO, a key molecule in vascular endothelial function, plays a critical role in subduing sympathetic outflow. Endogenous NO production suppresses the SNS, as observed in experiments where BP and HR rise in response to NO blockade (6, 16, 23). On the other hand, ROS, ET-1, and angiontensin II (RAAS) potentiate sympathetic outflow that leads to increased HR, BP, and vascular tone (3). The relationship between the chronically elevated SNS activation and long-term endothelial dysfunction is one that is clear based on population studies have shown its shared prevalence in many chronic conditions and diseases. However, although some research groups have attempted to investigate the endothelial function responses to brief sympathoexcitatory stimuli, which is most relevant to the interventions in our study, the literature is unclear (10, 15, 25, 33). It is possible withdrawal of sympathetic activity after HEAT and HGEX, even after only a brief period of HR elevation, transiently enhanced NO bioavailability to cause improved endothelial function.

Another consequence of sympathetic activation may be the attenuation of retrograde shear stress during HGEX. We observed in our study that HGEX increased MAP during the intervention. Previous research has demonstrated that the MSNA-associated increase in retrograde shear rate is attenuated by concurrent increases in MAP, a finding that may explain the lack of observed increases in retrograde shear stress during HGEX that we hypothesized would occur (21). Whether or not the diminished retrograde

shear response had an effect on the FMD% response is unclear, but it is something to consider when interpreting the results from interventions that concurrently change MAP.

Limitations and Future Directions

Our study had several limitations that we wish to address in future investigations. First, although the brief intervention time was sufficient to cause changes in endothelial function in HEAT and HGEX conditions, 10 minutes is not representative of the typical duration of activity that humans would experience in their day-to-day lives. More often, interventions such as exercise are performed in 30 to 60-minute bouts, as modeled in other similarly designed studies. Moreover, some stimuli activate time-dependent regulatory mechanisms, resulting in flow and shear responses that differ greatly for short- and long-duration interventions. For example, NO-mediated maximum skin blood flow due to heating is only achieved after 35-55 minutes (18). Therefore, for widespread applicability and comparison to previous work, longer intervention durations of at least 30 minutes should be used in future studies. Second, in the interest of simplifying our study design, we did not randomize limbs to the control and experimental conditions. That is, in all participants and for all visits, the right arm served as the control limb and the left arm served as the experimental limb. Our results show that there are between-limb differences in arterial diameter, such that brachial arteries from the right arm are larger than the left arm, possibly due to handedness. Furthermore, for all 3 interventions, there was a main effect of limb for FMD% where the control limb values were smaller than the experimental limb values. Since baseline arterial diameter is responsible for 64% of the

variability in the FMD response, the difference in this measure may have confounded our results (1, 5). Randomizing limb between participants, but not between visits, is an easy way to avoid this issue altogether. Third, upon deciding to use the right arm as a within-subject time control during the interventions, we assumed that this limb would be completely unaffected by the intervention applied to the experimental limb. Although alterations in blood flow and shear stress parameters were successfully isolated to the experimental limb during the intervention, our findings of a main effect of time for FMD% in HEAT and HGEX suggest that there may be crossover effects at play in these interventions. Sympathetic activation, as evidenced by increases in HR and BP, has a systemic effect, which in turn may have had a transient endothelial function effect on the control limb. Adding a fourth visit where the intervention is 10 minutes of supine rest will allow for the examination of a true time control, without the confounding effect of neural modulation.

Conclusion

Although at first glance, anterograde-dominant shear stress patterns appear to result in the greatest improvements in endothelial function, for shorter duration interventions such as the ones explored in this study, neuromodulation through the sympathetic nervous system may be the dominant regulatory system in these conditions. Specifically, sympathetic withdrawal as demonstrated by heart rate recovery to resting levels after HEAT and HGEX interventions, prior to FMD assessment may have a

positive, transient effect on NO bioavailability that influences the capacity of the artery to dilate shortly thereafter.

2.5 References

1. **Atkinson G**, **Batterham AM**, **Thijssen DHJ**, **Green DJ**. A new approach to improve the specificity of flow-mediated dilation for indicating endothelial function in cardiovascular research. *J Hypertens* 31: 287–91, 2013.
2. **Birk G**, **Dawson E**, **Atkinson C**, **Haynes A**, **Cable N**, **Thijssen D**, **Green D**. Brachial artery adaptation to lower limb exercise training: role of shear stress. *J Appl Physiol* 112: 1653–1658, 2012.
3. **Bruno RM**, **Ghiadoni L**, **Seravalle G**, **Dell'Oro R**, **Taddei S**, **Grassi G**. Sympathetic regulation of vascular function in health and disease. *Front Physiol* 3: 1–15, 2012.
4. **Carter HH**, **Dawson EA**, **Birk GK**, **Spence AL**, **Naylor LH**, **Cable NT**, **Thijssen DHJ**, **Green DJ**. Effect of SR manipulation on conduit artery dilation in humans. *Hypertension* 61: 143–150, 2013.
5. **Corretti MC**, **Anderson TJ**, **Benjamin EJ**, **Celermajer D**, **Charbonneau F**, **Creager MA**, **Deanfield J**, **Drexler H**, **Gerhard-Herman M**, **Herrington D**, **Vallance P**, **Vita J**, **Vogel R**. Guidelines for the ultrasound assessment of endothelial-dependent flow-mediated vasodilation of the brachial artery: A report of the international brachial artery reactivity task force. *J Am Coll Cardiol* 39: 257–265, 2002.
6. **Cunha RS**, **Cabral AM**, **Vasquez EC**. Evidence that the autonomic nervous system plays a major role in the L-NAME-induced hypertension in conscious rats. *Am J Hypertens* 6: 806–809, 1993.

7. **Currie KD**, **McKelvie RS**, **MacDonald MJ**. Flow-mediated dilation is acutely improved after high-intensity interval exercise. *Med Sci Sports Exerc* 44: 2057–2064, 2012.

8. **Deanfield JE**, **Halcox JP**, **Rabelink TJ**. Endothelial function and dysfunction: Testing and clinical relevance. *Circulation* 115: 1285–1295, 2007.

9. **Di Francescomarino S**, **Sciartilli A**, **Di Valerio V**, **Di Baldassarre A**, **Gallina S**. The effect of physical exercise on endothelial function. *Sports Med* 39: 797–812, 2009.

10. **Ghiadoni L**, **Donald a E**, **Cropley M**, **Mullen MJ**, **Oakley G**, **Taylor M**, **O'Connor G**, **Betteridge J**, **Klein N**, **Steptoe a**, **Deanfield JE**. Mental stress induces transient endothelial dysfunction in humans. *Circulation* 102: 2473–2478, 2000.

11. **Glazer NL**, **Lyass A**, **Esliger DW**, **Blease SJ**, **Freedson PS**, **Massaro JM**, **Murabito JM**, **Vasan RS**. Sustained and Shorter Bouts of Physical Activity are Related to Cardiovascular Health. *Med Sci Sport Exer* 45: 109–115, 2013.

12. **Gonzales JU**, **Thompson BC**, **Thistlethwaite JR**, **Scheuermann BW**. Association between exercise hemodynamics and changes in local vascular function following acute exercise. *Appl Physiol Nutr Metab* 36: 137–144, 2011.

13. **Gurovich AN**, **Braith RW**. Enhanced external counterpulsation creates acute blood flow patterns responsible for improved flow-mediated dilation in humans. *Hypertens Res* 36: 1–9, 2013.

14. **Harris RA**, **Padilla J**, **Hanlon KP**, **Rink LD**, **Wallace JP**. The flow-mediated

dilation response to acute exercise in overweight active and inactive men. *Obesity* 16: 578–584, 2008.

15. **Hijmering ML**, **Stroes ESG**, **Olijhoek J**, **Hutten BA**, **Blankestijn PJ**, **Rabelink TJ**. Sympathetic activation markedly reduces endothelium-dependent, flow-mediated vasodilation. *J Am Coll Cardiol* 39: 683–688, 2002.
16. **Huang M**, **Leblanc ML**, **Hester RL**. Systemic and regional hemodynamics after nitric oxide synthase inhibition: role of a neurogenic mechanism. *Am J Physiol* 267: R84–R88, 1994.
17. **Kamijo Y-I**, **Lee K**, **Mack GW**. Active cutaneous vasodilation in resting humans during mild heat stress. *J Appl Physiol* 98: 829–837, 2005.
18. **Kellogg DL**. In vivo mechanisms of cutaneous vasodilation and vasoconstriction in humans during thermoregulatory challenges. *J Appl Physiol* 100: 1709–1718, 2006.
19. **Li YSJ**, **Haga JH**, **Chien S**. Molecular basis of the effects of shear stress on vascular endothelial cells. *J Biomech* 38: 1949–1971, 2005.
20. **Newcomer SC**, **Sauder CL**, **Kuipers NT**, **Laughlin MH**, **Ray CA**. Effects of posture on shear rates in human brachial and superficial femoral arteries. *Am J Physiol Hear Circ Physiol* 294: H1833-9, 2008.
21. **Padilla J**, **Young CN**, **Simmons GH**, **Deo SH**, **Newcomer SC**, **Sullivan JP**, **Laughlin MH**, **Fadel PJ**. Increased muscle sympathetic nerve activity acutely alters conduit artery shear rate patterns. *Am J Physiol Hear Circ Physiol* 298: H1128-35, 2010.

22. **Reneman RS**, **Arts T**, **Hoeks APG**. Wall Shear Stress - an Important Determinant of Endothelial Cell Function and Structure - in the Arterial System in vivo. *J Vasc Res* 43: 251–269, 2006.

23. **Sander M**, **Hansen PG**, **Victor RG**. Sympathetically mediated hypertension caused by chronic inhibition of nitric oxide. [Online]. *Hypertension* 26: 691–695, 1995. http://www.ncbi.nlm.nih.gov/pubmed/7558232.

24. **Savage M V**, **Brengelmann GL**. Control of skin blood flow in the neutral zone of human body temperature regulation. [Online]. *J Appl Physiol* 80: 1249–57, 1996. http://www.ncbi.nlm.nih.gov/pubmed/8926253.

25. **Thijssen DH**, **de Groot P**, **Kooijman M**, **Smits P**, **Hopman MT**. Sympathetic nervous system contributes to the age-related impairment of flow-mediated dilation of the superficial femoral artery. *Am J Physiol Hear Circ Physiol* 291: H3122-9, 2006.

26. **Thijssen DHJ**, **Black M a**, **Pyke KE**, **Padilla J**, **Atkinson G**, **Harris R a**, **Parker B**, **Widlansky ME**, **Tschakovsky ME**, **Green DJ**. Assessment of flow-mediated dilation in humans: a methodological and physiological guideline. *Am J Physiol Heart Circ Physiol* 300: H2–H12, 2011.

27. **Thijssen DHJ**, **Dawson EA**, **Black MA**, **Hopman MTE**, **Cable NT**, **Green DJ**. Brachial artery blood flow responses to different modalities of lower limb exercise. *Med Sci Sports Exerc* 41: 1072–1079, 2009.

28. **Thomas KN**, **Rij AM van**, **Lucas SJE**, **Gray AR**, **Cotter JD**. Substantive hemodynamic and thermal strain upon completing lower-limb hot-water immersion;

comparisons with treadmill running. *Temperature* 8940, 2016.

29. **Tinken TM**, **Thijssen DHJ**, **Hopkins N**, **Black MA**, **Dawson EA**, **Minson CT**, **Newcomer SC**, **Laughlin MH**, **Cable NT**, **Green DJ**. Impact of shear rate modulation on vascular function in humans. *Hypertension* 54: 278–285, 2009.
30. **Tinken TM**, **Thijssen DHJ**, **Hopkins N**, **Dawson EA**, **Cable NT**, **Green DJ**. Shear stress mediates endothelial adaptations to exercise training in humans. *Hypertension* 55: 312–318, 2010.
31. **Topper JN**, **Gimbrone MAJ**. Blood flow and vascular gene expression: fluid shear stress as a modulator of endothelial phenotype. *Mol Med Today* 5: 40–46, 1999.
32. **Totosy de Zepetnek JO**, **Ditor DS**, **Au JS**, **Macdonald MJ**. Impact of shear rate pattern on upper and lower limb conduit artery endothelial function in both spinal cord-injured and able-bodied men. *Exp Physiol Exp Physiol Exp Physiol* 1001010: 1107–1117, 2015.
33. **Victor RG**, **Leimbach WN**, **Seals DR**, **Wallin BG**, **Mark AL**. Effects of the Cold Pressor Test on Muscle Sympathetic Nerve Activity in Humans. *Hypertension* 9: 429–436, 1987.
34. **Wang C**, **Baker BM**, **Chen CS**, **Schwartz MA**. Endothelial cell sensing of flow direction. *Arterioscler Thromb Vasc Biol* 33: 2130–2136, 2013.

APPENDIX A – Raw Data

Table A1. Resting blood pressure and heart rate (Dinamap)

HEAT				
	SBP (mmHg)	**DBP (mmHg)**	**MAP (mmHg)**	**HR (bpm)**
ASPEN01	131	60	87	70
ASPEN02	104	58	76	66
ASPEN03	119	70	90	66
ASPEN04	121	56	81	59
ASPEN05	130	68	93	60
ASPEN06	122	61	85	62
ASPEN07	125	67	88	55
ASPEN08	124	65	87	57
ASPEN09	128	75	94	51
ASPEN10	102	68	81	55
CUFF				
	SBP (mmHg)	**DBP (mmHg)**	**MAP (mmHg)**	**HR (bpm)**
ASPEN01	115	58	81	56
ASPEN02	115	60	81	63
ASPEN03	148	79	106	62
ASPEN04	123	60	85	74
ASPEN05	135	67	93	63
ASPEN06	108	60	77	60
ASPEN07	121	62	85	69
ASPEN08	119	57	83	62
ASPEN09	121	77	93	55
ASPEN10	109	70	84	53
HGEX				
	SBP (mmHg)	**DBP (mmHg)**	**MAP (mmHg)**	**HR (bpm)**
ASPEN01	112	58	80	55
ASPEN02	115	69	86	63
ASPEN03	118	65	86	73
ASPEN04	129	62	87	73
ASPEN05	121	63	86	69
ASPEN06	116	64	84	60
ASPEN07	127	72	93	59
ASPEN08	127	60	86	60
ASPEN09	127	77	96	51
ASPEN10	103	70	82	53

Table A2. Central Hemodynamics

HEAT																		
	SBP (mmHg)			**DBP (mmHg)**			**MAP (mmHg)**			**HR (bpm)**			**CO (L/min)**			**SV (mL)**		
	BL	**9 m**	**15 m**	**BL**	**9 m**	**15 m**	**BL**	**9 m**	**15 m**	**BL**	**9 m**	**15 m**	**BL**	**9 m**	**15 m**	**BL**	**9 m**	**15 m**
ASPEN01	129	141	140	68	74	77	87	93	102	65	70	66	8.6	9.9	9.5	137.0	138.0	140.0
ASPEN02	129	103	131	67	58	72	85	77	90	72	76	66	6.2	6.5	5.8	86.0	87.0	89.0
ASPEN03	124	135	131	82	87	85	98	105	102	68	72	65	6.1	6.4	6.2	90.0	84.0	93.0
ASPEN04	141	142	140	71	79	79	85	99	99	62	60	56	7.1	6.7	6.6	110.0	109.0	120.0
ASPEN05	122	139	134	75	82	77	91	99	96	57	64	62	4.9	5.5	5.7	82.0	90.0	94.0
ASPEN06	116	124	130	67	63	69	91	82	88	64	67	59	6.4	6.9	6.4	102.0	106.0	115.0
ASPEN07	143	161	136	82	87	86	101	112	109	61	68	65	6.5	7.7	7.4	112.0	115.0	112.0
ASPEN08	121	128	137	75	78	89	93	94	104	52	58	59	5.0	4.7	4.3	80.0	81.0	73.0
ASPEN09	153	159	157	89	95	96	113	112	121	50	54	55	5.6	6.0	6.5	114.0	111.0	107.0
ASPEN10	123	130	125	73	78	74	92	94	93	53	54	52	4.9	4.8	5.0	95.0	85.0	93.0
CUFF																		
	SBP (mmHg)			**DBP (mmHg)**			**MAP (mmHg)**			**HR (bpm)**			**CO (L/min)**			**SV (mL)**		
	BL	**9 m**	**15 m**	**BL**	**9 m**	**15 m**	**BL**	**9 m**	**15 m**	**BL**	**9 m**	**15 m**	**BL**	**9 m**	**15 m**	**BL**	**9 m**	**15 m**
ASPEN01	147	154	160	81	90	90	100	102	108	51	65	54	6.4	7.0	5.9	121.0	124.0	111.0
ASPEN02	140	126	133	78	69	76	95	87	95	69	64	61	7.9	6.1	5.5	98.0	93.0	90.0
ASPEN03	131	132	134	79	83	85	96	108	106	62	69	64	6.8	7.3	6.5	108.0	105.0	99.0
ASPEN04	154	168	158	86	89	88	112	113	113	62	67	60	7.7	7.5	7.0	113.0	110.0	118.0
ASPEN05	133	129	135	78	81	79	99	100	99	64	62	64	6.0	5.1	6.1	97.0	85.0	93.0
ASPEN06	127	137	125	69	76	77	84	90	92	59	57	50	5.9	6.5	5.9	105.0	105.0	103.0
ASPEN07	189	183	192	116	108	113	140	133	140	64	63	64	5.0	5.9	5.3	81.0	94.0	87.0
ASPEN08	109	123	136	72	73	85	89	89	100	63	63	60	5.8	5.6	5.5	93.0	86.0	85.0
ASPEN09	135	158	136	84	101	91	100	125	114	57	52	56	5.9	5.9	6.7	101.0	109.0	106.0
ASPEN10	164	158	157	106	99	99	133	119	120	60	57	51	3.9	3.7	3.6	67.0	66.0	70.0
HGEX																		
	SBP (mmHg)			**DBP (mmHg)**			**MAP (mmHg)**			**HR (bpm)**			**CO (L/min)**			**SV (mL)**		
	BL	**9 m**	**15 m**	**BL**	**9 m**	**15 m**	**BL**	**9 m**	**15 m**	**BL**	**9 m**	**15 m**	**BL**	**9 m**	**15 m**	**BL**	**9 m**	**15 m**
ASPEN01	139	148	147	79	85	82	98	107	104	62	60	66	7.9	7.5	8.2	126.0	132.0	129.0
ASPEN02	113	108	134	63	65	73	83	81	95	60	71	69	2.3	2.4	2.7	39.0	33.0	39.0
ASPEN03	129	145	132	76	88	77	95	110	93	72	79	68	8.9	9.0	8.3	128.0	114.0	121.0
ASPEN04	135	147	141	73	77	74	96	99	97	75	82	79	8.2	8.6	9.0	111.0	105.0	106.0
ASPEN05	128	123	127	79	74	73	91	92	90	58	66	75	5.4	5.6	6.9	80.0	82.0	92.0
ASPEN06	126	150	146	74	87	91	92	113	113	56	79	58	5.1	6.8	6.2	96.0	93.0	100.0
ASPEN07	135	120	154	73	67	87	94	98	108	58	82	58	6.6	9.6	6.8	111.0	117.0	118.0
ASPEN08	122	129	133	75	85	79	88	102	95	56	70	61	4.9	5.4	5.6	88.0	79.0	93.0
ASPEN09	143	147	149	81	83	88	103	105	111	51	68	54	5.9	8.1	5.6	120.0	119.0	95.0
ASPEN10	125	n.d.	126	74	n.d.	80	92	n.d.	100	60	n.d.	58	5.5	n.d.	5.2	94.0	n.d.	87.0

Table A3. Core Temperature (°C)

HEAT			
	BL	**9 m**	**15 m**
ASPEN01	37.6	37.1	36.8
ASPEN02	37.5	36.3	37.1
ASPEN03	37.4	37.4	37.4
ASPEN04	36.9	37.0	36.8
ASPEN05	36.2	36.2	36.1
ASPEN06	36.8	36.6	36.6
ASPEN07	36.6	36.6	36.5
ASPEN08	37.0	37.0	37.1
ASPEN09	37.0	36.7	36.7
ASPEN10	37.0	37.0	36.6
CUFF			
	BL	**9 m**	**15 m**
ASPEN01	37.3	37.2	36.9
ASPEN02	36.7	37.0	36.8
ASPEN03	36.8	36.3	36.5
ASPEN04	37.0	37.1	37.4
ASPEN05	36.3	36.2	36.3
ASPEN06	36.3	36.2	36.1
ASPEN07	37.0	37.1	37.1
ASPEN08	36.9	37.3	36.8
ASPEN09	37.0	36.8	36.7
ASPEN10	37.3	37.2	37.1
HGEX			
	BL	**9 m**	**15 m**
ASPEN01	37.3	37.2	36.8
ASPEN02	37.2	36.7	36.6
ASPEN03	37.4	37.6	37.3
ASPEN04	37.9	38.5	38.1
ASPEN05	35.6	36.3	36.0
ASPEN06	36.3	36.5	36.2
ASPEN07	36.9	37.1	36.7
ASPEN08	37.0	37.2	36.9
ASPEN09	37.3	36.8	36.6
ASPEN10	37.3	37.1	37.2

Table A4. Skin Temperature (°C)

HEAT						
	CON			**EXP**		
	BL	**9 m**	**15 m**	**BL**	**9 m**	**15 m**
ASPEN01	33.2	33.4	33.4	34.6	42.7	36.4
ASPEN02	31.9	32.7	32.1	33.0	41.7	36.2
ASPEN03	32.1	32.9	33.5	32.7	42.6	36.0
ASPEN04	33.0	33.0	32.8	33.9	41.1	36.0
ASPEN05	31.2	31.5	30.8	33.4	40.8	34.7
ASPEN06	34.0	33.8	34.0	35.0	42.2	35.8
ASPEN07	32.3	32.6	32.8	33.8	43.2	36.4
ASPEN08	31.3	31.7	31.2	32.7	42.1	35.6
ASPEN09	32.8	32.9	32.4	33.8	42.4	35.3
ASPEN10	32.8	32.9	32.6	33.9	41.3	35.5
CUFF						
	CON			**EXP**		
	BL	**9 m**	**15 m**	**BL**	**9 m**	**15 m**
ASPEN01	33.2	33.0	33.2	34.3	34.3	34.5
ASPEN02	29.1	29.0	28.9	33.1	33.3	33.5
ASPEN03	32.6	32.6	32.9	33.7	33.4	34.1
ASPEN04	32.8	33.0	32.3	34.9	34.6	34.5
ASPEN05	31.8	31.8	31.8	33.7	33.5	33.9
ASPEN06	32.3	32.4	32.3	32.5	32.8	32.8
ASPEN07	32.1	32.7	32.7	33.3	33.3	33.6
ASPEN08	30.9	31.3	31.4	33.1	33.6	33.8
ASPEN09	33.2	34.0	34.3	33.6	34.0	34.5
ASPEN10	34.8	34.3	34.4	29.7	28.6	28.6
HGEX						
	CON			**EXP**		
	BL	**9 m**	**15 m**	**BL**	**9 m**	**15 m**
ASPEN01	33.6	33.4	33.7	34.1	34.8	34.9
ASPEN02	32.0	32.0	32.6	33.5	35.3	35.4
ASPEN03	32.5	32.6	32.6	35.2	36.4	36.8
ASPEN04	32.0	31.8	31.6	34.8	36.2	36.3
ASPEN05	30.9	31.0	31.0	32.4	33.6	35.0
ASPEN06	32.9	32.8	32.8	33.6	34.4	34.8
ASPEN07	32.0	32.7	33.4	32.1	32.4	32.9
ASPEN08	32.0	31.6	31.8	33.5	33.8	34.9
ASPEN09	34.4	34.9	35.2	32.6	33.2	33.5
ASPEN10	33.7	34.2	34.3	34.7	35.7	36.3

Table A5. Blood Parameters: ρ = blood density (kg/m^3), μ = blood viscosity (10^{-1}Nm^{-2}s^{-1})

HEAT														
			CON						EXP					
	Hct%	ρ	SR_p		μ_p		μ		SR_p		μ_p		μ	
			BL	9 m	BL	9 m	BL	9 m	BL	9 m	BL	9 m	BL	9 m
ASPEN01	45.0	1059.8	84.1	100.0	0.014	0.012	0.039	0.033	100.0	100.0	0.012	0.012	0.033	0.033
ASPEN02	42.0	1058.1	86.6	90.9	0.014	0.013	0.036	0.035	100.0	100.0	0.012	0.012	0.031	0.032
ASPEN03	48.0	1061.4	77.8	82.1	0.015	0.014	0.046	0.043	68.6	100.0	0.017	0.012	0.052	0.036
ASPEN04	48.0	1061.4	100.0	95.6	0.012	0.012	0.036	0.037	100.0	100.0	0.012	0.012	0.036	0.036
ASPEN05	51.0	1063.1	89.0	71.9	0.013	0.017	0.044	0.054	94.9	100.0	0.013	0.012	0.041	0.039
ASPEN06	44.5	1059.5	100.0	100.0	0.012	0.012	0.033	0.033	100.0	100.0	0.012	0.012	0.033	0.033
ASPEN07	43.0	1058.7	93.1	96.0	0.013	0.012	0.034	0.033	100.0	100.0	0.012	0.012	0.032	0.032
ASPEN08	44.0	1059.2	79.9	82.1	0.015	0.014	0.041	0.040	100.0	100.0	0.012	0.012	0.033	0.033
ASPEN09	44.0	1059.2	100.0	80.4	0.012	0.015	0.033	0.041	100.0	100.0	0.012	0.012	0.033	0.033
ASPEN10	47.5	1061.1	100.0	73.6	0.012	0.016	0.035	0.048	100.0	100.0	0.012	0.012	0.035	0.035
CUFF														
			CON						EXP					
	Hct%	ρ	SR_p		μ_p		μ		SR_p		μ_p		μ	
			BL	9 m	BL	9 m	BL	9 m	BL	9 m	BL	9 m	BL	9 m
ASPEN01	43.5	1058.9	100.0	83.0	0.012	0.014	0.032	0.039	100.0	100.0	0.012	0.012	0.032	0.032
ASPEN02	41.0	1057.6	75.5	71.1	0.016	0.017	0.041	0.043	100.0	100.0	0.012	0.012	0.031	0.030
ASPEN03	51.0	1063.1	74.9	100.0	0.016	0.012	0.051	0.039	60.0	100.0	0.020	0.012	0.064	0.039
ASPEN04	47.0	1060.9	72.4	80.5	0.016	0.015	0.048	0.043	100.0	100.0	0.012	0.012	0.035	0.035
ASPEN05	48.0	1061.4	67.1	66.8	0.018	0.018	0.054	0.054	91.0	99.0	0.013	0.012	0.040	0.037
ASPEN06	51.0	1063.1	99.7	74.3	0.012	0.016	0.039	0.052	100.0	100.0	0.012	0.012	0.039	0.039
ASPEN07	43.5	1058.9	100.0	94.0	0.012	0.013	0.032	0.034	100.0	100.0	0.012	0.012	0.032	0.032
ASPEN08	46.0	1060.3	100.0	71.1	0.012	0.017	0.034	0.048	100.0	100.0	0.012	0.012	0.034	0.034
ASPEN09	45.5	1060.0	100.0	90.4	0.012	0.013	0.034	0.038	100.0	100.0	0.012	0.012	0.034	0.034
ASPEN10	47.0	1060.9	100.0	75.3	0.012	0.016	0.035	0.046	100.0	100.0	0.012	0.012	0.035	0.035
HGEX														
			CON						EXP					
	Hct%	ρ	SR_p		μ_p		μ		SR_p		μ_p		μ	
			BL	9 m	BL	9 m	BL	9 m	BL	9 m	BL	9 m	BL	9 m
ASPEN01	47.5	1061.1	100.0	100.0	0.012	0.012	0.035	0.035	100.0	100.0	0.012	0.012	0.035	0.035
ASPEN02	43.0	1058.7	69.6	100.0	0.017	0.012	0.046	0.032	100.0	100.0	0.012	0.012	0.032	0.032
ASPEN03	51.0	1063.1	63.7	100.0	0.018	0.012	0.060	0.038	100.0	100.0	0.012	0.012	0.038	0.038
ASPEN04	52.0	1063.6	90.8	89.5	0.013	0.013	0.043	0.043	84.5	100.0	0.014	0.011	0.046	0.038
ASPEN05	49.0	1062.0	56.4	72.9	0.022	0.016	0.067	0.051	100.0	100.0	0.012	0.012	0.038	0.037
ASPEN06	48.5	1061.7	100.0	100.0	0.012	0.012	0.037	0.037	100.0	100.0	0.012	0.012	0.037	0.037
ASPEN07	42.0	1058.1	100.0	100.0	0.012	0.012	0.031	0.031	100.0	100.0	0.012	0.012	0.031	0.031
ASPEN08	44.0	1059.2	100.0	100.0	0.012	0.012	0.033	0.032	100.0	100.0	0.012	0.012	0.033	0.032
ASPEN09	43.5	1058.9	83.0	99.8	0.014	0.012	0.039	0.032	100.0	100.0	0.012	0.012	0.032	0.032
ASPEN10	49.0	1062.0	98.7	100.0	0.012	0.012	0.037	0.037	100.0	100.0	0.012	0.012	0.036	0.037

Table A6. Blood Velocity (m/s)

HEAT								
	CON				**EXP**			
	Antero		**Retro**		**Antero**		**Retro**	
	BL	**9 m**	**BL**	**9 m**	**BL**	**9 m**	**BL**	**9 m**
ASPEN01	9.08	12.73	-3.92	-2.43	14.57	23.43	-2.48	-1.89
ASPEN02	7.12	6.09	-2.38	-1.12	9.94	14.34	-3.25	-1.56
ASPEN03	6.87	7.46	-1.64	-2.01	6.64	15.65	-2.15	-1.76
ASPEN04	8.85	7.97	-2.53	-2.49	9.65	15.10	-1.64	-1.72
ASPEN05	7.00	6.67	-1.75	-2.46	7.84	16.85	-2.54	-1.32
ASPEN06	9.64	9.80	-1.29	-1.35	13.68	22.46	-0.97	-0.86
ASPEN07	7.63	8.37	-2.17	-2.78	8.64	25.26	-1.59	-0.06
ASPEN08	5.69	6.58	-1.65	-2.26	7.82	10.06	-1.15	-1.47
ASPEN09	7.82	6.77	-1.07	-1.34	9.07	17.08	-1.81	-0.88
ASPEN10	6.21	4.63	-0.10	-0.58	10.39	11.91	-0.16	-0.15
CUFF								
	CON				**EXP**			
	Antero		**Retro**		**Antero**		**Retro**	
	BL	**9 m**	**BL**	**9 m**	**BL**	**9 m**	**BL**	**9 m**
ASPEN01	9.04	7.13	-2.29	-2.07	16.55	23.96	-1.54	-13.85
ASPEN02	4.97	5.69	-1.18	-2.14	14.64	26.70	-0.95	-12.85
ASPEN03	5.81	7.75	-0.78	-0.50	5.78	18.23	-1.81	-10.86
ASPEN04	5.74	6.76	-1.51	-2.01	9.86	31.21	-1.79	-13.31
ASPEN05	5.85	5.78	-1.71	-1.67	7.37	18.33	-2.09	-12.27
ASPEN06	6.71	5.57	-0.97	-1.26	8.22	18.61	-0.79	-10.62
ASPEN07	7.19	6.45	-1.50	-1.43	8.84	25.31	-1.88	-15.35
ASPEN08	9.17	7.28	-2.39	-2.93	9.85	27.89	-4.24	-15.09
ASPEN09	7.97	6.88	-0.84	-0.95	12.82	27.54	-1.29	-12.02
ASPEN10	5.95	4.54	-0.38	-0.47	14.44	18.80	-0.39	-8.58
HGEX								
	CON				**EXP**			
	Antero		**Retro**		**Antero**		**Retro**	
	BL	**9 m**	**BL**	**9 m**	**BL**	**9 m**	**BL**	**9 m**
ASPEN01	13.40	13.58	-2.39	-3.95	14.49	26.13	-1.84	-3.71
ASPEN02	6.21	10.31	-2.78	-0.44	9.40	44.48	-2.76	-5.66
ASPEN03	7.29	8.98	-3.18	-1.22	9.48	49.28	-2.81	-2.88
ASPEN04	8.74	8.46	-3.42	-3.40	7.75	30.15	-3.11	-1.12
ASPEN05	5.60	4.96	-2.22	-0.73	9.17	37.80	-1.53	-6.73
ASPEN06	11.37	9.06	-0.79	-1.11	11.98	32.74	-1.56	-4.63
ASPEN07	7.25	7.99	-1.28	-1.40	8.16	34.49	-1.02	-2.21
ASPEN08	7.94	7.52	-2.44	-1.99	16.23	42.55	-1.30	-4.71
ASPEN09	6.25	7.51	-0.85	-0.99	12.28	38.84	-1.53	-3.02
ASPEN10	5.26	11.95	-0.07	-0.14	14.97	30.59	-0.15	-1.79

Table A7. Blood Flow (mL/min)

HEAT								
	CON				**EXP**			
	Antero		**Retro**		**Antero**		**Retro**	
	BL	**9 m**	**BL**	**9 m**	**BL**	**9 m**	**BL**	**9 m**
ASPEN01	103.63	142.87	-44.66	-27.25	160.83	196.61	-27.40	-15.82
ASPEN02	64.41	55.09	-21.55	-10.09	82.22	88.05	-26.87	-9.61
ASPEN03	93.72	99.54	-22.37	-26.76	85.54	153.97	-27.72	-17.35
ASPEN04	91.00	78.74	-26.02	-24.62	84.44	101.68	-14.33	-11.58
ASPEN05	73.46	68.85	-18.35	-25.44	73.85	121.42	-23.90	-9.48
ASPEN06	91.63	91.08	-12.21	-12.53	133.42	160.16	-9.44	-6.13
ASPEN07	79.14	85.69	-22.54	-28.47	69.79	153.40	-12.83	-0.36
ASPEN08	44.02	54.92	-12.76	-18.85	67.19	63.18	-9.90	-9.25
ASPEN09	107.52	92.97	-14.72	-18.35	101.74	147.45	-20.26	-7.61
ASPEN10	58.47	42.25	-0.92	-5.30	92.62	83.17	-1.41	-1.08
CUFF								
	CON				**EXP**			
	Antero		**Retro**		**Antero**		**Retro**	
	BL	**9 m**	**BL**	**9 m**	**BL**	**9 m**	**BL**	**9 m**
ASPEN01	108.16	80.00	-27.36	-23.18	185.73	208.75	-17.27	-120.69
ASPEN02	37.64	42.69	-8.96	-16.08	113.14	156.78	-7.34	-75.47
ASPEN03	78.93	101.03	-10.64	-6.55	76.20	164.02	-23.89	-97.70
ASPEN04	58.98	70.62	-15.54	-21.05	87.55	207.91	-15.90	-88.68
ASPEN05	66.98	66.25	-19.63	-19.12	74.82	207.42	-21.25	-138.82
ASPEN06	67.24	56.48	-9.69	-12.74	73.98	130.00	-7.07	-74.20
ASPEN07	62.64	55.38	-13.08	-12.26	59.83	149.48	-12.76	-90.65
ASPEN08	71.56	82.40	-18.63	-33.16	44.03	101.56	-18.97	-54.96
ASPEN09	102.79	89.41	-10.79	-12.37	154.07	229.99	-15.48	-100.37
ASPEN10	49.00	40.15	-3.11	-4.14	121.75	129.25	-3.27	-58.98
HGEX								
	CON				**EXP**			
	Antero		**Retro**		**Antero**		**Retro**	
	BL	**9 m**	**BL**	**9 m**	**BL**	**9 m**	**BL**	**9 m**
ASPEN01	166.85	163.81	-29.75	-47.66	173.51	319.02	-22.01	-45.25
ASPEN02	45.43	73.90	-20.37	-3.12	74.50	418.84	-21.83	-53.32
ASPEN03	91.48	110.48	-39.93	-15.00	113.93	625.59	-33.72	-36.51
ASPEN04	90.64	81.44	-35.46	-32.78	70.40	287.72	-28.28	-10.64
ASPEN05	60.58	50.31	-24.05	-7.43	86.34	360.70	-14.41	-64.19
ASPEN06	110.90	88.39	-7.67	-10.85	105.36	291.98	-13.73	-41.28
ASPEN07	62.91	66.09	-11.14	-11.55	64.30	296.35	-8.04	-19.01
ASPEN08	55.72	51.46	-17.13	-13.61	88.43	283.50	-7.06	-31.35
ASPEN09	79.58	96.85	-10.83	-12.74	135.60	468.60	-16.92	-36.47
ASPEN10	43.97	101.73	-0.58	-1.15	122.65	288.01	-1.19	-16.89

Table A8. Reynolds number

HEAT								
	CON				**EXP**			
	Antero		**Retro**		**Antero**		**Retro**	
	BL	**9 m**	**BL**	**9 m**	**BL**	**9 m**	**BL**	**9 m**
ASPEN01	1205	1975	-519	-377	2261	3143	-385	-253
ASPEN02	925	814	-310	-149	1426	1735	-466	-189
ASPEN03	859	974	-205	-262	711	2137	-231	-241
ASPEN04	1224	1035	-350	-324	1230	1693	-209	-193
ASPEN05	803	612	-200	-226	909	1798	-294	-140
ASPEN06	1384	1386	-184	-191	1988	2781	-141	-106
ASPEN07	1099	1233	-313	-410	1179	2986	-217	-7
ASPEN08	598	737	-173	-253	1084	1191	-160	-175
ASPEN09	1370	948	-188	-187	1435	2358	-286	-122
ASPEN10	833	450	-13	-56	1356	1374	-21	-18
CUFF								
	CON				**EXP**			
	Antero		**Retro**		**Antero**		**Retro**	
	BL	**9 m**	**BL**	**9 m**	**BL**	**9 m**	**BL**	**9 m**
ASPEN01	1502	951	-380	-275	2664	3392	-248	-1961
ASPEN02	519	561	-124	-211	2046	3273	-133	-1576
ASPEN03	645	1114	-87	-72	506	2177	-159	-1297
ASPEN04	589	779	-155	-232	1299	3567	-236	-1522
ASPEN05	566	556	-166	-160	912	2596	-259	-1737
ASPEN06	843	524	-122	-118	982	1957	-94	-1117
ASPEN07	1015	851	-212	-188	1100	2948	-234	-1788
ASPEN08	1156	791	-301	-318	940	2419	-405	-1309
ASPEN09	1309	1021	-137	-141	2032	3623	-204	-1581
ASPEN10	758	451	-48	-47	1862	2186	-50	-997
HGEX								
	CON				**EXP**			
	Antero		**Retro**		**Antero**		**Retro**	
	BL	**9 m**	**BL**	**9 m**	**BL**	**9 m**	**BL**	**9 m**
ASPEN01	2076	2069	-370	-602	2202	4006	-279	-568
ASPEN02	567	1327	-254	-56	1285	6560	-376	-835
ASPEN03	669	1285	-292	-174	1337	7163	-396	-418
ASPEN04	1026	953	-401	-384	792	3782	-318	-140
ASPEN05	427	479	-170	-71	1157	4864	-193	-866
ASPEN06	1498	1197	-104	-147	1499	4137	-195	-585
ASPEN07	1055	1139	-187	-199	1131	5010	-141	-321
ASPEN08	995	934	-306	-247	1792	5215	-143	-577
ASPEN09	890	1283	-121	-169	1964	6430	-245	-500
ASPEN10	638	1476	-8	-17	1821	3974	-18	-233

Table A9. Shear stress (dynes/cm^2)

HEAT								
	CON				**EXP**			
	Antero		**Retro**		**Antero**		**Retro**	
	BL	**9 m**	**BL**	**9 m**	**BL**	**9 m**	**BL**	**9 m**
ASPEN01	14.52	17.39	-6.26	-3.32	19.90	37.01	-3.39	-2.98
ASPEN02	11.61	9.66	-3.88	-1.77	14.66	25.07	-4.79	-2.74
ASPEN03	11.67	12.14	-2.78	-3.26	13.14	24.31	-4.26	-2.74
ASPEN04	13.60	13.01	-3.89	-4.07	16.05	28.58	-2.72	-3.25
ASPEN05	12.97	15.45	-3.24	-5.71	14.39	33.60	-4.66	-2.62
ASPEN06	14.25	14.70	-1.90	-2.02	19.93	38.44	-1.41	-1.47
ASPEN07	11.23	12.04	-3.20	-4.00	13.41	45.24	-2.47	-0.11
ASPEN08	11.48	12.43	-3.33	-4.27	11.95	18.01	-1.76	-2.64
ASPEN09	9.46	10.23	-1.30	-2.02	12.13	26.21	-2.42	-1.35
ASPEN10	9.83	10.12	-0.15	-1.27	16.89	21.90	-0.26	-0.28
CUFF								
	CON				**EXP**			
	Antero		**Retro**		**Antero**		**Retro**	
	BL	**9 m**	**BL**	**9 m**	**BL**	**9 m**	**BL**	**9 m**
ASPEN01	11.51	11.32	-2.91	-3.28	21.77	35.84	-2.02	-20.72
ASPEN02	10.05	12.21	-2.39	-4.60	22.15	46.06	-1.44	-22.17
ASPEN03	11.12	11.46	-1.50	-0.74	14.02	32.44	-4.40	-19.33
ASPEN04	11.86	12.43	-3.13	-3.70	15.89	57.92	-2.89	-24.71
ASPEN05	12.82	12.78	-3.76	-3.69	12.66	27.48	-3.60	-18.39
ASPEN06	11.36	12.57	-1.64	-2.83	14.63	37.63	-1.40	-21.48
ASPEN07	10.79	10.33	-2.25	-2.29	15.05	46.02	-3.21	-27.91
ASPEN08	15.42	14.22	-4.01	-5.72	21.89	68.19	-9.43	-36.90
ASPEN09	10.30	9.84	-1.08	-1.36	17.14	44.36	-1.72	-19.36
ASPEN10	9.91	9.71	-0.63	-1.00	23.76	34.29	-0.64	-15.65
HGEX								
	CON				**EXP**			
	Antero		**Retro**		**Antero**		**Retro**	
	BL	**9 m**	**BL**	**9 m**	**BL**	**9 m**	**BL**	**9 m**
ASPEN01	18.36	18.91	-3.27	-5.50	20.25	36.17	-2.57	-5.13
ASPEN02	14.40	16.97	-6.46	-0.72	14.58	63.87	-4.27	-8.13
ASPEN03	16.89	13.34	-7.37	-1.81	14.29	72.09	-4.23	-4.21
ASPEN04	15.85	15.97	-6.20	-6.43	16.13	51.13	-6.48	-1.89
ASPEN05	15.60	10.89	-6.19	-1.61	15.44	62.39	-2.58	-11.10
ASPEN06	18.32	14.56	-1.27	-1.79	20.34	55.03	-2.65	-7.78
ASPEN07	10.55	11.86	-1.87	-2.07	12.45	50.25	-1.56	-3.22
ASPEN08	13.41	12.83	-4.12	-3.39	31.15	73.56	-2.49	-8.13
ASPEN09	9.28	9.32	-1.26	-1.23	16.27	49.68	-2.03	-3.87
ASPEN10	9.22	20.55	-0.12	-0.23	26.13	50.01	-0.25	-2.93

Table A10. Shear rate (s^{-1})

HEAT								
	CON				**EXP**			
	Antero		**Retro**		**Antero**		**Retro**	
	BL	**9 m**	**BL**	**9 m**	**BL**	**9 m**	**BL**	**9 m**
ASPEN01	147.72	208.70	-63.66	-39.81	240.81	444.13	-41.03	-35.74
ASPEN02	130.13	111.30	-43.55	-20.38	189.74	317.71	-62.02	-34.67
ASPEN03	102.17	112.23	-24.38	-30.17	101.51	273.87	-32.89	-30.86
ASPEN04	151.68	139.13	-43.37	-43.50	179.05	319.59	-30.38	-36.39
ASPEN05	118.60	114.03	-29.63	-42.13	140.37	344.84	-45.44	-26.93
ASPEN06	171.84	176.66	-22.90	-24.31	240.46	461.92	-17.01	-17.68
ASPEN07	130.23	143.75	-37.09	-47.77	166.98	562.85	-30.69	-1.33
ASPEN08	112.49	124.95	-32.61	-42.90	146.51	220.56	-21.59	-32.31
ASPEN09	115.92	100.23	-15.86	-19.79	148.62	319.27	-29.60	-16.48
ASPEN10	111.14	84.21	-1.74	-10.56	191.02	247.43	-2.91	-3.20
CUFF								
	CON				**EXP**			
	Antero		**Retro**		**Antero**		**Retro**	
	BL	**9 m**	**BL**	**9 m**	**BL**	**9 m**	**BL**	**9 m**
ASPEN01	143.42	116.87	-36.28	-33.86	271.32	445.74	-25.23	-257.70
ASPEN02	99.09	114.09	-23.59	-42.97	289.14	605.07	-18.77	-291.26
ASPEN03	86.53	117.86	-11.66	-7.65	87.38	333.66	-27.40	-198.74
ASPEN04	98.32	114.74	-25.90	-34.20	181.82	663.99	-33.02	-283.21
ASPEN05	94.90	93.86	-27.80	-27.08	127.15	299.31	-36.12	-200.32
ASPEN06	116.50	95.98	-16.79	-21.65	150.48	386.73	-14.38	-220.74
ASPEN07	133.75	120.76	-27.93	-26.73	186.57	572.03	-39.78	-346.91
ASPEN08	180.20	118.91	-46.91	-47.84	255.83	802.52	-110.21	-434.25
ASPEN09	121.98	104.90	-12.81	-14.51	203.09	523.25	-20.41	-228.35
ASPEN10	113.90	83.95	-7.24	-8.66	273.07	393.64	-7.33	-179.61
HGEX								
	CON				**EXP**			
	Antero		**Retro**		**Antero**		**Retro**	
	BL	**9 m**	**BL**	**9 m**	**BL**	**9 m**	**BL**	**9 m**
ASPEN01	208.59	214.65	-37.20	-62.45	230.08	410.69	-29.19	-58.25
ASPEN02	126.09	211.50	-56.54	-8.93	183.50	796.10	-53.76	-101.35
ASPEN03	113.03	140.56	-49.34	-19.08	150.19	759.69	-44.45	-44.33
ASPEN04	149.16	149.71	-58.36	-60.26	141.26	536.02	-56.75	-19.83
ASPEN05	93.58	85.49	-37.15	-12.63	164.11	671.98	-27.39	-119.59
ASPEN06	199.86	159.30	-13.82	-19.56	221.86	602.19	-28.91	-85.14
ASPEN07	135.26	152.52	-23.94	-26.66	159.55	646.21	-19.94	-41.46
ASPEN08	164.49	157.96	-50.56	-41.78	381.95	905.40	-30.48	-100.11
ASPEN09	96.09	114.93	-13.08	-15.12	203.04	614.05	-25.34	-47.79
ASPEN10	100.03	224.98	-1.31	-2.55	287.16	547.43	-2.79	-32.11

Table A11. Oscillatory shear index

HEAT				
	CON		**EXP**	
	BL	**9 m**	**BL**	**9 m**
ASPEN01	0.30	0.16	0.15	0.07
ASPEN02	0.25	0.15	0.25	0.10
ASPEN03	0.19	0.21	0.24	0.10
ASPEN04	0.22	0.24	0.15	0.10
ASPEN05	0.20	0.27	0.24	0.07
ASPEN06	0.12	0.12	0.07	0.04
ASPEN07	0.22	0.25	0.16	0.00
ASPEN08	0.22	0.26	0.13	0.13
ASPEN09	0.12	0.16	0.17	0.05
ASPEN10	0.02	0.11	0.01	0.01
CUFF				
	CON		**EXP**	
	BL	**9 m**	**BL**	**9 m**
ASPEN01	0.20	0.22	0.09	0.37
ASPEN02	0.19	0.27	0.06	0.32
ASPEN03	0.12	0.06	0.24	0.37
ASPEN04	0.21	0.23	0.15	0.30
ASPEN05	0.23	0.22	0.22	0.40
ASPEN06	0.13	0.18	0.09	0.36
ASPEN07	0.17	0.18	0.18	0.38
ASPEN08	0.21	0.29	0.30	0.35
ASPEN09	0.10	0.12	0.09	0.30
ASPEN10	0.06	0.09	0.03	0.31
HGEX				
	CON		**EXP**	
	BL	**9 m**	**BL**	**9 m**
ASPEN01	0.15	0.23	0.11	0.12
ASPEN02	0.31	0.04	0.23	0.11
ASPEN03	0.30	0.12	0.23	0.06
ASPEN04	0.28	0.29	0.29	0.04
ASPEN05	0.28	0.13	0.14	0.15
ASPEN06	0.06	0.11	0.12	0.12
ASPEN07	0.15	0.15	0.11	0.06
ASPEN08	0.24	0.21	0.07	0.10
ASPEN09	0.12	0.12	0.11	0.07
ASPEN10	0.01	0.01	0.01	0.06

Table A12. 9 minute arterial diameter (mm)

HEAT		
	CON	**EXP**
ASPEN01	4.88	4.22
ASPEN02	4.38	3.61
ASPEN03	5.32	4.57
ASPEN04	4.58	3.78
ASPEN05	4.68	3.91
ASPEN06	4.44	3.89
ASPEN07	4.66	3.59
ASPEN08	4.21	3.65
ASPEN09	5.40	4.28
ASPEN10	4.40	3.85
CUFF		
	CON	**EXP**
ASPEN01	4.88	4.30
ASPEN02	3.99	3.53
ASPEN03	5.26	4.37
ASPEN04	4.71	3.76
ASPEN05	4.93	4.90
ASPEN06	4.64	3.85
ASPEN07	4.27	3.54
ASPEN08	4.90	2.78
ASPEN09	5.25	4.21
ASPEN10	4.33	3.82
HGEX		
	CON	**EXP**
ASPEN01	5.06	5.09
ASPEN02	3.90	4.47
ASPEN03	5.11	5.19
ASPEN04	4.52	4.50
ASPEN05	4.64	4.50
ASPEN06	4.55	4.35
ASPEN07	4.19	4.27
ASPEN08	3.81	3.76
ASPEN09	5.23	5.06
ASPEN10	4.25	4.47

Table A13. Flow-mediated dilation (%)

HEAT																
	CON								EXP							
	D_{base}		D_{peak}		Abs. FMD		FMD%		D_{base}		D_{peak}		Abs. FMD		FMD%	
	BL	15 m	BL	15 m	BL	15 m	BL	15 m	BL	15 m	BL	15 m	BL	15 m	BL	15 m
ASPEN01	4.92	5.09	5.09	5.35	0.17	0.26	3.35	4.97	4.84	4.97	5.10	5.26	0.26	0.29	5.48	5.82
ASPEN02	4.38	4.52	4.48	4.65	0.10	0.13	2.42	2.94	4.19	4.29	4.47	4.57	0.28	0.28	6.68	6.61
ASPEN03	5.38	5.35	5.47	5.46	0.09	0.11	1.67	2.05	5.23	5.07	5.36	5.32	0.13	0.25	2.58	4.96
ASPEN04	4.67	4.61	4.77	4.80	0.10	0.19	2.28	4.12	4.31	4.29	4.61	4.85	0.30	0.56	6.90	13.14
ASPEN05	4.72	4.66	4.94	4.83	0.22	0.17	4.63	3.54	4.47	4.53	4.87	4.85	0.40	0.32	8.96	7.09
ASPEN06	4.49	4.44	4.58	4.79	0.09	0.35	2.00	6.04	4.55	4.46	4.71	4.72	0.16	0.26	3.41	5.89
ASPEN07	4.69	4.61	4.82	4.83	0.13	0.22	3.73	4.72	4.14	4.06	4.40	4.51	0.26	0.45	6.22	11.02
ASPEN08	4.05	3.94	4.12	4.09	0.07	0.15	3.88	3.60	4.27	4.22	4.42	4.44	0.15	0.22	3.15	6.18
ASPEN09	5.40	5.16	5.56	5.38	0.16	0.22	3.03	4.30	4.88	4.98	5.14	5.35	0.26	0.37	5.25	7.51
ASPEN10	4.47	4.32	4.71	4.55	0.24	0.23	5.29	5.19	4.35	4.39	4.74	5.08	0.39	0.69	8.86	15.62
CUFF																
	CON								EXP							
	D_{base}		D_{peak}		Abs. FMD		FMD%		D_{base}		D_{peak}		Abs. FMD		FMD%	
	BL	15 m	BL	15 m	BL	15 m	BL	15 m	BL	15 m	BL	15 m	BL	15 m	BL	15 m
ASPEN01	5.04	5.03	5.24	5.23	0.20	0.20	3.91	3.98	4.88	4.99	5.19	5.26	0.31	0.27	6.24	5.55
ASPEN02	4.01	4.02	4.12	4.14	0.11	0.12	2.73	2.95	4.05	4.22	4.29	4.44	0.24	0.22	5.81	5.03
ASPEN03	5.37	5.23	5.47	5.35	0.10	0.12	1.90	2.26	5.29	5.25	5.42	5.49	0.13	0.24	2.55	4.63
ASPEN04	4.67	4.62	4.92	4.93	0.25	0.31	5.17	6.76	4.34	4.34	4.66	4.81	0.32	0.47	7.39	10.83
ASPEN05	4.93	4.91	5.07	5.08	0.14	0.17	2.67	3.52	4.64	4.54	4.97	4.80	0.33	0.26	7.11	5.71
ASPEN06	4.61	4.52	4.74	4.74	0.13	0.22	2.79	5.01	4.37	4.17	4.66	4.54	0.29	0.37	4.76	8.96
ASPEN07	4.30	4.31	4.63	4.53	0.33	0.22	4.93	5.03	3.79	3.81	4.14	4.15	0.35	0.34	9.06	8.74
ASPEN08	4.07	4.07	4.26	4.24	0.19	0.17	4.64	4.17	3.08	3.20	3.48	3.56	0.40	0.36	12.94	11.24
ASPEN09	5.23	5.13	5.43	5.34	0.20	0.21	3.93	4.25	5.05	4.70	5.30	4.97	0.25	0.27	4.85	5.73
ASPEN10	4.18	4.35	4.46	4.59	0.28	0.24	6.65	5.54	4.23	4.27	4.53	4.81	0.30	0.54	7.12	12.50
HGEX																
	CON								EXP							
	D_{base}		D_{peak}		Abs. FMD		FMD%		D_{base}		D_{peak}		Abs. FMD		FMD%	
	BL	15 m	BL	15 m	BL	15 m	BL	15 m	BL	15 m	BL	15 m	BL	15 m	BL	15 m
ASPEN01	5.14	5.06	5.38	5.33	0.24	0.27	4.68	5.28	5.04	5.04	5.29	5.25	0.25	0.21	4.98	4.17
ASPEN02	3.94	3.93	4.09	4.17	0.15	0.24	3.73	6.33	4.10	4.32	4.39	4.72	0.29	0.40	6.99	9.18
ASPEN03	5.16	5.00	5.29	5.23	0.13	0.23	2.56	4.62	5.05	5.09	5.24	5.39	0.19	0.30	3.85	5.98
ASPEN04	4.69	4.60	4.87	4.83	0.18	0.23	3.90	4.96	4.39	4.35	4.62	4.58	0.23	0.23	5.34	5.28
ASPEN05	4.79	4.80	4.91	4.90	0.12	0.10	2.60	2.08	4.47	4.42	4.66	4.69	0.19	0.27	4.43	6.11
ASPEN06	4.55	4.50	4.67	4.71	0.12	0.21	2.77	4.57	4.32	4.22	4.51	4.52	0.19	0.30	4.34	7.27
ASPEN07	4.29	4.37	4.54	4.64	0.25	0.27	5.80	6.27	4.09	4.03	4.39	4.39	0.30	0.36	7.23	9.08
ASPEN08	3.86	3.83	4.15	3.97	0.29	0.14	6.30	3.64	3.40	3.54	3.63	3.91	0.23	0.37	6.72	10.47
ASPEN09	5.20	5.24	5.35	5.40	0.15	0.16	2.89	3.08	4.84	4.85	5.11	5.14	0.27	0.29	5.62	6.01
ASPEN10	4.21	4.11	4.46	4.47	.25	0.36	5.90	8.77	4.17	4.29	4.57	4.93	0.40	0.64	9.65	14.96

APPENDIX B – SPSS Outputs

Table B1. HEAT Anterograde Shear Stress

General Linear Model

Notes		
Output Created	11-JUL-2017 10:45:02	
Comments		
Input	Data	/Users/jemcheng/Documents/VDL | M.Sc/Projects/ASPEN/Statistics/ASPEN complete.sav
	Active Dataset	DataSet1
	Filter	<none>
	Weight	<none>
	Split File	<none>
	N of Rows in Working Data File	20
Missing Value Handling	Definition of Missing	User-defined missing values are treated as missing.
	Cases Used	Statistics are based on all cases with valid data for all variables in the model.
Syntax	GLM CON_HEAT_ESSAntero_Pre CON_HEAT_ESSAntero_Dur EXP_HEAT_ESSAntero_Pre EXP_HEAT_ESSAntero_Dur /WSFACTOR=Limb 2 Polynomial Time 2 Polynomial /METHOD=SSTYPE(3) /PLOT=PROFILE(Time*Limb) /PRINT=DESCRIPTIVE	

	ETASQ OPOWER HOMOGENEITY /CRITERIA=ALPHA(.05) /WSDESIGN=Limb Time Limb*Time.	
Resources	Processor Time	00:00:00.25
	Elapsed Time	00:00:00.00

[DataSet1] /Users/jemcheng/Documents/VDL | M.Sc/Projects/ASPEN/Statistics/ASPEN complete.sav

Warnings
The HOMOGENEITY specification in the PRINT subcommand will be ignored because there are no between-subjects factors.

Within-Subjects Factors

Measure: MEASURE_1

Limb	Time	Dependent Variable
1	1	CON_HEAT_ESSAntero_Pre
	2	CON_HEAT_ESSAntero_Dur
2	1	EXP_HEAT_ESSAntero_Pre
	2	EXP_HEAT_ESSAntero_Dur

Descriptive Statistics

	Mean	Std.	N

		Deviation	
CON_HEAT_ESSAntero_Pre	12.0620	1.73718	10
CON_HEAT_ESSAntero_Dur	12.7170	2.50495	10
EXP_HEAT_ESSAntero_Pre	15.2450	2.91365	10
EXP_HEAT_ESSAntero_Dur	29.8370	8.48369	10

Multivariate Tests[a]

Effect	Value	F	Hypothesis df	Error df	Sig.	Partial Eta Squared	Noncent. Parameter	Observed Power[c]	
Limb	Pillai's Trace	.874	62.450[b]	1.000	9.000	.000	.874	62.450	1.000
	Wilks' Lambda	.126	62.450[b]	1.000	9.000	.000	.874	62.450	1.000
	Hotelling's Trace	6.939	62.450[b]	1.000	9.000	.000	.874	62.450	1.000
	Roy's Largest Root	6.939	62.450[b]	1.000	9.000	.000	.874	62.450	1.000
Time	Pillai's Trace	.790	33.900[b]	1.000	9.000	.000	.790	33.900	.999
	Wilks' Lambda	.210	33.900[b]	1.000	9.000	.000	.790	33.900	.999
	Hotelling's Trace	3.767	33.900[b]	1.000	9.000	.000	.790	33.900	.999
	Roy's Largest Root	3.767	33.900[b]	1.000	9.000	.000	.790	33.900	.999
Limb * Time	Pillai's Trace	.797	35.415[b]	1.000	9.000	.000	.797	35.415	.999
	Wilks' Lambda	.203	35.415[b]	1.000	9.000	.000	.797	35.415	.999
	Hotelling's Trace	3.935	35.415[b]	1.000	9.000	.000	.797	35.415	.999
	Roy's Largest Root	3.935	35.415[b]	1.000	9.000	.000	.797	35.415	.999

a. Design: Intercept

Within Subjects Design: Limb + Time + Limb * Time
b. Exact statistic
c. Computed using alpha =

Mauchly's Test of Sphericity[a]

Measure: MEASURE_1

Within Subjects Effect	Mauchly's W	Approx. Chi-Square	df	Sig.	Epsilon[b]		
					Greenhouse-Geisser	Huynh-Feldt	Lower-bound
Limb	1.000	.000	0	.	1.000	1.000	1.000
Time	1.000	.000	0	.	1.000	1.000	1.000
Limb * Time	1.000	.000	0	.	1.000	1.000	1.000

Tests the null hypothesis that the error covariance matrix of the orthonormalized transformed dependent variables is proportional to an identity matrix.

a. Design: Intercept
Within Subjects Design: Limb + Time + Limb * Time

b. May be used to adjust the degrees of freedom for the averaged tests of significance. Corrected tests are displayed in the Tests of Within-Subjects Effects table.

Tests of Within-Subjects Effects

Measure: MEASURE_1

Source	Type III Sum of Squares	df	Mean Square	F	Sig.	Partial Eta Squared	Noncent. Parameter	Observed Power[a]	
Limb	Sphericity	1030.530	1	1030.530	62.450	.000	.874	62.450	1.000

	Assumed								
	Greenhouse-Geisser	1030.530	1.000	1030.530	62.450	.000	.874	62.450	1.000
	Huynh-Feldt	1030.530	1.000	1030.530	62.450	.000	.874	62.450	1.000
	Lower-bound	1030.530	1.000	1030.530	62.450	.000	.874	62.450	1.000
Error(Limb)	Sphericity Assumed	148.515	9	16.502					
	Greenhouse-Geisser	148.515	9.000	16.502					
	Huynh-Feldt	148.515	9.000	16.502					
	Lower-bound	148.515	9.000	16.502					
Time	Sphericity Assumed	581.178	1	581.178	33.900	.000	.790	33.900	.999
	Greenhouse-Geisser	581.178	1.000	581.178	33.900	.000	.790	33.900	.999
	Huynh-Feldt	581.178	1.000	581.178	33.900	.000	.790	33.900	.999
	Lower-bound	581.178	1.000	581.178	33.900	.000	.790	33.900	.999
Error(Time)	Sphericity Assumed	154.294	9	17.144					
	Greenhouse-Geisser	154.294	9.000	17.144					
	Huynh-Feldt	154.294	9.000	17.144					
	Lower-bound	154.294	9.000	17.144					
Limb * Time	Sphericity Assumed	485.600	1	485.600	35.415	.000	.797	35.415	.999
	Greenhouse-Geisser	485.600	1.000	485.600	35.415	.000	.797	35.415	.999
	Huynh-Feldt	485.600	1.000	485.600	35.415	.000	.797	35.415	.999
	Lower-bound	485.600	1.000	485.600	35.415	.000	.797	35.415	.999
Error(Limb*Time)	Sphericity Assumed	123.404	9	13.712					
	Greenhouse-Geisser	123.404	9.000	13.712					
	Huynh-Feldt	123.404	9.000	13.712					

	Lower-bound	123.404	9.000	13.712						
a. Computed using alpha =										

Tests of Within-Subjects Contrasts

Measure: MEASURE_1

Source	Limb	Time	Type III Sum of Squares	df	Mean Square	F	Sig.	Partial Eta Squared	Noncent. Parameter	Observed Power[a]
Limb	Linear		1030.530	1	1030.530	62.450	.000	.874	62.450	1.000
Error(Limb)	Linear		148.515	9	16.502					
Time		Linear	581.178	1	581.178	33.900	.000	.790	33.900	.999
Error(Time)		Linear	154.294	9	17.144					
Limb * Time	Linear	Linear	485.600	1	485.600	35.415	.000	.797	35.415	.999
Error(Limb*Time)	Linear	Linear	123.404	9	13.712					
a. Computed using alpha =										

Tests of Between-Subjects Effects

Measure: MEASURE_1

Transformed Variable: Average

Source	Type III Sum of Squares	df	Mean Square	F	Sig.	Partial Eta Squared	Noncent. Parameter	Observed Power[a]
Intercept	12201.398	1	12201.398	287.783	.000	.970	287.783	1.000
Error	381.582	9	42.398					
a. Computed using alpha =								

Table B2. HEAT Retrograde Shear Stress

General Linear Model

Notes		
Output Created	11-JUL-2017 10:44:28	
Comments		
Input	Data	/Users/jemcheng/Documents/VDL | M.Sc/Projects/ASPEN/Statistics/ASPEN complete.sav
	Active Dataset	DataSet1
	Filter	<none>
	Weight	<none>
	Split File	<none>
	N of Rows in Working Data File	20
Missing Value Handling	Definition of Missing	User-defined missing values are treated as missing.
	Cases Used	Statistics are based on all cases with valid data for all variables in the model.
Syntax	GLM CON_HEAT_ESSRetro_Pre CON_HEAT_ESSRetro_Dur EXP_HEAT_ESSRetro_Pre EXP_HEAT_ESSRetro_Dur /WSFACTOR=Limb 2 Polynomial Time 2 Polynomial /METHOD=SSTYPE(3) /PLOT=PROFILE(Time*Limb) /PRINT=DESCRIPTIVE ETASQ OPOWER HOMOGENEITY /CRITERIA=ALPHA(.05) /WSDESIGN=Limb Time Limb*Time.	

Resources	Processor Time	00:00:01.23
	Elapsed Time	00:00:01.00

[DataSet1] /Users/jemcheng/Documents/VDL | M.Sc/Projects/ASPEN/Statistics/ASPEN complete.sav

Warnings
The HOMOGENEITY specification in the PRINT subcommand will be ignored because there are no between-subjects factors.

Within-Subjects Factors

Measure: MEASURE_1

Limb	Time	Dependent Variable
1	1	CON_HEAT_ESSRetro_Pre
	2	CON_HEAT_ESSRetro_Dur
2	1	EXP_HEAT_ESSRetro_Pre
	2	EXP_HEAT_ESSRetro_Dur

Descriptive Statistics

	Mean	Std. Deviation	N
CON_HEAT_ESSRetro_Pre	-2.9930	1.65566	10
CON_HEAT_ESSRetro_Dur	-3.1710	1.39069	10
EXP_HEAT_ESSRetro_Pre	-2.8140	1.47657	10
EXP_HEAT_ESSRetro_Dur	-2.0180	1.13738	10

Multivariate Tests[a]

Effect	Value	F	Hypothesis df	Error df	Sig.	Partial Eta Squared	Noncent. Parameter	Observed Power[c]	
Limb	Pillai's Trace	.322	4.268[b]	1.000	9.000	.069	.322	4.268	.454
	Wilks' Lambda	.678	4.268[b]	1.000	9.000	.069	.322	4.268	.454
	Hotelling's Trace	.474	4.268[b]	1.000	9.000	.069	.322	4.268	.454
	Roy's Largest Root	.474	4.268[b]	1.000	9.000	.069	.322	4.268	.454
Time	Pillai's Trace	.102	1.021[b]	1.000	9.000	.339	.102	1.021	.148
	Wilks' Lambda	.898	1.021[b]	1.000	9.000	.339	.102	1.021	.148
	Hotelling's Trace	.113	1.021[b]	1.000	9.000	.339	.102	1.021	.148
	Roy's Largest Root	.113	1.021[b]	1.000	9.000	.339	.102	1.021	.148
Limb * Time	Pillai's Trace	.210	2.386[b]	1.000	9.000	.157	.210	2.386	.282
	Wilks' Lambda	.790	2.386[b]	1.000	9.000	.157	.210	2.386	.282
	Hotelling's Trace	.265	2.386[b]	1.000	9.000	.157	.210	2.386	.282
	Roy's Largest Root	.265	2.386[b]	1.000	9.000	.157	.210	2.386	.282

a. Design: Intercept

Within Subjects Design: Limb + Time + Limb * Time
b. Exact statistic
c. Computed using alpha =

Mauchly's Test of Sphericity[a]

Measure: MEASURE_1

Within Subjects Effect	Mauchly's W	Approx. Chi-Square	df	Sig.	Epsilon[b]		
					Greenhouse-Geisser	Huynh-Feldt	Lower-bound
Limb	1.000	.000	0	.	1.000	1.000	1.000
Time	1.000	.000	0	.	1.000	1.000	1.000
Limb * Time	1.000	.000	0	.	1.000	1.000	1.000

Tests the null hypothesis that the error covariance matrix of the orthonormalized transformed dependent variables is proportional to an identity matrix.

a. Design: Intercept
Within Subjects Design: Limb + Time + Limb * Time

b. May be used to adjust the degrees of freedom for the averaged tests of significance. Corrected tests are displayed in the Tests of Within-Subjects Effects table.

Tests of Within-Subjects Effects

Measure: MEASURE_1

Source		Type III Sum of Squares	df	Mean Square	F	Sig.	Partial Eta Squared	Noncent. Parameter	Observed Power[a]	
Limb	Sphericity	4.436	1	4.436	4.268	.069	.322	4.268	.454	

	Assumed								
	Greenhouse-Geisser	4.436	1.000	4.436	4.268	.069	.322	4.268	.454
	Huynh-Feldt	4.436	1.000	4.436	4.268	.069	.322	4.268	.454
	Lower-bound	4.436	1.000	4.436	4.268	.069	.322	4.268	.454
Error(Limb)	Sphericity Assumed	9.352	9	1.039					
	Greenhouse-Geisser	9.352	9.000	1.039					
	Huynh-Feldt	9.352	9.000	1.039					
	Lower-bound	9.352	9.000	1.039					
Time	Sphericity Assumed	.955	1	.955	1.021	.339	.102	1.021	.148
	Greenhouse-Geisser	.955	1.000	.955	1.021	.339	.102	1.021	.148
	Huynh-Feldt	.955	1.000	.955	1.021	.339	.102	1.021	.148
	Lower-bound	.955	1.000	.955	1.021	.339	.102	1.021	.148
Error(Time)	Sphericity Assumed	8.420	9	.936					
	Greenhouse-Geisser	8.420	9.000	.936					
	Huynh-Feldt	8.420	9.000	.936					
	Lower-bound	8.420	9.000	.936					
Limb * Time	Sphericity Assumed	2.372	1	2.372	2.386	.157	.210	2.386	.282
	Greenhouse-Geisser	2.372	1.000	2.372	2.386	.157	.210	2.386	.282
	Huynh-Feldt	2.372	1.000	2.372	2.386	.157	.210	2.386	.282
	Lower-bound	2.372	1.000	2.372	2.386	.157	.210	2.386	.282
Error(Limb*Time)	Sphericity Assumed	8.947	9	.994					
	Greenhouse-Geisser	8.947	9.000	.994					
	Huynh-Feldt	8.947	9.000	.994					

	Lower-bound	8.947	9.000	.994						
a. Computed using alpha =										

Tests of Within-Subjects Contrasts

Measure: MEASURE_1

Source	Limb	Time	Type III Sum of Squares	df	Mean Square	F	Sig.	Partial Eta Squared	Noncent. Parameter	Observed Power[a]
Limb	Linear		4.436	1	4.436	4.268	.069	.322	4.268	.454
Error(Limb)	Linear		9.352	9	1.039					
Time		Linear	.955	1	.955	1.021	.339	.102	1.021	.148
Error(Time)		Linear	8.420	9	.936					
Limb * Time	Linear	Linear	2.372	1	2.372	2.386	.157	.210	2.386	.282
Error(Limb*Time)	Linear	Linear	8.947	9	.994					
a. Computed using alpha =										

Tests of Between-Subjects Effects

Measure: MEASURE_1
Transformed Variable: Average

Source	Type III Sum of Squares	df	Mean Square	F	Sig.	Partial Eta Squared	Noncent. Parameter	Observed Power[a]
Intercept	302.280	1	302.280	58.351	.000	.866	58.351	1.000
Error	46.623	9	5.180					
a. Computed using alpha =								

Table B3. HEAT Oscillatory Shear Index

General Linear Model

Notes		
Output Created	11-JUL-2017 10:47:39	
Comments		
Input	Data	/Users/jemcheng/Documents/VDL | M.Sc/Projects/ASPEN/Statistics/ASPEN complete.sav
	Active Dataset	DataSet1
	Filter	<none>
	Weight	<none>
	Split File	<none>
	N of Rows in Working Data File	20
Missing Value Handling	Definition of Missing	User-defined missing values are treated as missing.
	Cases Used	Statistics are based on all cases with valid data for all variables in the model.
Syntax	GLM CON_HEAT_OSI_Pre CON_HEAT_OSI_Dur EXP_HEAT_OSI_Pre EXP_HEAT_OSI_Dur /WSFACTOR=Limb 2 Polynomial Time 2 Polynomial /METHOD=SSTYPE(3) /PLOT=PROFILE(Time*Limb) /PRINT=DESCRIPTIVE ETASQ OPOWER HOMOGENEITY /CRITERIA=ALPHA(.05) /WSDESIGN=Limb Time Limb*Time.	
Resources	Processor Time	00:00:00.28

	Elapsed Time	00:00:00.00

[DataSet1] /Users/jemcheng/Documents/VDL | M.Sc/Projects/ASPEN/Statistics/ASPEN complete.sav

Warnings
The HOMOGENEITY specification in the PRINT subcommand will be ignored because there are no between-subjects factors.

Within-Subjects Factors

Measure: MEASURE_1

Limb	Time	Dependent Variable
1	1	CON_HEAT_OSI_Pre
	2	CON_HEAT_OSI_Dur
2	1	EXP_HEAT_OSI_Pre
	2	EXP_HEAT_OSI_Dur

Descriptive Statistics

	Mean	Std. Deviation	N
CON_HEAT_OSI_Pre	.1867	.08156	10
CON_HEAT_OSI_Dur	.1937	.05827	10
EXP_HEAT_OSI_Pre	.1557	.07667	10
EXP_HEAT_OSI_Dur	.0678	.04152	10

Multivariate Tests[a]

Effect	Value	F	Hypothesis df	Error df	Sig.	Partial Eta Squared	Noncent. Parameter	Observed Power[c]	
Limb	Pillai's Trace	.780	31.838[b]	1.000	9.000	.000	.780	31.838	.999
	Wilks' Lambda	.220	31.838[b]	1.000	9.000	.000	.780	31.838	.999
	Hotelling's Trace	3.538	31.838[b]	1.000	9.000	.000	.780	31.838	.999
	Roy's Largest Root	3.538	31.838[b]	1.000	9.000	.000	.780	31.838	.999
Time	Pillai's Trace	.403	6.074[b]	1.000	9.000	.036	.403	6.074	.594
	Wilks' Lambda	.597	6.074[b]	1.000	9.000	.036	.403	6.074	.594
	Hotelling's Trace	.675	6.074[b]	1.000	9.000	.036	.403	6.074	.594
	Roy's Largest Root	.675	6.074[b]	1.000	9.000	.036	.403	6.074	.594
Limb * Time	Pillai's Trace	.542	10.650[b]	1.000	9.000	.010	.542	10.650	.827
	Wilks' Lambda	.458	10.650[b]	1.000	9.000	.010	.542	10.650	.827
	Hotelling's Trace	1.183	10.650[b]	1.000	9.000	.010	.542	10.650	.827
	Roy's Largest Root	1.183	10.650[b]	1.000	9.000	.010	.542	10.650	.827

a. Design: Intercept
Within Subjects Design: Limb + Time + Limb

* Time
b. Exact statistic
c. Computed using alpha =

Mauchly's Test of Sphericity[a]

Measure: MEASURE_1

Within Subjects Effect	Mauchly's W	Approx. Chi-Square	df	Sig.	Epsilon[b]		
					Greenhouse-Geisser	Huynh-Feldt	Lower-bound
Limb	1.000	.000	0	.	1.000	1.000	1.000
Time	1.000	.000	0	.	1.000	1.000	1.000
Limb * Time	1.000	.000	0	.	1.000	1.000	1.000

Tests the null hypothesis that the error covariance matrix of the orthonormalized transformed dependent variables is proportional to an identity matrix.

a. Design: Intercept
Within Subjects Design: Limb + Time + Limb * Time

b. May be used to adjust the degrees of freedom for the averaged tests of significance. Corrected tests are displayed in the Tests of Within-Subjects Effects table.

Tests of Within-Subjects Effects

Measure: MEASURE_1

Source	Type III Sum of Squares	df	Mean Square	F	Sig.	Partial Eta Squared	Noncent. Parameter	Observed Power[a]	
Limb	Sphericity Assumed	.062	1	.062	31.838	.000	.780	31.838	.999

	Greenhouse-Geisser	.062	1.000	.062	31.838	.000	.780	31.838	.999
	Huynh-Feldt	.062	1.000	.062	31.838	.000	.780	31.838	.999
	Lower-bound	.062	1.000	.062	31.838	.000	.780	31.838	.999
Error(Limb)	Sphericity Assumed	.017	9	.002					
	Greenhouse-Geisser	.017	9.000	.002					
	Huynh-Feldt	.017	9.000	.002					
	Lower-bound	.017	9.000	.002					
Time	Sphericity Assumed	.016	1	.016	6.074	.036	.403	6.074	.594
	Greenhouse-Geisser	.016	1.000	.016	6.074	.036	.403	6.074	.594
	Huynh-Feldt	.016	1.000	.016	6.074	.036	.403	6.074	.594
	Lower-bound	.016	1.000	.016	6.074	.036	.403	6.074	.594
Error(Time)	Sphericity Assumed	.024	9	.003					
	Greenhouse-Geisser	.024	9.000	.003					
	Huynh-Feldt	.024	9.000	.003					
	Lower-bound	.024	9.000	.003					
Limb * Time	Sphericity Assumed	.023	1	.023	10.650	.010	.542	10.650	.827
	Greenhouse-Geisser	.023	1.000	.023	10.650	.010	.542	10.650	.827
	Huynh-Feldt	.023	1.000	.023	10.650	.010	.542	10.650	.827
	Lower-bound	.023	1.000	.023	10.650	.010	.542	10.650	.827
Error(Limb*Time)	Sphericity Assumed	.019	9	.002					
	Greenhouse-Geisser	.019	9.000	.002					
	Huynh-Feldt	.019	9.000	.002					
	Lower-bound	.019	9.000	.002					

a. Computed using alpha =

Tests of Within-Subjects Contrasts

Measure: MEASURE_1

Source	Limb	Time	Type III Sum of Squares	df	Mean Square	F	Sig.	Partial Eta Squared	Noncent. Parameter	Observed Power[a]
Limb	Linear		.062	1	.062	31.838	.000	.780	31.838	.999
Error(Limb)	Linear		.017	9	.002					
Time		Linear	.016	1	.016	6.074	.036	.403	6.074	.594
Error(Time)		Linear	.024	9	.003					
Limb * Time	Linear	Linear	.023	1	.023	10.650	.010	.542	10.650	.827
Error(Limb*Time)	Linear	Linear	.019	9	.002					

a. Computed using alpha =

Tests of Between-Subjects Effects

Measure: MEASURE_1
Transformed Variable: Average

Source	Type III Sum of Squares	df	Mean Square	F	Sig.	Partial Eta Squared	Noncent. Parameter	Observed Power[a]
Intercept	.912	1	.912	83.586	.000	.903	83.586	1.000
Error	.098	9	.011					

a. Computed using alpha =

Table B4. HEAT FMD%

General Linear Model

Notes		
Output Created	17-JUL-2017 13:00:06	
Comments		
Input	Data	/Users/jemcheng/Documents/VDL | M.Sc/Projects/ASPEN/Statistics/ASPEN complete.sav
	Active Dataset	DataSet1
	Filter	<none>
	Weight	<none>
	Split File	<none>
	N of Rows in Working Data File	20
Missing Value Handling	Definition of Missing	User-defined missing values are treated as missing.
	Cases Used	Statistics are based on all cases with valid data for all variables in the model.
Syntax	GLM CON_HEAT_FMD_Pre CON_HEAT_FMD_Post EXP_HEAT_FMD_Pre EXP_HEAT_FMD_Post /WSFACTOR=Limb 2 Polynomial Time 2 Polynomial /METHOD=SSTYPE(3) /PLOT=PROFILE(Time*Limb) /PRINT=DESCRIPTIVE ETASQ OPOWER HOMOGENEITY /CRITERIA=ALPHA(.05) /WSDESIGN=Limb Time Limb*Time.	
Resources	Processor Time	00:00:00.19
	Elapsed Time	00:00:00.00

[DataSet1] /Users/jemcheng/Documents/VDL | M.Sc/Projects/ASPEN/Statistics/ASPEN complete.sav

Warnings

The HOMOGENEITY specification in the PRINT subcommand will be ignored because there are no between-subjects factors.

Within-Subjects Factors

Measure: MEASURE_1

Limb	Time	Dependent Variable
1	1	CON_HEAT_FMD_Pre
	2	CON_HEAT_FMD_Post
2	1	EXP_HEAT_FMD_Pre
	2	EXP_HEAT_FMD_Post

Descriptive Statistics

	Mean	Std. Deviation	N
CON_HEAT_FMD_Pre	3.2280	1.17547	10
CON_HEAT_FMD_Post	4.1470	1.16538	10
EXP_HEAT_FMD_Pre	5.7490	2.23587	10
EXP_HEAT_FMD_Post	8.3840	3.60383	10

Multivariate Tests[a]

Effect	Value	F	Hypothesis df	Error df	Sig.	Partial Eta Squared	Noncent. Parameter	Observed Power[c]	
Limb	Pillai's Trace	.711	22.152[b]	1.000	9.000	.001	.711	22.152	.986
	Wilks' Lambda	.289	22.152[b]	1.000	9.000	.001	.711	22.152	.986
	Hotelling's Trace	2.461	22.152[b]	1.000	9.000	.001	.711	22.152	.986
	Roy's Largest Root	2.461	22.152[b]	1.000	9.000	.001	.711	22.152	.986
Time	Pillai's Trace	.559	11.389[b]	1.000	9.000	.008	.559	11.389	.851
	Wilks' Lambda	.441	11.389[b]	1.000	9.000	.008	.559	11.389	.851
	Hotelling's Trace	1.265	11.389[b]	1.000	9.000	.008	.559	11.389	.851
	Roy's Largest Root	1.265	11.389[b]	1.000	9.000	.008	.559	11.389	.851
Limb * Time	Pillai's Trace	.289	3.658[b]	1.000	9.000	.088	.289	3.658	.401
	Wilks' Lambda	.711	3.658[b]	1.000	9.000	.088	.289	3.658	.401
	Hotelling's Trace	.406	3.658[b]	1.000	9.000	.088	.289	3.658	.401
	Roy's Largest Root	.406	3.658[b]	1.000	9.000	.088	.289	3.658	.401

a. Design: Intercept
Within Subjects Design: Limb + Time + Limb * Time

b. Exact statistic
c. Computed using alpha =

Mauchly's Test of Sphericity[a]

Measure: MEASURE_1

Within Subjects Effect	Mauchly's W	Approx. Chi-Square	df	Sig.	Epsilon[b]		
					Greenhouse-Geisser	Huynh-Feldt	Lower-bound
Limb	1.000	.000	0	.	1.000	1.000	1.000
Time	1.000	.000	0	.	1.000	1.000	1.000
Limb * Time	1.000	.000	0	.	1.000	1.000	1.000

Tests the null hypothesis that the error covariance matrix of the orthonormalized transformed dependent variables is proportional to an identity matrix.

a. Design: Intercept
Within Subjects Design: Limb + Time + Limb * Time

b. May be used to adjust the degrees of freedom for the averaged tests of significance. Corrected tests are displayed in the Tests of Within-Subjects Effects table.

Tests of Within-Subjects Effects

Measure: MEASURE_1

Source	Type III Sum of Squares	df	Mean Square	F	Sig.	Partial Eta Squared	Noncent. Parameter	Observed Power[a]	
Limb	Sphericity Assumed	114.176	1	114.176	22.152	.001	.711	22.152	.986
	Greenhouse-	114.176	1.000	114.176	22.152	.001	.711	22.152	.986

	Geisser								
	Huynh-Feldt	114.176	1.000	114.176	22.152	.001	.711	22.152	.986
	Lower-bound	114.176	1.000	114.176	22.152	.001	.711	22.152	.986
Error(Limb)	Sphericity Assumed	46.389	9	5.154					
	Greenhouse-Geisser	46.389	9.000	5.154					
	Huynh-Feldt	46.389	9.000	5.154					
	Lower-bound	46.389	9.000	5.154					
Time	Sphericity Assumed	31.577	1	31.577	11.389	.008	.559	11.389	.851
	Greenhouse-Geisser	31.577	1.000	31.577	11.389	.008	.559	11.389	.851
	Huynh-Feldt	31.577	1.000	31.577	11.389	.008	.559	11.389	.851
	Lower-bound	31.577	1.000	31.577	11.389	.008	.559	11.389	.851
Error(Time)	Sphericity Assumed	24.954	9	2.773					
	Greenhouse-Geisser	24.954	9.000	2.773					
	Huynh-Feldt	24.954	9.000	2.773					
	Lower-bound	24.954	9.000	2.773					
Limb * Time	Sphericity Assumed	7.362	1	7.362	3.658	.088	.289	3.658	.401
	Greenhouse-Geisser	7.362	1.000	7.362	3.658	.088	.289	3.658	.401
	Huynh-Feldt	7.362	1.000	7.362	3.658	.088	.289	3.658	.401
	Lower-bound	7.362	1.000	7.362	3.658	.088	.289	3.658	.401
Error(Limb*Time)	Sphericity Assumed	18.113	9	2.013					
	Greenhouse-Geisser	18.113	9.000	2.013					
	Huynh-Feldt	18.113	9.000	2.013					
	Lower-bound	18.113	9.000	2.013					
a. Computed using alpha =									

Tests of Within-Subjects Contrasts

Measure: MEASURE_1

Source	Limb	Time	Type III Sum of Squares	df	Mean Square	F	Sig.	Partial Eta Squared	Noncent. Parameter	Observed Power[a]
Limb	Linear		114.176	1	114.176	22.152	.001	.711	22.152	.986
Error(Limb)	Linear		46.389	9	5.154					
Time		Linear	31.577	1	31.577	11.389	.008	.559	11.389	.851
Error(Time)		Linear	24.954	9	2.773					
Limb * Time	Linear	Linear	7.362	1	7.362	3.658	.088	.289	3.658	.401
Error(Limb*Time)	Linear	Linear	18.113	9	2.013					

a. Computed using alpha =

Tests of Between-Subjects Effects

Measure: MEASURE_1
Transformed Variable: Average

Source	Type III Sum of Squares	df	Mean Square	F	Sig.	Partial Eta Squared	Noncent. Parameter	Observed Power[a]
Intercept	1156.485	1	1156.485	107.211	.000	.923	107.211	1.000
Error	97.083	9	10.787					

a. Computed using alpha =

Table B5. CUFF Anterograde Shear Stress

General Linear Model

Notes		
Output Created	11-JUL-2017 10:55:12	
Comments		
Input	Data	/Users/jemcheng/Documents/VDL | M.Sc/Projects/ASPEN/Statistics/ASPEN complete.sav
	Active Dataset	DataSet1
	Filter	<none>
	Weight	<none>
	Split File	<none>
	N of Rows in Working Data File	20
Missing Value Handling	Definition of Missing	User-defined missing values are treated as missing.
	Cases Used	Statistics are based on all cases with valid data for all variables in the model.
Syntax	GLM CON_CUFF_ESSAntero_Pre CON_CUFF_ESSAntero_Dur EXP_CUFF_ESSAntero_Pre EXP_CUFF_ESSAntero_Dur /WSFACTOR=Limb 2 Polynomial Time 2 Polynomial /METHOD=SSTYPE(3) /PLOT=PROFILE(Time*Limb) /PRINT=DESCRIPTIVE ETASQ OPOWER HOMOGENEITY /CRITERIA=ALPHA(.05) /WSDESIGN=Limb Time Limb*Time.	
Resources	Processor Time	00:00:00.31
	Elapsed Time	00:00:00.00

[DataSet1] /Users/jemcheng/Documents/VDL | M.Sc/Projects/ASPEN/Statistics/ASPEN complete.sav

Warnings
The HOMOGENEITY specification in the PRINT subcommand will be ignored because there are no between-subjects factors.

Within-Subjects Factors

Measure: MEASURE_1

Limb	Time	Dependent Variable
1	1	CON_CUFF_ESSAntero_Pre
	2	CON_CUFF_ESSAntero_Dur
2	1	EXP_CUFF_ESSAntero_Pre
	2	EXP_CUFF_ESSAntero_Dur

Descriptive Statistics

	Mean	Std. Deviation	N
CON_CUFF_ESSAntero_Pre	11.5140	1.63215	10
CON_CUFF_ESSAntero_Dur	11.6870	1.43618	10
EXP_CUFF_ESSAntero_Pre	17.8960	4.07218	10
EXP_CUFF_ESSAntero_Dur	43.0230	12.40887	10

Multivariate Tests[a]

Effect	Value	F	Hypothesis df	Error df	Sig.	Partial Eta Squared	Noncent. Parameter	Observed Power[c]	
Limb	Pillai's Trace	.901	81.679[b]	1.000	9.000	.000	.901	81.679	1.000
	Wilks' Lambda	.099	81.679[b]	1.000	9.000	.000	.901	81.679	1.000
	Hotelling's Trace	9.075	81.679[b]	1.000	9.000	.000	.901	81.679	1.000
	Roy's Largest Root	9.075	81.679[b]	1.000	9.000	.000	.901	81.679	1.000
Time	Pillai's Trace	.839	46.823[b]	1.000	9.000	.000	.839	46.823	1.000
	Wilks' Lambda	.161	46.823[b]	1.000	9.000	.000	.839	46.823	1.000
	Hotelling's Trace	5.203	46.823[b]	1.000	9.000	.000	.839	46.823	1.000
	Roy's Largest Root	5.203	46.823[b]	1.000	9.000	.000	.839	46.823	1.000
Limb * Time	Pillai's Trace	.826	42.578[b]	1.000	9.000	.000	.826	42.578	1.000
	Wilks' Lambda	.174	42.578[b]	1.000	9.000	.000	.826	42.578	1.000
	Hotelling's Trace	4.731	42.578[b]	1.000	9.000	.000	.826	42.578	1.000
	Roy's Largest Root	4.731	42.578[b]	1.000	9.000	.000	.826	42.578	1.000

a. Design: Intercept
Within Subjects Design: Limb + Time + Limb * Time

b. Exact statistic
c. Computed using alpha =

Mauchly's Test of Sphericity[a]

Measure: MEASURE_1

Within Subjects Effect	Mauchly's W	Approx. Chi-Square	df	Sig.	Epsilon[b]		
					Greenhouse-Geisser	Huynh-Feldt	Lower-bound
Limb	1.000	.000	0	.	1.000	1.000	1.000
Time	1.000	.000	0	.	1.000	1.000	1.000
Limb * Time	1.000	.000	0	.	1.000	1.000	1.000

Tests the null hypothesis that the error covariance matrix of the orthonormalized transformed dependent variables is proportional to an identity matrix.

a. Design: Intercept
Within Subjects Design: Limb + Time + Limb * Time

b. May be used to adjust the degrees of freedom for the averaged tests of significance. Corrected tests are displayed in the Tests of Within-Subjects Effects table.

Tests of Within-Subjects Effects

Measure: MEASURE_1

Source	Type III Sum of Squares	df	Mean Square	F	Sig.	Partial Eta Squared	Noncent. Parameter	Observed Power[a]	
Limb	Sphericity Assumed	3556.619	1	3556.619	81.679	.000	.901	81.679	1.000
	Greenhouse-	3556.619	1.000	3556.619	81.679	.000	.901	81.679	1.000

	Geisser								
	Huynh-Feldt	3556.619	1.000	3556.619	81.679	.000	.901	81.679	1.000
	Lower-bound	3556.619	1.000	3556.619	81.679	.000	.901	81.679	1.000
Error(Limb)	Sphericity Assumed	391.893	9	43.544					
	Greenhouse-Geisser	391.893	9.000	43.544					
	Huynh-Feldt	391.893	9.000	43.544					
	Lower-bound	391.893	9.000	43.544					
Time	Sphericity Assumed	1600.225	1	1600.225	46.823	.000	.839	46.823	1.000
	Greenhouse-Geisser	1600.225	1.000	1600.225	46.823	.000	.839	46.823	1.000
	Huynh-Feldt	1600.225	1.000	1600.225	46.823	.000	.839	46.823	1.000
	Lower-bound	1600.225	1.000	1600.225	46.823	.000	.839	46.823	1.000
Error(Time)	Sphericity Assumed	307.586	9	34.176					
	Greenhouse-Geisser	307.586	9.000	34.176					
	Huynh-Feldt	307.586	9.000	34.176					
	Lower-bound	307.586	9.000	34.176					
Limb * Time	Sphericity Assumed	1556.755	1	1556.755	42.578	.000	.826	42.578	1.000
	Greenhouse-Geisser	1556.755	1.000	1556.755	42.578	.000	.826	42.578	1.000
	Huynh-Feldt	1556.755	1.000	1556.755	42.578	.000	.826	42.578	1.000
	Lower-bound	1556.755	1.000	1556.755	42.578	.000	.826	42.578	1.000
Error(Limb*Time)	Sphericity Assumed	329.060	9	36.562					
	Greenhouse-Geisser	329.060	9.000	36.562					
	Huynh-Feldt	329.060	9.000	36.562					
	Lower-bound	329.060	9.000	36.562					
a. Computed using alpha =									

Tests of Within-Subjects Contrasts

Measure: MEASURE_1

Source	Limb	Time	Type III Sum of Squares	df	Mean Square	F	Sig.	Partial Eta Squared	Noncent. Parameter	Observed Power[a]
Limb	Linear		3556.619	1	3556.619	81.679	.000	.901	81.679	1.000
Error(Limb)	Linear		391.893	9	43.544					
Time		Linear	1600.225	1	1600.225	46.823	.000	.839	46.823	1.000
Error(Time)		Linear	307.586	9	34.176					
Limb * Time	Linear	Linear	1556.755	1	1556.755	42.578	.000	.826	42.578	1.000
Error(Limb*Time)	Linear	Linear	329.060	9	36.562					

a. Computed using alpha =

Tests of Between-Subjects Effects

Measure: MEASURE_1
Transformed Variable: Average

Source	Type III Sum of Squares	df	Mean Square	F	Sig.	Partial Eta Squared	Noncent. Parameter	Observed Power[a]
Intercept	17690.436	1	17690.436	289.973	.000	.970	289.973	1.000
Error	549.065	9	61.007					

a. Computed using alpha =

Table B6. CUFF Retrograde Shear Stress

General Linear Model

Notes		
Output Created	11-JUL-2017 10:54:48	
Comments		
Input	Data	/Users/jemcheng/Documents/VDL | M.Sc/Projects/ASPEN/Statistics/ASPEN complete.sav
	Active Dataset	DataSet1
	Filter	<none>
	Weight	<none>
	Split File	<none>
	N of Rows in Working Data File	20
Missing Value Handling	Definition of Missing	User-defined missing values are treated as missing.
	Cases Used	Statistics are based on all cases with valid data for all variables in the model.
Syntax	GLM CON_CUFF_ESSRetro_Pre CON_CUFF_ESSRetro_Dur EXP_CUFF_ESSRetro_Pre EXP_CUFF_ESSRetro_Dur /WSFACTOR=Limb 2 Polynomial Time 2 Polynomial /METHOD=SSTYPE(3) /PLOT=PROFILE(Time*Limb) /PRINT=DESCRIPTIVE ETASQ OPOWER HOMOGENEITY /CRITERIA=ALPHA(.05) /WSDESIGN=Limb Time Limb*Time.	
Resources	Processor Time	00:00:00.33
	Elapsed Time	00:00:01.00

[DataSet1] /Users/jemcheng/Documents/VDL | M.Sc/Projects/ASPEN/Statistics/ASPEN complete.sav

Warnings

The HOMOGENEITY specification in the PRINT subcommand will be ignored because there are no between-subjects factors.

Within-Subjects Factors

Measure: MEASURE_1

Limb	Time	Dependent Variable
1	1	CON_CUFF_ESSRetro_Pre
	2	CON_CUFF_ESSRetro_Dur
2	1	EXP_CUFF_ESSRetro_Pre
	2	EXP_CUFF_ESSRetro_Dur

Descriptive Statistics

	Mean	Std. Deviation	N
CON_CUFF_ESSRetro_Pre	-2.3300	1.12897	10
CON_CUFF_ESSRetro_Dur	-2.9210	1.60799	10
EXP_CUFF_ESSRetro_Pre	-3.0750	2.51279	10
EXP_CUFF_ESSRetro_Dur	-22.6620	6.04879	10

Multivariate Tests[a]

Effect	Value	F	Hypothesis df	Error df	Sig.	Partial Eta Squared	Noncent. Parameter	Observed Power[c]	
Limb	Pillai's Trace	.912	93.183[b]	1.000	9.000	.000	.912	93.183	1.000
	Wilks' Lambda	.088	93.183[b]	1.000	9.000	.000	.912	93.183	1.000
	Hotelling's Trace	10.354	93.183[b]	1.000	9.000	.000	.912	93.183	1.000
	Roy's Largest Root	10.354	93.183[b]	1.000	9.000	.000	.912	93.183	1.000
Time	Pillai's Trace	.951	173.836[b]	1.000	9.000	.000	.951	173.836	1.000
	Wilks' Lambda	.049	173.836[b]	1.000	9.000	.000	.951	173.836	1.000
	Hotelling's Trace	19.315	173.836[b]	1.000	9.000	.000	.951	173.836	1.000
	Roy's Largest Root	19.315	173.836[b]	1.000	9.000	.000	.951	173.836	1.000
Limb * Time	Pillai's Trace	.964	243.667[b]	1.000	9.000	.000	.964	243.667	1.000
	Wilks' Lambda	.036	243.667[b]	1.000	9.000	.000	.964	243.667	1.000
	Hotelling's Trace	27.074	243.667[b]	1.000	9.000	.000	.964	243.667	1.000
	Roy's Largest Root	27.074	243.667[b]	1.000	9.000	.000	.964	243.667	1.000

a. Design: Intercept
Within Subjects Design: Limb + Time + Limb * Time

b. Exact statistic
c. Computed using alpha =

Mauchly's Test of Sphericity[a]

Measure: MEASURE_1

Within Subjects Effect	Mauchly's W	Approx. Chi-Square	df	Sig.	Epsilon[b]		
					Greenhouse-Geisser	Huynh-Feldt	Lower-bound
Limb	1.000	.000	0	.	1.000	1.000	1.000
Time	1.000	.000	0	.	1.000	1.000	1.000
Limb * Time	1.000	.000	0	.	1.000	1.000	1.000

Tests the null hypothesis that the error covariance matrix of the orthonormalized transformed dependent variables is proportional to an identity matrix.

a. Design: Intercept
Within Subjects Design: Limb + Time + Limb * Time

b. May be used to adjust the degrees of freedom for the averaged tests of significance. Corrected tests are displayed in the Tests of Within-Subjects Effects table.

Tests of Within-Subjects Effects

Measure: MEASURE_1

Source	Type III Sum of Squares	df	Mean Square	F	Sig.	Partial Eta Squared	Noncent. Parameter	Observed Power[a]	
Limb	Sphericity Assumed	1049.190	1	1049.190	93.183	.000	.912	93.183	1.000
	Greenhouse-	1049.190	1.000	1049.190	93.183	.000	.912	93.183	1.000

	Geisser								
	Huynh-Feldt	1049.190	1.000	1049.190	93.183	.000	.912	93.183	1.000
	Lower-bound	1049.190	1.000	1049.190	93.183	.000	.912	93.183	1.000
Error(Limb)	Sphericity Assumed	101.335	9	11.259					
	Greenhouse-Geisser	101.335	9.000	11.259					
	Huynh-Feldt	101.335	9.000	11.259					
	Lower-bound	101.335	9.000	11.259					
Time	Sphericity Assumed	1017.879	1	1017.879	173.836	.000	.951	173.836	1.000
	Greenhouse-Geisser	1017.879	1.000	1017.879	173.836	.000	.951	173.836	1.000
	Huynh-Feldt	1017.879	1.000	1017.879	173.836	.000	.951	173.836	1.000
	Lower-bound	1017.879	1.000	1017.879	173.836	.000	.951	173.836	1.000
Error(Time)	Sphericity Assumed	52.699	9	5.855					
	Greenhouse-Geisser	52.699	9.000	5.855					
	Huynh-Feldt	52.699	9.000	5.855					
	Lower-bound	52.699	9.000	5.855					
Limb * Time	Sphericity Assumed	902.120	1	902.120	243.667	.000	.964	243.667	1.000
	Greenhouse-Geisser	902.120	1.000	902.120	243.667	.000	.964	243.667	1.000
	Huynh-Feldt	902.120	1.000	902.120	243.667	.000	.964	243.667	1.000
	Lower-bound	902.120	1.000	902.120	243.667	.000	.964	243.667	1.000
Error(Limb*Time)	Sphericity Assumed	33.320	9	3.702					
	Greenhouse-Geisser	33.320	9.000	3.702					
	Huynh-Feldt	33.320	9.000	3.702					
	Lower-bound	33.320	9.000	3.702					
a. Computed using alpha =									

Tests of Within-Subjects Contrasts

Measure: MEASURE_1

Source	Limb	Time	Type III Sum of Squares	df	Mean Square	F	Sig.	Partial Eta Squared	Noncent. Parameter	Observed Power[a]
Limb	Linear		1049.190	1	1049.190	93.183	.000	.912	93.183	1.000
Error(Limb)	Linear		101.335	9	11.259					
Time		Linear	1017.879	1	1017.879	173.836	.000	.951	173.836	1.000
Error(Time)		Linear	52.699	9	5.855					
Limb * Time	Linear	Linear	902.120	1	902.120	243.667	.000	.964	243.667	1.000
Error(Limb*Time)	Linear	Linear	33.320	9	3.702					

a. Computed using alpha =

Tests of Between-Subjects Effects

Measure: MEASURE_1
Transformed Variable: Average

Source	Type III Sum of Squares	df	Mean Square	F	Sig.	Partial Eta Squared	Noncent. Parameter	Observed Power[a]
Intercept	2400.640	1	2400.640	92.528	.000	.911	92.528	1.000
Error	233.505	9	25.945					

a. Computed using alpha =

Table B7. CUFF Oscillatory Shear Index

General Linear Model

Notes		
Output Created	11-JUL-2017 10:56:22	
Comments		
Input	Data	/Users/jemcheng/Documents/VDL | M.Sc/Projects/ASPEN/Statistics/ASPEN complete.sav
	Active Dataset	DataSet1
	Filter	<none>
	Weight	<none>
	Split File	<none>
	N of Rows in Working Data File	20
Missing Value Handling	Definition of Missing	User-defined missing values are treated as missing.
	Cases Used	Statistics are based on all cases with valid data for all variables in the model.
Syntax	GLM CON_CUFF_OSI_Pre CON_CUFF_OSI_Dur EXP_CUFF_OSI_Pre EXP_CUFF_OSI_Dur /WSFACTOR=Limb 2 Polynomial Time 2 Polynomial /METHOD=SSTYPE(3) /PLOT=PROFILE(Time*Limb) /PRINT=DESCRIPTIVE ETASQ OPOWER HOMOGENEITY /CRITERIA=ALPHA(.05) /WSDESIGN=Limb Time Limb*Time.	
Resources	Processor Time	00:00:00.22
	Elapsed Time	00:00:00.00

[DataSet1] /Users/jemcheng/Documents/VDL | M.Sc/Projects/ASPEN/Statistics/ASPEN complete.sav

Warnings

The HOMOGENEITY specification in the PRINT subcommand will be ignored because there are no between-subjects factors.

Within-Subjects Factors

Measure: MEASURE_1

Limb	Time	Dependent Variable
1	1	CON_CUFF_OSI_Pre
	2	CON_CUFF_OSI_Dur
2	1	EXP_CUFF_OSI_Pre
	2	EXP_CUFF_OSI_Dur

Descriptive Statistics

	Mean	Std. Deviation	N
CON_CUFF_OSI_Pre	.1608	.05681	10
CON_CUFF_OSI_Dur	.1880	.07530	10
EXP_CUFF_OSI_Pre	.1441	.08879	10
EXP_CUFF_OSI_Dur	.3474	.03493	10

Multivariate Tests[a]

Effect	Value	F	Hypothesis df	Error df	Sig.	Partial Eta Squared	Noncent. Parameter	Observed Power[c]	
Limb	Pillai's Trace	.543	10.700[b]	1.000	9.000	.010	.543	10.700	.829
	Wilks' Lambda	.457	10.700[b]	1.000	9.000	.010	.543	10.700	.829
	Hotelling's Trace	1.189	10.700[b]	1.000	9.000	.010	.543	10.700	.829
	Roy's Largest Root	1.189	10.700[b]	1.000	9.000	.010	.543	10.700	.829
Time	Pillai's Trace	.871	60.793[b]	1.000	9.000	.000	.871	60.793	1.000
	Wilks' Lambda	.129	60.793[b]	1.000	9.000	.000	.871	60.793	1.000
	Hotelling's Trace	6.755	60.793[b]	1.000	9.000	.000	.871	60.793	1.000
	Roy's Largest Root	6.755	60.793[b]	1.000	9.000	.000	.871	60.793	1.000
Limb * Time	Pillai's Trace	.837	46.062[b]	1.000	9.000	.000	.837	46.062	1.000
	Wilks' Lambda	.163	46.062[b]	1.000	9.000	.000	.837	46.062	1.000
	Hotelling's Trace	5.118	46.062[b]	1.000	9.000	.000	.837	46.062	1.000
	Roy's Largest Root	5.118	46.062[b]	1.000	9.000	.000	.837	46.062	1.000

a. Design: Intercept
Within Subjects Design: Limb + Time + Limb * Time

b. Exact statistic

c. Computed using alpha =	

Mauchly's Test of Sphericity[a]

Measure: MEASURE_1

Within Subjects Effect	Mauchly's W	Approx. Chi-Square	df	Sig.	Epsilon[b]		
					Greenhouse-Geisser	Huynh-Feldt	Lower-bound
Limb	1.000	.000	0	.	1.000	1.000	1.000
Time	1.000	.000	0	.	1.000	1.000	1.000
Limb * Time	1.000	.000	0	.	1.000	1.000	1.000

Tests the null hypothesis that the error covariance matrix of the orthonormalized transformed dependent variables is proportional to an identity matrix.

a. Design: Intercept
Within Subjects Design: Limb + Time + Limb * Time

b. May be used to adjust the degrees of freedom for the averaged tests of significance. Corrected tests are displayed in the Tests of Within-Subjects Effects table.

Tests of Within-Subjects Effects

Measure: MEASURE_1

Source	Type III Sum of Squares	df	Mean Square	F	Sig.	Partial Eta Squared	Noncent. Parameter	Observed Power[a]	
Limb	Sphericity Assumed	.051	1	.051	10.700	.010	.543	10.700	.829
	Greenhouse-Geisser	.051	1.000	.051	10.700	.010	.543	10.700	.829

	Huynh-Feldt	.051	1.000	.051	10.700	.010	.543	10.700	.829
	Lower-bound	.051	1.000	.051	10.700	.010	.543	10.700	.829
Error(Limb)	Sphericity Assumed	.043	9	.005					
	Greenhouse-Geisser	.043	9.000	.005					
	Huynh-Feldt	.043	9.000	.005					
	Lower-bound	.043	9.000	.005					
Time	Sphericity Assumed	.133	1	.133	60.793	.000	.871	60.793	1.000
	Greenhouse-Geisser	.133	1.000	.133	60.793	.000	.871	60.793	1.000
	Huynh-Feldt	.133	1.000	.133	60.793	.000	.871	60.793	1.000
	Lower-bound	.133	1.000	.133	60.793	.000	.871	60.793	1.000
Error(Time)	Sphericity Assumed	.020	9	.002					
	Greenhouse-Geisser	.020	9.000	.002					
	Huynh-Feldt	.020	9.000	.002					
	Lower-bound	.020	9.000	.002					
Limb * Time	Sphericity Assumed	.077	1	.077	46.062	.000	.837	46.062	1.000
	Greenhouse-Geisser	.077	1.000	.077	46.062	.000	.837	46.062	1.000
	Huynh-Feldt	.077	1.000	.077	46.062	.000	.837	46.062	1.000
	Lower-bound	.077	1.000	.077	46.062	.000	.837	46.062	1.000
Error(Limb*Time)	Sphericity Assumed	.015	9	.002					
	Greenhouse-Geisser	.015	9.000	.002					
	Huynh-Feldt	.015	9.000	.002					
	Lower-bound	.015	9.000	.002					

a. Computed using alpha =

Tests of Within-Subjects Contrasts

Measure: MEASURE_1

Source	Limb	Time	Type III Sum of Squares	df	Mean Square	F	Sig.	Partial Eta Squared	Noncent. Parameter	Observed Power[a]
Limb	Linear		.051	1	.051	10.700	.010	.543	10.700	.829
Error(Limb)	Linear		.043	9	.005					
Time		Linear	.133	1	.133	60.793	.000	.871	60.793	1.000
Error(Time)		Linear	.020	9	.002					
Limb * Time	Linear	Linear	.077	1	.077	46.062	.000	.837	46.062	1.000
Error(Limb*Time)	Linear	Linear	.015	9	.002					

a. Computed using alpha =

Tests of Between-Subjects Effects

Measure: MEASURE_1
Transformed Variable: Average

Source	Type III Sum of Squares	df	Mean Square	F	Sig.	Partial Eta Squared	Noncent. Parameter	Observed Power[a]
Intercept	1.765	1	1.765	188.217	.000	.954	188.217	1.000
Error	.084	9	.009					

a. Computed using alpha =

Table B8. CUFF FMD%

General Linear Model

Notes		
Output Created	17-JUL-2017 13:18:07	
Comments		
Input	Data	/Users/jemcheng/Documents/VDL | M.Sc/Projects/ASPEN/Statistics/ASPEN complete.sav
	Active Dataset	DataSet1
	Filter	<none>
	Weight	<none>
	Split File	<none>
	N of Rows in Working Data File	20
Missing Value Handling	Definition of Missing	User-defined missing values are treated as missing.
	Cases Used	Statistics are based on all cases with valid data for all variables in the model.
Syntax	GLM CON_CUFF_FMD_Pre CON_CUFF_FMD_Post EXP_CUFF_FMD_Pre EXP_CUFF_FMD_Post /WSFACTOR=Limb 2 Polynomial Time 2 Polynomial /METHOD=SSTYPE(3) /PLOT=PROFILE(Time*Limb) /PRINT=DESCRIPTIVE ETASQ OPOWER HOMOGENEITY /CRITERIA=ALPHA(.05) /WSDESIGN=Limb Time Limb*Time.	
Resources	Processor Time	00:00:00.23
	Elapsed Time	00:00:01.00

[DataSet1] /Users/jemcheng/Documents/VDL | M.Sc/Projects/ASPEN/Statistics/ASPEN complete.sav

Warnings

The HOMOGENEITY specification in the PRINT subcommand will be ignored because there are no between-subjects factors.

Within-Subjects Factors

Measure: MEASURE_1

Limb	Time	Dependent Variable
1	1	CON_CUFF_FMD_Pre
	2	CON_CUFF_FMD_Post
2	1	EXP_CUFF_FMD_Pre
	2	EXP_CUFF_FMD_Post

Descriptive Statistics

	Mean	Std. Deviation	N
CON_CUFF_FMD_Pre	3.9320	1.44870	10
CON_CUFF_FMD_Post	4.3470	1.30462	10
EXP_CUFF_FMD_Pre	6.7830	2.80221	10
EXP_CUFF_FMD_Post	7.8920	2.91902	10

Multivariate Tests[a]

Effect	Value	F	Hypothesis df	Error df	Sig.	Partial Eta Squared	Noncent. Parameter	Observed Power[c]	
Limb	Pillai's Trace	.775	30.913[b]	1.000	9.000	.000	.775	30.913	.998
	Wilks' Lambda	.225	30.913[b]	1.000	9.000	.000	.775	30.913	.998
	Hotelling's Trace	3.435	30.913[b]	1.000	9.000	.000	.775	30.913	.998
	Roy's Largest Root	3.435	30.913[b]	1.000	9.000	.000	.775	30.913	.998
Time	Pillai's Trace	.237	2.799[b]	1.000	9.000	.129	.237	2.799	.322
	Wilks' Lambda	.763	2.799[b]	1.000	9.000	.129	.237	2.799	.322
	Hotelling's Trace	.311	2.799[b]	1.000	9.000	.129	.237	2.799	.322
	Roy's Largest Root	.311	2.799[b]	1.000	9.000	.129	.237	2.799	.322
Limb * Time	Pillai's Trace	.079	.771[b]	1.000	9.000	.403	.079	.771	.123
	Wilks' Lambda	.921	.771[b]	1.000	9.000	.403	.079	.771	.123
	Hotelling's Trace	.086	.771[b]	1.000	9.000	.403	.079	.771	.123
	Roy's Largest Root	.086	.771[b]	1.000	9.000	.403	.079	.771	.123

a. Design: Intercept
Within Subjects Design: Limb + Time + Limb * Time

b. Exact statistic

c. Computed using alpha =	

Mauchly's Test of Sphericity[a]

Measure: MEASURE_1

Within Subjects Effect	Mauchly's W	Approx. Chi-Square	df	Sig.	Epsilon[b]		
					Greenhouse-Geisser	Huynh-Feldt	Lower-bound
Limb	1.000	.000	0	.	1.000	1.000	1.000
Time	1.000	.000	0	.	1.000	1.000	1.000
Limb * Time	1.000	.000	0	.	1.000	1.000	1.000

Tests the null hypothesis that the error covariance matrix of the orthonormalized transformed dependent variables is proportional to an identity matrix.

a. Design: Intercept
Within Subjects Design: Limb + Time + Limb * Time

b. May be used to adjust the degrees of freedom for the averaged tests of significance. Corrected tests are displayed in the Tests of Within-Subjects Effects table.

Tests of Within-Subjects Effects

Measure: MEASURE_1

Source	Type III Sum of Squares	df	Mean Square	F	Sig.	Partial Eta Squared	Noncent. Parameter	Observed Power[a]	
Limb	Sphericity Assumed	102.272	1	102.272	30.913	.000	.775	30.913	.998
	Greenhouse-Geisser	102.272	1.000	102.272	30.913	.000	.775	30.913	.998

	Huynh-Feldt	102.272	1.000	102.272	30.913	.000	.775	30.913	.998
	Lower-bound	102.272	1.000	102.272	30.913	.000	.775	30.913	.998
Error(Limb)	Sphericity Assumed	29.776	9	3.308					
	Greenhouse-Geisser	29.776	9.000	3.308					
	Huynh-Feldt	29.776	9.000	3.308					
	Lower-bound	29.776	9.000	3.308					
Time	Sphericity Assumed	5.806	1	5.806	2.799	.129	.237	2.799	.322
	Greenhouse-Geisser	5.806	1.000	5.806	2.799	.129	.237	2.799	.322
	Huynh-Feldt	5.806	1.000	5.806	2.799	.129	.237	2.799	.322
	Lower-bound	5.806	1.000	5.806	2.799	.129	.237	2.799	.322
Error(Time)	Sphericity Assumed	18.669	9	2.074					
	Greenhouse-Geisser	18.669	9.000	2.074					
	Huynh-Feldt	18.669	9.000	2.074					
	Lower-bound	18.669	9.000	2.074					
Limb * Time	Sphericity Assumed	1.204	1	1.204	.771	.403	.079	.771	.123
	Greenhouse-Geisser	1.204	1.000	1.204	.771	.403	.079	.771	.123
	Huynh-Feldt	1.204	1.000	1.204	.771	.403	.079	.771	.123
	Lower-bound	1.204	1.000	1.204	.771	.403	.079	.771	.123
Error(Limb*Time)	Sphericity Assumed	14.062	9	1.562					
	Greenhouse-Geisser	14.062	9.000	1.562					
	Huynh-Feldt	14.062	9.000	1.562					
	Lower-bound	14.062	9.000	1.562					
a. Computed using alpha =									

Tests of Within-Subjects Contrasts

Measure: MEASURE_1

Source	Limb	Time	Type III Sum of Squares	df	Mean Square	F	Sig.	Partial Eta Squared	Noncent. Parameter	Observed Power[a]
Limb	Linear		102.272	1	102.272	30.913	.000	.775	30.913	.998
Error(Limb)	Linear		29.776	9	3.308					
Time		Linear	5.806	1	5.806	2.799	.129	.237	2.799	.322
Error(Time)		Linear	18.669	9	2.074					
Limb * Time	Linear	Linear	1.204	1	1.204	.771	.403	.079	.771	.123
Error(Limb*Time)	Linear	Linear	14.062	9	1.562					

a. Computed using alpha =

Tests of Between-Subjects Effects

Measure: MEASURE_1
Transformed Variable: Average

Source	Type III Sum of Squares	df	Mean Square	F	Sig.	Partial Eta Squared	Noncent. Parameter	Observed Power[a]
Intercept	1317.215	1	1317.215	99.573	.000	.917	99.573	1.000
Error	119.058	9	13.229					

a. Computed using alpha =

Table B9. HGEX Anterograde Shear Stress

General Linear Model

Notes		
Output Created	11-JUL-2017 10:58:08	
Comments		
Input	Data	/Users/jemcheng/Documents/VDL | M.Sc/Projects/ASPEN/Statistics/ASPEN complete.sav
	Active Dataset	DataSet1
	Filter	<none>
	Weight	<none>
	Split File	<none>
	N of Rows in Working Data File	20
Missing Value Handling	Definition of Missing	User-defined missing values are treated as missing.
	Cases Used	Statistics are based on all cases with valid data for all variables in the model.
Syntax	GLM CON_HGEX_ESSAntero_Pre CON_HGEX_ESSAntero_Dur EXP_HGEX_ESSAntero_Pre EXP_HGEX_ESSAntero_Dur /WSFACTOR=Limb 2 Polynomial Time 2 Polynomial /METHOD=SSTYPE(3) /PLOT=PROFILE(Time*Limb) /PRINT=DESCRIPTIVE ETASQ OPOWER HOMOGENEITY /CRITERIA=ALPHA(.05) /WSDESIGN=Limb Time Limb*Time.	
Resources	Processor Time	00:00:00.22
	Elapsed Time	00:00:01.00

[DataSet1] /Users/jemcheng/Documents/VDL | M.Sc/Projects/ASPEN/Statistics/ASPEN complete.sav

Warnings

The HOMOGENEITY specification in the PRINT subcommand will be ignored because there are no between-subjects factors.

Within-Subjects Factors

Measure: MEASURE_1

Limb	Time	Dependent Variable
1	1	CON_HGEX_ESSAntero_Pre
	2	CON_HGEX_ESSAntero_Dur
2	1	EXP_HGEX_ESSAntero_Pre
	2	EXP_HGEX_ESSAntero_Dur

Descriptive Statistics

	Mean	Std. Deviation	N
CON_HGEX_ESSAntero_Pre	14.1880	3.48314	10
CON_HGEX_ESSAntero_Dur	14.5200	3.57896	10
EXP_HGEX_ESSAntero_Pre	18.7030	5.90595	10
EXP_HGEX_ESSAntero_Dur	56.4180	11.52309	10

Multivariate Tests[a]

Effect	Value	F	Hypothesis df	Error df	Sig.	Partial Eta Squared	Noncent. Parameter	Observed Power[c]	
Limb	Pillai's Trace	.913	93.904[b]	1.000	9.000	.000	.913	93.904	1.000
	Wilks' Lambda	.087	93.904[b]	1.000	9.000	.000	.913	93.904	1.000
	Hotelling's Trace	10.434	93.904[b]	1.000	9.000	.000	.913	93.904	1.000
	Roy's Largest Root	10.434	93.904[b]	1.000	9.000	.000	.913	93.904	1.000
Time	Pillai's Trace	.933	125.232[b]	1.000	9.000	.000	.933	125.232	1.000
	Wilks' Lambda	.067	125.232[b]	1.000	9.000	.000	.933	125.232	1.000
	Hotelling's Trace	13.915	125.232[b]	1.000	9.000	.000	.933	125.232	1.000
	Roy's Largest Root	13.915	125.232[b]	1.000	9.000	.000	.933	125.232	1.000
Limb * Time	Pillai's Trace	.874	62.190[b]	1.000	9.000	.000	.874	62.190	1.000
	Wilks' Lambda	.126	62.190[b]	1.000	9.000	.000	.874	62.190	1.000
	Hotelling's Trace	6.910	62.190[b]	1.000	9.000	.000	.874	62.190	1.000
	Roy's Largest Root	6.910	62.190[b]	1.000	9.000	.000	.874	62.190	1.000

a. Design: Intercept
Within Subjects Design: Limb + Time + Limb * Time

b. Exact statistic
c. Computed using alpha =

Mauchly's Test of Sphericity[a]

Measure: MEASURE_1

Within Subjects Effect	Mauchly's W	Approx. Chi-Square	df	Sig.	Epsilon[b]		
					Greenhouse-Geisser	Huynh-Feldt	Lower-bound
Limb	1.000	.000	0	.	1.000	1.000	1.000
Time	1.000	.000	0	.	1.000	1.000	1.000
Limb * Time	1.000	.000	0	.	1.000	1.000	1.000

Tests the null hypothesis that the error covariance matrix of the orthonormalized transformed dependent variables is proportional to an identity matrix.

a. Design: Intercept
Within Subjects Design: Limb + Time + Limb * Time

b. May be used to adjust the degrees of freedom for the averaged tests of significance. Corrected tests are displayed in the Tests of Within-Subjects Effects table.

Tests of Within-Subjects Effects

Measure: MEASURE_1

Source	Type III Sum of Squares	df	Mean Square	F	Sig.	Partial Eta Squared	Noncent. Parameter	Observed Power[a]	
Limb	Sphericity Assumed	5385.416	1	5385.416	93.904	.000	.913	93.904	1.000
	Greenhouse-	5385.416	1.000	5385.416	93.904	.000	.913	93.904	1.000

	Geisser								
	Huynh-Feldt	5385.416	1.000	5385.416	93.904	.000	.913	93.904	1.000
	Lower-bound	5385.416	1.000	5385.416	93.904	.000	.913	93.904	1.000
Error(Limb)	Sphericity Assumed	516.155	9	57.351					
	Greenhouse-Geisser	516.155	9.000	57.351					
	Huynh-Feldt	516.155	9.000	57.351					
	Lower-bound	516.155	9.000	57.351					
Time	Sphericity Assumed	3618.936	1	3618.936	125.232	.000	.933	125.232	1.000
	Greenhouse-Geisser	3618.936	1.000	3618.936	125.232	.000	.933	125.232	1.000
	Huynh-Feldt	3618.936	1.000	3618.936	125.232	.000	.933	125.232	1.000
	Lower-bound	3618.936	1.000	3618.936	125.232	.000	.933	125.232	1.000
Error(Time)	Sphericity Assumed	260.081	9	28.898					
	Greenhouse-Geisser	260.081	9.000	28.898					
	Huynh-Feldt	260.081	9.000	28.898					
	Lower-bound	260.081	9.000	28.898					
Limb * Time	Sphericity Assumed	3493.722	1	3493.722	62.190	.000	.874	62.190	1.000
	Greenhouse-Geisser	3493.722	1.000	3493.722	62.190	.000	.874	62.190	1.000
	Huynh-Feldt	3493.722	1.000	3493.722	62.190	.000	.874	62.190	1.000
	Lower-bound	3493.722	1.000	3493.722	62.190	.000	.874	62.190	1.000
Error(Limb*Time)	Sphericity Assumed	505.606	9	56.178					
	Greenhouse-Geisser	505.606	9.000	56.178					
	Huynh-Feldt	505.606	9.000	56.178					
	Lower-bound	505.606	9.000	56.178					
a. Computed using alpha =									

Tests of Within-Subjects Contrasts

Measure: MEASURE_1

Source	Limb	Time	Type III Sum of Squares	df	Mean Square	F	Sig.	Partial Eta Squared	Noncent. Parameter	Observed Power[a]
Limb	Linear		5385.416	1	5385.416	93.904	.000	.913	93.904	1.000
Error(Limb)	Linear		516.155	9	57.351					
Time		Linear	3618.936	1	3618.936	125.232	.000	.933	125.232	1.000
Error(Time)		Linear	260.081	9	28.898					
Limb * Time	Linear	Linear	3493.722	1	3493.722	62.190	.000	.874	62.190	1.000
Error(Limb*Time)	Linear	Linear	505.606	9	56.178					

a. Computed using alpha =

Tests of Between-Subjects Effects

Measure: MEASURE_1
Transformed Variable: Average

Source	Type III Sum of Squares	df	Mean Square	F	Sig.	Partial Eta Squared	Noncent. Parameter	Observed Power[a]
Intercept	26951.153	1	26951.153	537.130	.000	.984	537.130	1.000
Error	451.586	9	50.176					

a. Computed using alpha =

Table B10. HGEX Retrograde Shear Stress

General Linear Model

Notes		
Output Created	11-JUL-2017 10:57:46	
Comments		
Input	Data	/Users/jemcheng/Documents/VDL | M.Sc/Projects/ASPEN/Statistics/ASPEN complete.sav
	Active Dataset	DataSet1
	Filter	<none>
	Weight	<none>
	Split File	<none>
	N of Rows in Working Data File	20
Missing Value Handling	Definition of Missing	User-defined missing values are treated as missing.
	Cases Used	Statistics are based on all cases with valid data for all variables in the model.
Syntax	GLM CON_HGEX_ESSRetro_Pre CON_HGEX_ESSRetro_Dur EXP_HGEX_ESSRetro_Pre EXP_HGEX_ESSRetro_Dur /WSFACTOR=Limb 2 Polynomial Time 2 Polynomial /METHOD=SSTYPE(3) /PLOT=PROFILE(Time*Limb) /PRINT=DESCRIPTIVE ETASQ OPOWER HOMOGENEITY /CRITERIA=ALPHA(.05) /WSDESIGN=Limb Time Limb*Time.	
Resources	Processor Time	00:00:00.31
	Elapsed Time	00:00:00.00

[DataSet1] /Users/jemcheng/Documents/VDL | M.Sc/Projects/ASPEN/Statistics/ASPEN complete.sav

Warnings

The HOMOGENEITY specification in the PRINT subcommand will be ignored because there are no between-subjects factors.

Within-Subjects Factors

Measure: MEASURE_1

Limb	Time	Dependent Variable
1	1	CON_HGEX_ESSRetro_Pre
	2	CON_HGEX_ESSRetro_Dur
2	1	EXP_HGEX_ESSRetro_Pre
	2	EXP_HGEX_ESSRetro_Dur

Descriptive Statistics

	Mean	Std. Deviation	N
CON_HGEX_ESSRetro_Pre	-3.8130	2.62031	10
CON_HGEX_ESSRetro_Dur	-2.4780	2.03097	10
EXP_HGEX_ESSRetro_Pre	-2.9110	1.71522	10
EXP_HGEX_ESSRetro_Dur	-5.6390	2.97195	10

Multivariate Tests[a]

Effect	Value	F	Hypothesis df	Error df	Sig.	Partial Eta Squared	Noncent. Parameter	Observed Power[c]	
Limb	Pillai's Trace	.307	3.995[b]	1.000	9.000	.077	.307	3.995	.431
	Wilks' Lambda	.693	3.995[b]	1.000	9.000	.077	.307	3.995	.431
	Hotelling's Trace	.444	3.995[b]	1.000	9.000	.077	.307	3.995	.431
	Roy's Largest Root	.444	3.995[b]	1.000	9.000	.077	.307	3.995	.431
Time	Pillai's Trace	.119	1.219[b]	1.000	9.000	.298	.119	1.219	.167
	Wilks' Lambda	.881	1.219[b]	1.000	9.000	.298	.119	1.219	.167
	Hotelling's Trace	.135	1.219[b]	1.000	9.000	.298	.119	1.219	.167
	Roy's Largest Root	.135	1.219[b]	1.000	9.000	.298	.119	1.219	.167
Limb * Time	Pillai's Trace	.421	6.551[b]	1.000	9.000	.031	.421	6.551	.626
	Wilks' Lambda	.579	6.551[b]	1.000	9.000	.031	.421	6.551	.626
	Hotelling's Trace	.728	6.551[b]	1.000	9.000	.031	.421	6.551	.626
	Roy's Largest Root	.728	6.551[b]	1.000	9.000	.031	.421	6.551	.626

a. Design: Intercept
Within Subjects Design: Limb + Time + Limb * Time

b. Exact statistic
c. Computed using alpha =

Mauchly's Test of Sphericity[a]

Measure: MEASURE_1

Within Subjects Effect	Mauchly's W	Approx. Chi-Square	df	Sig.	Epsilon[b]		
					Greenhouse-Geisser	Huynh-Feldt	Lower-bound
Limb	1.000	.000	0	.	1.000	1.000	1.000
Time	1.000	.000	0	.	1.000	1.000	1.000
Limb * Time	1.000	.000	0	.	1.000	1.000	1.000

Tests the null hypothesis that the error covariance matrix of the orthonormalized transformed dependent variables is proportional to an identity matrix.

a. Design: Intercept
Within Subjects Design: Limb + Time + Limb * Time

b. May be used to adjust the degrees of freedom for the averaged tests of significance. Corrected tests are displayed in the Tests of Within-Subjects Effects table.

Tests of Within-Subjects Effects

Measure: MEASURE_1

Source	Type III Sum of Squares	df	Mean Square	F	Sig.	Partial Eta Squared	Noncent. Parameter	Observed Power[a]	
Limb	Sphericity Assumed	12.758	1	12.758	3.995	.077	.307	3.995	.431
	Greenhouse-	12.758	1.000	12.758	3.995	.077	.307	3.995	.431

	Geisser								
	Huynh-Feldt	12.758	1.000	12.758	3.995	.077	.307	3.995	.431
	Lower-bound	12.758	1.000	12.758	3.995	.077	.307	3.995	.431
Error(Limb)	Sphericity Assumed	28.741	9	3.193					
	Greenhouse-Geisser	28.741	9.000	3.193					
	Huynh-Feldt	28.741	9.000	3.193					
	Lower-bound	28.741	9.000	3.193					
Time	Sphericity Assumed	4.851	1	4.851	1.219	.298	.119	1.219	.167
	Greenhouse-Geisser	4.851	1.000	4.851	1.219	.298	.119	1.219	.167
	Huynh-Feldt	4.851	1.000	4.851	1.219	.298	.119	1.219	.167
	Lower-bound	4.851	1.000	4.851	1.219	.298	.119	1.219	.167
Error(Time)	Sphericity Assumed	35.824	9	3.980					
	Greenhouse-Geisser	35.824	9.000	3.980					
	Huynh-Feldt	35.824	9.000	3.980					
	Lower-bound	35.824	9.000	3.980					
Limb * Time	Sphericity Assumed	41.270	1	41.270	6.551	.031	.421	6.551	.626
	Greenhouse-Geisser	41.270	1.000	41.270	6.551	.031	.421	6.551	.626
	Huynh-Feldt	41.270	1.000	41.270	6.551	.031	.421	6.551	.626
	Lower-bound	41.270	1.000	41.270	6.551	.031	.421	6.551	.626
Error(Limb*Time)	Sphericity Assumed	56.696	9	6.300					
	Greenhouse-Geisser	56.696	9.000	6.300					
	Huynh-Feldt	56.696	9.000	6.300					
	Lower-bound	56.696	9.000	6.300					
a. Computed using alpha =									

Tests of Within-Subjects Contrasts

Measure: MEASURE_1

Source	Limb	Time	Type III Sum of Squares	df	Mean Square	F	Sig.	Partial Eta Squared	Noncent. Parameter	Observed Power[a]
Limb	Linear		12.758	1	12.758	3.995	.077	.307	3.995	.431
Error(Limb)	Linear		28.741	9	3.193					
Time		Linear	4.851	1	4.851	1.219	.298	.119	1.219	.167
Error(Time)		Linear	35.824	9	3.980					
Limb * Time	Linear	Linear	41.270	1	41.270	6.551	.031	.421	6.551	.626
Error(Limb*Time)	Linear	Linear	56.696	9	6.300					

a. Computed using alpha =

Tests of Between-Subjects Effects

Measure: MEASURE_1
Transformed Variable: Average

Source	Type III Sum of Squares	df	Mean Square	F	Sig.	Partial Eta Squared	Noncent. Parameter	Observed Power[a]
Intercept	550.638	1	550.638	59.260	.000	.868	59.260	1.000
Error	83.627	9	9.292					

a. Computed using alpha =

Table B11. HGEX Oscillatory Shear Index

General Linear Model

Notes		
Output Created	11-JUL-2017 10:59:30	
Comments		
Input	Data	/Users/jemcheng/Documents/VDL | M.Sc/Projects/ASPEN/Statistics/ASPEN complete.sav
	Active Dataset	DataSet1
	Filter	<none>
	Weight	<none>
	Split File	<none>
	N of Rows in Working Data File	20
Missing Value Handling	Definition of Missing	User-defined missing values are treated as missing.
	Cases Used	Statistics are based on all cases with valid data for all variables in the model.
Syntax	GLM CON_HGEX_OSI_Pre CON_HGEX_OSI_Dur EXP_HGEX_OSI_Pre EXP_HGEX_OSI_Dur /WSFACTOR=Limb 2 Polynomial Time 2 Polynomial /METHOD=SSTYPE(3) /PLOT=PROFILE(Time*Limb) /PRINT=DESCRIPTIVE ETASQ OPOWER HOMOGENEITY /CRITERIA=ALPHA(.05) /WSDESIGN=Limb Time Limb*Time.	
Resources	Processor Time	00:00:00.22
	Elapsed Time	00:00:00.00

[DataSet1] /Users/jemcheng/Documents/VDL | M.Sc/Projects/ASPEN/Statistics/ASPEN complete.sav

Warnings

The HOMOGENEITY specification in the PRINT subcommand will be ignored because there are no between-subjects factors.

Within-Subjects Factors

Measure: MEASURE_1

Limb	Time	Dependent Variable
1	1	CON_HGEX_OSI_Pre
	2	CON_HGEX_OSI_Dur
2	1	EXP_HGEX_OSI_Pre
	2	EXP_HGEX_OSI_Dur

Descriptive Statistics

	Mean	Std. Deviation	N
CON_HGEX_OSI_Pre	.1913	.10620	10
CON_HGEX_OSI_Dur	.1396	.08321	10
EXP_HGEX_OSI_Pre	.1418	.08246	10
EXP_HGEX_OSI_Dur	.0890	.03833	10

Multivariate Tests[a]

Effect	Value	F	Hypothesis df	Error df	Sig.	Partial Eta Squared	Noncent. Parameter	Observed Power[c]	
Limb	Pillai's Trace	.472	8.036[b]	1.000	9.000	.020	.472	8.036	.714
	Wilks' Lambda	.528	8.036[b]	1.000	9.000	.020	.472	8.036	.714
	Hotelling's Trace	.893	8.036[b]	1.000	9.000	.020	.472	8.036	.714
	Roy's Largest Root	.893	8.036[b]	1.000	9.000	.020	.472	8.036	.714
Time	Pillai's Trace	.293	3.728[b]	1.000	9.000	.086	.293	3.728	.407
	Wilks' Lambda	.707	3.728[b]	1.000	9.000	.086	.293	3.728	.407
	Hotelling's Trace	.414	3.728[b]	1.000	9.000	.086	.293	3.728	.407
	Roy's Largest Root	.414	3.728[b]	1.000	9.000	.086	.293	3.728	.407
Limb * Time	Pillai's Trace	.000	.001[b]	1.000	9.000	.979	.000	.001	.050
	Wilks' Lambda	1.000	.001[b]	1.000	9.000	.979	.000	.001	.050
	Hotelling's Trace	.000	.001[b]	1.000	9.000	.979	.000	.001	.050
	Roy's Largest Root	.000	.001[b]	1.000	9.000	.979	.000	.001	.050

a. Design: Intercept
Within Subjects Design: Limb + Time + Limb * Time

b. Exact statistic

c. Computed using alpha =	

Mauchly's Test of Sphericity[a]

Measure: MEASURE_1

Within Subjects Effect	Mauchly's W	Approx. Chi-Square	df	Sig.	Epsilon[b]		
					Greenhouse-Geisser	Huynh-Feldt	Lower-bound
Limb	1.000	.000	0	.	1.000	1.000	1.000
Time	1.000	.000	0	.	1.000	1.000	1.000
Limb * Time	1.000	.000	0	.	1.000	1.000	1.000

Tests the null hypothesis that the error covariance matrix of the orthonormalized transformed dependent variables is proportional to an identity matrix.

a. Design: Intercept
Within Subjects Design: Limb + Time + Limb * Time

b. May be used to adjust the degrees of freedom for the averaged tests of significance. Corrected tests are displayed in the Tests of Within-Subjects Effects table.

Tests of Within-Subjects Effects

Measure: MEASURE_1

Source	Type III Sum of Squares	df	Mean Square	F	Sig.	Partial Eta Squared	Noncent. Parameter	Observed Power[a]	
Limb	Sphericity Assumed	.025	1	.025	8.036	.020	.472	8.036	.714
	Greenhouse-Geisser	.025	1.000	.025	8.036	.020	.472	8.036	.714

	Huynh-Feldt	.025	1.000	.025	8.036	.020	.472	8.036	.714
	Lower-bound	.025	1.000	.025	8.036	.020	.472	8.036	.714
Error(Limb)	Sphericity Assumed	.028	9	.003					
	Greenhouse-Geisser	.028	9.000	.003					
	Huynh-Feldt	.028	9.000	.003					
	Lower-bound	.028	9.000	.003					
Time	Sphericity Assumed	.027	1	.027	3.728	.086	.293	3.728	.407
	Greenhouse-Geisser	.027	1.000	.027	3.728	.086	.293	3.728	.407
	Huynh-Feldt	.027	1.000	.027	3.728	.086	.293	3.728	.407
	Lower-bound	.027	1.000	.027	3.728	.086	.293	3.728	.407
Error(Time)	Sphericity Assumed	.066	9	.007					
	Greenhouse-Geisser	.066	9.000	.007					
	Huynh-Feldt	.066	9.000	.007					
	Lower-bound	.066	9.000	.007					
Limb * Time	Sphericity Assumed	2.652E-006	1	2.652E-006	.001	.979	.000	.001	.050
	Greenhouse-Geisser	2.652E-006	1.000	2.652E-006	.001	.979	.000	.001	.050
	Huynh-Feldt	2.652E-006	1.000	2.652E-006	.001	.979	.000	.001	.050
	Lower-bound	2.652E-006	1.000	2.652E-006	.001	.979	.000	.001	.050
Error(Limb*Time)	Sphericity Assumed	.033	9	.004					
	Greenhouse-Geisser	.033	9.000	.004					
	Huynh-Feldt	.033	9.000	.004					
	Lower-bound	.033	9.000	.004					

a. Computed using alpha =	

Tests of Within-Subjects Contrasts

Measure: MEASURE_1

Source	Limb	Time	Type III Sum of Squares	df	Mean Square	F	Sig.	Partial Eta Squared	Noncent. Parameter	Observed Power[a]
Limb	Linear		.025	1	.025	8.036	.020	.472	8.036	.714
Error(Limb)	Linear		.028	9	.003					
Time		Linear	.027	1	.027	3.728	.086	.293	3.728	.407
Error(Time)		Linear	.066	9	.007					
Limb * Time	Linear	Linear	2.652E-006	1	2.652E-006	.001	.979	.000	.001	.050
Error(Limb*Time)	Linear	Linear	.033	9	.004					

a. Computed using alpha =

Tests of Between-Subjects Effects

Measure: MEASURE_1
Transformed Variable: Average

Source	Type III Sum of Squares	df	Mean Square	F	Sig.	Partial Eta Squared	Noncent. Parameter	Observed Power[a]
Intercept	.789	1	.789	63.621	.000	.876	63.621	1.000
Error	.112	9	.012					

a. Computed using alpha =

Table B12. HGEX FMD%

General Linear Model

Notes		
Output Created	17-JUL-2017 13:25:27	
Comments		
Input	Data	/Users/jemcheng/Documents/VDL | M.Sc/Projects/ASPEN/Statistics/ASPEN complete.sav
	Active Dataset	DataSet1
	Filter	<none>
	Weight	<none>
	Split File	<none>
	N of Rows in Working Data File	20
Missing Value Handling	Definition of Missing	User-defined missing values are treated as missing.
	Cases Used	Statistics are based on all cases with valid data for all variables in the model.
Syntax	GLM CON_HGEX_FMD_Pre CON_HGEX_FMD_Post EXP_HGEX_FMD_Pre EXP_HGEX_FMD_Post /WSFACTOR=Limb 2 Polynomial Time 2 Polynomial /METHOD=SSTYPE(3) /PLOT=PROFILE(Time*Limb) /PRINT=DESCRIPTIVE ETASQ OPOWER HOMOGENEITY /CRITERIA=ALPHA(.05) /WSDESIGN=Limb Time Limb*Time.	
Resources	Processor Time	00:00:00.19

	Elapsed Time	00:00:00.00

[DataSet1] /Users/jemcheng/Documents/VDL | M.Sc/Projects/ASPEN/Statistics/ASPEN complete.sav

Warnings
The HOMOGENEITY specification in the PRINT subcommand will be ignored because there are no between-subjects factors.

Within-Subjects Factors

Measure: MEASURE_1

Limb	Time	Dependent Variable
1	1	CON_HGEX_FMD_Pre
	2	CON_HGEX_FMD_Post
2	1	EXP_HGEX_FMD_Pre
	2	EXP_HGEX_FMD_Post

Descriptive Statistics

	Mean	Std. Deviation	N
CON_HGEX_FMD_Pre	4.1130	1.46577	10
CON_HGEX_FMD_Post	4.9600	1.88710	10
EXP_HGEX_FMD_Pre	5.9150	1.75515	10
EXP_HGEX_FMD_Post	7.8510	3.18141	10

Multivariate Tests[a]

Effect	Value	F	Hypothesis df	Error df	Sig.	Partial Eta Squared	Noncent. Parameter	Observed Power[c]	
Limb	Pillai's Trace	.729	24.227[b]	1.000	9.000	.001	.729	24.227	.992
	Wilks' Lambda	.271	24.227[b]	1.000	9.000	.001	.729	24.227	.992
	Hotelling's Trace	2.692	24.227[b]	1.000	9.000	.001	.729	24.227	.992
	Roy's Largest Root	2.692	24.227[b]	1.000	9.000	.001	.729	24.227	.992
Time	Pillai's Trace	.557	11.310[b]	1.000	9.000	.008	.557	11.310	.848
	Wilks' Lambda	.443	11.310[b]	1.000	9.000	.008	.557	11.310	.848
	Hotelling's Trace	1.257	11.310[b]	1.000	9.000	.008	.557	11.310	.848
	Roy's Largest Root	1.257	11.310[b]	1.000	9.000	.008	.557	11.310	.848
Limb * Time	Pillai's Trace	.203	2.287[b]	1.000	9.000	.165	.203	2.287	.273
	Wilks' Lambda	.797	2.287[b]	1.000	9.000	.165	.203	2.287	.273
	Hotelling's Trace	.254	2.287[b]	1.000	9.000	.165	.203	2.287	.273
	Roy's Largest Root	.254	2.287[b]	1.000	9.000	.165	.203	2.287	.273

a. Design: Intercept
Within Subjects Design: Limb + Time + Limb

* Time
b. Exact statistic
c. Computed using alpha =

Mauchly's Test of Sphericity[a]

Measure: MEASURE_1

Within Subjects Effect	Mauchly's W	Approx. Chi-Square	df	Sig.	Epsilon[b]		
					Greenhouse-Geisser	Huynh-Feldt	Lower-bound
Limb	1.000	.000	0	.	1.000	1.000	1.000
Time	1.000	.000	0	.	1.000	1.000	1.000
Limb * Time	1.000	.000	0	.	1.000	1.000	1.000

Tests the null hypothesis that the error covariance matrix of the orthonormalized transformed dependent variables is proportional to an identity matrix.

a. Design: Intercept
Within Subjects Design: Limb + Time + Limb * Time

b. May be used to adjust the degrees of freedom for the averaged tests of significance. Corrected tests are displayed in the Tests of Within-Subjects Effects table.

Tests of Within-Subjects Effects

Measure: MEASURE_1

Source	Type III Sum of Squares	df	Mean Square	F	Sig.	Partial Eta Squared	Noncent. Parameter	Observed Power[a]	
Limb	Sphericity Assumed	55.061	1	55.061	24.227	.001	.729	24.227	.992

	Greenhouse-Geisser	55.061	1.000	55.061	24.227	.001	.729	24.227	.992
	Huynh-Feldt	55.061	1.000	55.061	24.227	.001	.729	24.227	.992
	Lower-bound	55.061	1.000	55.061	24.227	.001	.729	24.227	.992
Error(Limb)	Sphericity Assumed	20.454	9	2.273					
	Greenhouse-Geisser	20.454	9.000	2.273					
	Huynh-Feldt	20.454	9.000	2.273					
	Lower-bound	20.454	9.000	2.273					
Time	Sphericity Assumed	19.363	1	19.363	11.310	.008	.557	11.310	.848
	Greenhouse-Geisser	19.363	1.000	19.363	11.310	.008	.557	11.310	.848
	Huynh-Feldt	19.363	1.000	19.363	11.310	.008	.557	11.310	.848
	Lower-bound	19.363	1.000	19.363	11.310	.008	.557	11.310	.848
Error(Time)	Sphericity Assumed	15.408	9	1.712					
	Greenhouse-Geisser	15.408	9.000	1.712					
	Huynh-Feldt	15.408	9.000	1.712					
	Lower-bound	15.408	9.000	1.712					
Limb * Time	Sphericity Assumed	2.965	1	2.965	2.287	.165	.203	2.287	.273
	Greenhouse-Geisser	2.965	1.000	2.965	2.287	.165	.203	2.287	.273
	Huynh-Feldt	2.965	1.000	2.965	2.287	.165	.203	2.287	.273
	Lower-bound	2.965	1.000	2.965	2.287	.165	.203	2.287	.273
Error(Limb*Time)	Sphericity Assumed	11.665	9	1.296					
	Greenhouse-Geisser	11.665	9.000	1.296					
	Huynh-Feldt	11.665	9.000	1.296					
	Lower-bound	11.665	9.000	1.296					

a. Computed using alpha =	

Tests of Within-Subjects Contrasts

Measure: MEASURE_1

Source	Limb	Time	Type III Sum of Squares	df	Mean Square	F	Sig.	Partial Eta Squared	Noncent. Parameter	Observed Power[a]
Limb	Linear		55.061	1	55.061	24.227	.001	.729	24.227	.992
Error(Limb)	Linear		20.454	9	2.273					
Time		Linear	19.363	1	19.363	11.310	.008	.557	11.310	.848
Error(Time)		Linear	15.408	9	1.712					
Limb * Time	Linear	Linear	2.965	1	2.965	2.287	.165	.203	2.287	.273
Error(Limb*Time)	Linear	Linear	11.665	9	1.296					

a. Computed using alpha =

Tests of Between-Subjects Effects

Measure: MEASURE_1
Transformed Variable: Average

Source	Type III Sum of Squares	df	Mean Square	F	Sig.	Partial Eta Squared	Noncent. Parameter	Observed Power[a]
Intercept	1304.050	1	1304.050	95.670	.000	.914	95.670	1.000
Error	122.677	9	13.631					

a. Computed using alpha =

Table B13. HEAT Linear Regression for Allometric Scaling

Regression

Notes		
Output Created	20-JUL-2017 08:52:37	
Comments		
Input	Data	/Users/jemcheng/Documents/VDL | M.Sc/Projects/ASPEN/Statistics/ASPEN HEAT FMD allometric scaling.sav
	Active Dataset	DataSet2
	Filter	<none>
	Weight	<none>
	Split File	Limb
	N of Rows in Working Data File	40
Missing Value Handling	Definition of Missing	User-defined missing values are treated as missing.
	Cases Used	Statistics are based on cases with no missing values for any variable used.
Syntax	REGRESSION /MISSING LISTWISE /STATISTICS COEFF OUTS CI(95) R ANOVA /CRITERIA=PIN(.05) POUT(.10) /NOORIGIN /DEPENDENT LnDpeak /METHOD=ENTER LnDbase.	
Resources	Processor Time	00:00:00.01
	Elapsed Time	00:00:00.00
	Memory Required	3040 bytes
	Additional Memory	0 bytes

	Required for Residual Plots	

[DataSet2] /Users/jemcheng/Documents/VDL | M.Sc/Projects/ASPEN/Statistics/ASPEN HEAT FMD allometric scaling.sav

Limb = CON

Variables Entered/Removed[a,b]

Model	Variables Entered	Variables Removed	Method
1	LnDbase[c]	.	Enter

a. Limb = CON

b. Dependent Variable: LnDpeak

c. All requested variables entered.

Model Summary[a]

Model	R	R Square	Adjusted R Square	Std. Error of the Estimate
1	.985[b]	.970	.968	.01539

a. Limb = CON

b. Predictors:

(Constant), LnDbase	

ANOVA[a,b]

Model		Sum of Squares	df	Mean Square	F	Sig.
1	Regression	.139	1	.139	584.839	.000[c]
	Residual	.004	18	.000		
	Total	.143	19			

a. Limb = CON

b. Dependent Variable: LnDpeak

c. Predictors: (Constant), LnDbase

Coefficients[a,b]

Model		Unstandardized Coefficients	Standardized Coefficients	t	Sig.	95.0% Confidence Interval for B		
		B	Std. Error	Beta		Lower Bound	Upper Bound	
1	(Constant)	.079	.062		1.268	.221	-.052	.209
	LnDbase	.972	.040	.985	24.183	.000	.888	1.057

a. Limb = CON

b. Dependent Variable: LnDpeak

Limb = EXP

Variables Entered/Removed[a,b]

Model	Variables Entered	Variables Removed	Method
1	LnDbase[c]	.	Enter

a. Limb = EXP

b. Dependent Variable: LnDpeak

c. All requested variables entered.

Model Summary[a]

Model	R	R Square	Adjusted R Square	Std. Error of the Estimate
1	.918[b]	.843	.834	.02778

a. Limb = EXP

b. Predictors: (Constant), LnDbase

ANOVA[a,b]

Model		Sum of Squares	df	Mean Square	F	Sig.
1	Regression	.075	1	.075	96.666	.000[c]
	Residual	.014	18	.001		
	Total	.088	19			

a. Limb = EXP

b. Dependent Variable: LnDpeak

c. Predictors: (Constant), LnDbase

Coefficients[a,b]

Model		Unstandardized Coefficients	Standardized Coefficients	t	Sig.	95.0% Confidence Interval for B		
		B	Std. Error	Beta		Lower Bound	Upper Bound	
1	(Constant)	.314	.128		2.451	.025	.045	.584
	LnDbase	.836	.085	.918	9.832	.000	.657	1.015

a. Limb = EXP

b. Dependent Variable: LnDpeak

Table B14. HEAT Generalized Estimating Equations for Allometric Scaling

Generalized Linear Models

Notes

Output Created	20-JUL-2017 16:51:58	
Comments		
Input	Data	/Users/jemcheng/Documents/VDL | M.Sc/Projects/ASPEN/Statistics/ASPEN HEAT FMD allometric scaling.sav
	Active Dataset	DataSet5
	Filter	<none>
	Weight	<none>
	Split File	<none>

	N of Rows in Working Data File	40
Missing Value Handling	Definition of Missing	User-defined missing values for factor, subject and within-subject variables are treated as missing.
	Cases Used	Statistics are based on cases with valid data for all variables in the model.
Weight Handling	not applicable	
Syntax	GENLIN ScalingLnDdiff BY S_Time S_Limb (ORDER=ASCENDING) WITH ScalingLnDbase /MODEL S_Time S_Limb S_Time*S_Limb INTERCEPT=YES DISTRIBUTION=NORMAL LINK=IDENTITY /CRITERIA SCALE=MLE PCONVERGE=1E-006(ABSOLUTE) SINGULAR=1E-012 ANALYSISTYPE=3(WALD) CILEVEL=95 LIKELIHOOD=FULL /EMMEANS TABLES=S_Time SCALE=ORIGINAL /EMMEANS TABLES=S_Limb SCALE=ORIGINAL /EMMEANS TABLES=S_Time*S_Limb SCALE=ORIGINAL /REPEATED SUBJECT=S_ParticipantID WITHINSUBJECT=S_Time*S_Limb SORT=YES CORRTYPE=EXCHANGEABLE ADJUSTCORR=YES COVB=ROBUST MAXITERATIONS=100	

	PCONVERGE=1e-006(ABSOLUTE) UPDATECORR=1 /MISSING CLASSMISSING=EXCLUDE /PRINT CPS DESCRIPTIVES MODELINFO FIT SUMMARY SOLUTION.	
Resources	Processor Time	00:00:00.10
	Elapsed Time	00:00:00.00

```
[DataSet5] /Users/jemcheng/Documents/VDL | M.Sc/Projects/ASPEN/Statistics/ASPEN HEAT FMD
allometric scaling.sav
```

Model Information		
Dependent Variable	ScalingLnDdiff	
Probability Distribution	Normal	
Link Function	Identity	
Subject Effect	1	S_ParticipantID
Within-Subject Effect	1	S_Time
	2	S_Limb
Working Correlation Matrix Structure	Exchangeable	

Case Processing Summary		
	N	Percent
Included	40	100.0%

Excluded	0	0.0%
Total	40	100.0%

Correlated Data Summary

Number of Levels	Subject Effect	S_ParticipantID	10
	Within-Subject Effect	S_Time	2
		S_Limb	2
Number of Subjects	10		
Number of Measurements per Subject	Minimum	4	
	Maximum	4	
Correlation Matrix Dimension	4		

Categorical Variable Information

		N	Percent
Factor	S_Time	Pre	20	50.0%
		Post	20	50.0%
		Total	40	100.0%
	S_Limb	CON	20	50.0%
		EXP	20	50.0%
		Total	40	100.0%

Continuous Variable Information

	N	Minimum	Maximum	Mean	Std. Deviation	
Dependent Variable	ScalingLnDdiff	40	.02	.15	.0516	.02833

Covariate	ScalingLnDbase	40	1.37	1.69	1.5247	.08259

Goodness of Fit[a]	
	Value
Quasi Likelihood under Independence Model Criterion (QIC)[b]	8.018
Corrected Quasi Likelihood under Independence Model Criterion (QICC)[b]	8.018
Dependent Variable: ScalingLnDdiff Model: (Intercept), S_Time, S_Limb, S_Time * S_Limb	
a. Information criteria are in small-is-better form.	
b. Computed using the full log quasi-likelihood function.	

Tests of Model Effects

Source	Type III Wald Chi-Square	df	Sig.
(Intercept)	118.305	1	.000
S_Time	13.782	1	.000
S_Limb	23.298	1	.000
S_Time * S_Limb	1.057	1	.304
Dependent Variable: ScalingLnDdiff Model: (Intercept),			

S_Time, S_Limb, S_Time * S_Limb	

Parameter Estimates

Parameter	B	Std. Error	95% Wald Confidence Interval		Hypothesis Test		
			Lower	Upper	Wald Chi-Square	df	Sig.
(Intercept)	.079	.0101	.059	.099	60.843	1	.000
[S_Time=1.00]	-.023	.0074	-.037	-.008	9.339	1	.002
[S_Time=2.00]	0[a]	.	.	.	.	.	.
[S_Limb=1.00]	-.036	.0103	-.056	-.016	12.355	1	.000
[S_Limb=2.00]	0[a]	.	.	.	.	.	.
[S_Time=1.00] * [S_Limb=1.00]	.008	.0082	-.008	.025	1.057	1	.304
[S_Time=1.00] * [S_Limb=2.00]	0[a]	.	.	.	.	.	.
[S_Time=2.00] * [S_Limb=1.00]	0[a]	.	.	.	.	.	.
[S_Time=2.00] * [S_Limb=2.00]	0[a]	.	.	.	.	.	.
(Scale)	.000						

Dependent Variable: ScalingLnDdiff
Model: (Intercept), S_Time, S_Limb, S_Time * S_Limb

a. Set to zero because this parameter is redundant.

Estimated Marginal Means 1: S_Time

Estimates

S_Time	Mean	Std. Error	95% Wald Confidence Interval	
			Lower	Upper
Pre	.0424	.00474	.0331	.0517
Post	.0609	.00592	.0493	.0725

Covariates appearing in the model are fixed at the following values: ScalingLnDbase=1.5247

Estimated Marginal Means 2: S_Limb

Estimates

S_Limb	Mean	Std. Error	95% Wald Confidence Interval	
			Lower	Upper
CON	.0357	.00313	.0296	.0418
EXP	.0676	.00756	.0528	.0824

Covariates appearing in the model are fixed at the following values: ScalingLnDbase=1.5247

Estimated Marginal Means 3: S_Time* S_Limb

Estimates

S_Time	S_Limb	Mean	Std. Error	95% Wald Confidence Interval	
				Lower	Upper
Pre	CON	.0286	.00364	.0214	.0357
	EXP	.0562	.00628	.0439	.0685
Post	CON	.0428	.00451	.0340	.0517
	EXP	.0789	.01012	.0591	.0988

Covariates appearing in the model are fixed at the following values: ScalingLnDbase=1.5247

Table B15. CUFF Linear Regression for Allometric Scaling

Regression

Notes

Output Created	20-JUL-2017 09:17:53	
Comments		
Input	Data	/Users/jemcheng/Documents/VDL | M.Sc/Projects/ASPEN/Statistics/ASPEN CUFF FMD allometric scaling.sav
	Active Dataset	DataSet3
	Filter	<none>
	Weight	<none>

	Split File	Limb
	N of Rows in Working Data File	40
Missing Value Handling	Definition of Missing	User-defined missing values are treated as missing.
	Cases Used	Statistics are based on cases with no missing values for any variable used.
Syntax	REGRESSION /MISSING LISTWISE /STATISTICS COEFF OUTS CI(95) R ANOVA /CRITERIA=PIN(.05) POUT(.10) /NOORIGIN /DEPENDENT LnDpeak /METHOD=ENTER LnDbase.	
Resources	Processor Time	00:00:00.01
	Elapsed Time	00:00:00.00
	Memory Required	3040 bytes
	Additional Memory Required for Residual Plots	0 bytes

[DataSet3] /Users/jemcheng/Documents/VDL | M.Sc/Projects/ASPEN/Statistics/ASPEN CUFF FMD allometric scaling.sav

Limb = CON

Variables Entered/Removed[a,b]

Model	Variables Entered	Variables Removed	Method
1	LnDbase[c]	.	Enter

a. Limb = CON

b. Dependent Variable: LnDpeak

c. All requested variables entered.

Model Summary[a]

Model	R	R Square	Adjusted R Square	Std. Error of the Estimate
1	.989[b]	.978	.977	.01410

a. Limb = CON

b. Predictors: (Constant), LnDbase

ANOVA[a,b]

Model		Sum of Squares	df	Mean Square	F	Sig.	
1	Regression	.162	1	.162	813.128	.000[c]	
	Residual	.004	18	.000			
	Total	.165	19				

a. Limb = CON

b. Dependent Variable: LnDpeak
c. Predictors: (Constant), LnDbase

Coefficients[a,b]

Model		Unstandardized Coefficients	Standardized Coefficients	t	Sig.	95.0% Confidence Interval for B		
		B	Std. Error	Beta		Lower Bound	Upper Bound	
1	(Constant)	.133	.050		2.630	.017	.027	.239
	LnDbase	.940	.033	.989	28.515	.000	.871	1.010

a. Limb = CON

b. Dependent Variable: LnDpeak

Limb = EXP

Variables Entered/Removed[a,b]

Model	Variables Entered	Variables Removed	Method
1	LnDbase[c]	.	Enter

a. Limb = EXP

b. Dependent Variable: LnDpeak

c. All requested variables entered.

Model Summary[a]

Model	R	R Square	Adjusted R Square	Std. Error of the Estimate
1	.992[b]	.983	.982	.01667

a. Limb = EXP

b. Predictors: (Constant), LnDbase

ANOVA[a,b]

Model		Sum of Squares	df	Mean Square	F	Sig.
1	Regression	.294	1	.294	1058.056	.000[c]
	Residual	.005	18	.000		
	Total	.299	19			

a. Limb = EXP

b. Dependent Variable: LnDpeak

c. Predictors: (Constant), LnDbase

Coefficients[a,b]

Model		Unstandardized Coefficients		Standardized Coefficients	t	Sig.	95.0% Confidence Interval for B	
		B	Std. Error	Beta			Lower Bound	Upper Bound
1	(Constant)	.277	.039		7.123	.000	.195	.358
	LnDbase	.860	.026	.992	32.528	.000	.804	.915

a. Limb = EXP	
b. Dependent Variable: LnDpeak	

Table B16. CUFF Generalized Estimating Equations for Allometric Scaling

Generalized Linear Models

Notes		
Output Created	20-JUL-2017 16:42:54	
Comments		
Input	Data	/Users/jemcheng/Documents/VDL | M.Sc/Projects/ASPEN/Statistics/ASPEN CUFF FMD allometric scaling.sav
	Active Dataset	DataSet3
	Filter	<none>
	Weight	<none>
	Split File	<none>
	N of Rows in Working Data File	40
Missing Value Handling	Definition of Missing	User-defined missing values for factor, subject and within-subject variables are treated as missing.
	Cases Used	Statistics are based on cases with valid data for all variables in the model.
Weight Handling	not applicable	
Syntax	GENLIN ScalingLnDdiff BY S_Time S_Limb (ORDER=ASCENDING) WITH ScalingLnDbase /MODEL S_Time S_Limb	

	S_Time*S_Limb INTERCEPT=YES DISTRIBUTION=NORMAL LINK=IDENTITY /CRITERIA SCALE=MLE PCONVERGE=1E-006(ABSOLUTE) SINGULAR=1E-012 ANALYSISTYPE=3(WALD) CILEVEL=95 LIKELIHOOD=FULL /EMMEANS SCALE=ORIGINAL /EMMEANS TABLES=S_Time SCALE=ORIGINAL /EMMEANS TABLES=S_Limb SCALE=ORIGINAL /EMMEANS TABLES=S_Time*S_Limb SCALE=ORIGINAL /REPEATED SUBJECT=S_ParticipantID WITHINSUBJECT=S_Time*S_Limb SORT=YES CORRTYPE=EXCHANGEABLE ADJUSTCORR=YES COVB=ROBUST MAXITERATIONS=100 PCONVERGE=1e-006(ABSOLUTE) UPDATECORR=1 /MISSING CLASSMISSING=EXCLUDE /PRINT CPS DESCRIPTIVES MODELINFO FIT SUMMARY SOLUTION.	
Resources	Processor Time	00:00:00.11
	Elapsed Time	00:00:00.00

[DataSet3] /Users/jemcheng/Documents/VDL | M.Sc/Projects/ASPEN/Statistics/ASPEN CUFF FMD allometric scaling.sav

Model Information		
Dependent Variable	ScalingLnDdiff	
Probability Distribution	Normal	
Link Function	Identity	
Subject Effect	1	S_ParticipantID
Within-Subject Effect	1	S_Time
	2	S_Limb
Working Correlation Matrix Structure	Exchangeable	

Case Processing Summary		
	N	Percent
Included	40	100.0%
Excluded	0	0.0%
Total	40	100.0%

Correlated Data Summary			
Number of Levels	Subject Effect	S_ParticipantID	10
	Within-Subject Effect	S_Time	2
		S_Limb	2
Number of Subjects	10		
Number of Measurements per	Minimum	4	

Subject	Maximum	4	
Correlation Matrix Dimension	4		

Categorical Variable Information

	N	Percent		
Factor	S_Time	Pre	20	50.0%
		Post	20	50.0%
		Total	40	100.0%
	S_Limb	CON	20	50.0%
		EXP	20	50.0%
		Total	40	100.0%

Continuous Variable Information

	N	Minimum	Maximum	Mean	Std. Deviation	
Dependent Variable	ScalingLnDdiff	40	.02	.12	.0568	.02580
Covariate	ScalingLnDbase	40	1.12	1.68	1.4955	.12638

Goodness of Fit[a]

	Value
Quasi Likelihood under Independence Model Criterion (QIC)[b]	8.017
Corrected Quasi Likelihood under Independence Model Criterion (QICC)[b]	8.017

Dependent Variable: ScalingLnDdiff Model: (Intercept), S_Time, S_Limb, S_Time * S_Limb
a. Information criteria are in small-is-better form.
b. Computed using the full log quasi-likelihood function.

Tests of Model Effects

Source	Type III Wald Chi-Square	df	Sig.
(Intercept)	113.105	1	.000
S_Time	1.332	1	.248
S_Limb	35.950	1	.000
S_Time * S_Limb	1.168	1	.280

Dependent Variable: ScalingLnDdiff
Model: (Intercept), S_Time, S_Limb, S_Time * S_Limb

Parameter Estimates

Parameter	B	Std. Error	95% Wald Confidence Interval		Hypothesis Test		
			Lower	Upper	Wald Chi-Square	df	Sig.

(Intercept)	.076	.0082	.060	.092	86.463	1	.000
[S_Time=1.00]	-.008	.0066	-.021	.004	1.638	1	.201
[S_Time=2.00]	0[a]	.	.	.	.	.	.
[S_Limb=1.00]	-.034	.0057	-.045	-.023	35.216	1	.000
[S_Limb=2.00]	0[a]	.	.	.	.	.	.
[S_Time=1.00] * [S_Limb=1.00]	.008	.0070	-.006	.021	1.168	1	.280
[S_Time=1.00] * [S_Limb=2.00]	0[a]	.	.	.	.	.	.
[S_Time=2.00] * [S_Limb=1.00]	0[a]	.	.	.	.	.	.
[S_Time=2.00] * [S_Limb=2.00]	0[a]	.	.	.	.	.	.
(Scale)	.000						

Dependent Variable: ScalingLnDdiff
Model: (Intercept), S_Time, S_Limb, S_Time * S_Limb

a. Set to zero because this parameter is redundant.

Estimated Marginal Means 1: Grand Mean

Estimates

Mean	Std. Error	95% Wald Confidence Interval	
		Lower	Upper
.0568	.00534	.0463	.0672

Covariates appearing in the model are fixed at the following values: ScalingLnDbase=1.4955

Estimated Marginal Means 2: S_Time

Estimates

S_Time	Mean	Std. Error	95% Wald Confidence Interval	
			Lower	Upper
Pre	.0545	.00573	.0432	.0657
Post	.0590	.00566	.0479	.0701

Covariates appearing in the model are fixed at the following values: ScalingLnDbase=1.4955

Estimated Marginal Means 3: S_Limb

Estimates

S_Limb	Mean	Std. Error	95% Wald Confidence Interval	
			Lower	Upper
CON	.0418	.00421	.0336	.0501
EXP	.0717	.00718	.0576	.0858

Covariates appearing in the model are fixed at the

following values: ScalingLnDbase=1.4955	

Estimated Marginal Means 4: S_Time* S_Limb

Estimates

S_Time	S_Limb	Mean	Std. Error	95% Wald Confidence Interval	
				Lower	Upper
Pre	CON	.0414	.00535	.0310	.0519
	EXP	.0675	.00762	.0525	.0824
Post	CON	.0422	.00369	.0350	.0494
	EXP	.0759	.00816	.0599	.0919
Covariates appearing in the model are fixed at the following values: ScalingLnDbase=1.4955					

Table B17. HGEX Linear Regression for Allometric Scaling

Regression

Notes	
Output Created	20-JUL-2017 12:39:02
Comments	

Input	Data	/Users/jemcheng/Documents/VDL | M.Sc/Projects/ASPEN/Statistics/ASPEN HGEX FMD allometric scaling.sav
	Active Dataset	DataSet4
	Filter	<none>
	Weight	<none>
	Split File	Limb
	N of Rows in Working Data File	40
Missing Value Handling	Definition of Missing	User-defined missing values are treated as missing.
	Cases Used	Statistics are based on cases with no missing values for any variable used.
Syntax	REGRESSION /MISSING LISTWISE /STATISTICS COEFF OUTS CI(95) R ANOVA /CRITERIA=PIN(.05) POUT(.10) /NOORIGIN /DEPENDENT Dpeak /METHOD=ENTER Dbase.	
Resources	Processor Time	00:00:00.01
	Elapsed Time	00:00:00.00
	Memory Required	3040 bytes
	Additional Memory Required for Residual Plots	0 bytes

[DataSet4] /Users/jemcheng/Documents/VDL | M.Sc/Projects/ASPEN/Statistics/ASPEN HGEX FMD allometric scaling.sav

Limb = CON

Variables Entered/Removed[a,b]

Model	Variables Entered	Variables Removed	Method
1	Dbase[c]	.	Enter

a. Limb = CON

b. Dependent Variable: Dpeak

c. All requested variables entered.

Model Summary[a]

Model	R	R Square	Adjusted R Square	Std. Error of the Estimate
1	.990[b]	.980	.979	.06752

a. Limb = CON

b. Predictors: (Constant), Dbase

ANOVA[a,b]

Model		Sum of Squares	df	Mean Square	F	Sig.
1	Regression	3.985	1	3.985	874.241	.000[c]
	Residual	.082	18	.005		
	Total	4.067	19			

a. Limb = CON

b. Dependent Variable: Dpeak

c. Predictors: (Constant), Dbase

Coefficients[a,b]

Model		Unstandardized Coefficients		Standardized Coefficients	t	Sig.	95.0% Confidence Interval for B	
		B	Std. Error	Beta			Lower Bound	Upper Bound
1	(Constant)	.416	.148		2.814	.011	.105	.727
	Dbase	.954	.032	.990	29.568	.000	.886	1.021

a. Limb = CON

b. Dependent Variable: Dpeak

Limb = EXP

Variables Entered/Removed[a,b]

Model	Variables Entered	Variables Removed	Method

1	Dbase[c]	.	Enter

a. Limb = EXP

b. Dependent Variable: Dpeak

c. All requested variables entered.

Model Summary[a]

Model	R	R Square	Adjusted R Square	Std. Error of the Estimate
1	.976[b]	.952	.949	.10342

a. Limb = EXP

b. Predictors: (Constant), Dbase

ANOVA[a,b]

Model		Sum of Squares	df	Mean Square	F	Sig.	
1	Regression	3.806	1	3.806	355.804	.000[c]	
	Residual	.193	18	.011			
	Total	3.998	19				

a. Limb = EXP

b. Dependent Variable: Dpeak

c. Predictors: (Constant), Dbase

Coefficients[a,b]

Model		Unstandardized Coefficients	Standardized Coefficients	t	Sig.	95.0% Confidence Interval for B		
		B	Std. Error	Beta		Lower Bound	Upper Bound	
1	(Constant)	.554	.221		2.506	.022	.090	1.018
	Dbase	.941	.050	.976	18.863	.000	.837	1.046
a. Limb = EXP								
b. Dependent Variable: Dpeak								

Table B18. HGEX Generalized Estimating Equations for Allometric Scaling

Generalized Linear Models

Notes		
Output Created	20-JUL-2017 16:49:05	
Comments		
Input	Data	/Users/jemcheng/Documents/VDL | M.Sc/Projects/ASPEN/Statistics/ASPEN HGEX FMD allometric scaling.sav
	Active Dataset	DataSet4
	Filter	<none>
	Weight	<none>
	Split File	<none>
	N of Rows in Working Data File	40
Missing Value Handling	Definition of Missing	User-defined missing values for factor, subject and within-subject variables are treated as missing.
	Cases Used	Statistics are based on cases with valid data for all variables in the model.

Weight Handling	not applicable	
Syntax	GENLIN ScalingLnDdiff BY S_Time S_Limb (ORDER=ASCENDING) WITH ScalingLnDbase /MODEL S_Time S_Limb S_Time*S_Limb INTERCEPT=YES DISTRIBUTION=NORMAL LINK=IDENTITY /CRITERIA SCALE=MLE PCONVERGE=1E-006(ABSOLUTE) SINGULAR=1E-012 ANALYSISTYPE=3(WALD) CILEVEL=95 LIKELIHOOD=FULL /EMMEANS SCALE=ORIGINAL /EMMEANS TABLES=S_Time SCALE=ORIGINAL /EMMEANS TABLES=S_Limb SCALE=ORIGINAL /EMMEANS TABLES=S_Time*S_Limb SCALE=ORIGINAL /REPEATED SUBJECT=S_ParticipantID WITHINSUBJECT=S_Time*S_Limb SORT=YES CORRTYPE=EXCHANGEABLE ADJUSTCORR=YES COVB=ROBUST MAXITERATIONS=100 PCONVERGE=1e-006(ABSOLUTE) UPDATECORR=1 /MISSING CLASSMISSING=EXCLUDE	

	/PRINT CPS DESCRIPTIVES MODELINFO FIT SUMMARY SOLUTION.	
Resources	Processor Time	00:00:00.10
	Elapsed Time	00:00:00.00

```
[DataSet4] /Users/jemcheng/Documents/VDL | M.Sc/Projects/ASPEN/Statistics/ASPEN HGEX FMD
allometric scaling.sav
```

Model Information		
Dependent Variable	ScalingLnDdiff	
Probability Distribution	Normal	
Link Function	Identity	
Subject Effect	1	S_ParticipantID
Within-Subject Effect	1	S_Time
	2	S_Limb
Working Correlation Matrix Structure	Exchangeable	

Case Processing Summary		
	N	Percent
Included	40	100.0%
Excluded	0	0.0%
Total	40	100.0%

Correlated Data Summary

Number of Levels	Subject Effect	S_ParticipantID	10
	Within-Subject Effect	S_Time	2
		S_Limb	2
Number of Subjects	10		
Number of Measurements per Subject	Minimum	4	
	Maximum	4	
Correlation Matrix Dimension	4		

Categorical Variable Information

		N	Percent
Factor	S_Time	Pre	20	50.0%
		Post	20	50.0%
		Total	40	100.0%
	S_Limb	CON	20	50.0%
		EXP	20	50.0%
		Total	40	100.0%

Continuous Variable Information

	N	Minimum	Maximum	Mean	Std. Deviation	
Dependent Variable	ScalingLnDdiff	40	.02	.14	.0553	.02363
Covariate	ScalingLnDbase	40	1.22	1.66	1.4944	.10886

Goodness of Fit[a]

	Value
Quasi Likelihood under Independence Model Criterion (QIC)[b]	8.015
Corrected Quasi Likelihood under Independence Model Criterion (QICC)[b]	8.015
Dependent Variable: ScalingLnDdiff Model: (Intercept), S_Time, S_Limb, S_Time * S_Limb	
a. Information criteria are in small-is-better form.	
b. Computed using the full log quasi-likelihood function.	

Tests of Model Effects

Source	Type III Wald Chi-Square	df	Sig.
(Intercept)	110.457	1	.000
S_Time	11.021	1	.001
S_Limb	27.639	1	.000
S_Time * S_Limb	2.192	1	.139
Dependent Variable: ScalingLnDdiff Model: (Intercept), S_Time, S_Limb, S_Time * S_Limb			

Parameter Estimates

Parameter	B	Std. Error	95% Wald Confidence Interval		Hypothesis Test		
			Lower	Upper	Wald Chi-Square	df	Sig.
(Intercept)	.075	.0087	.058	.092	73.661	1	.000
[S_Time=1.00]	-.018	.0049	-.027	-.008	13.203	1	.000
[S_Time=2.00]	0[a]	.	.	.	.	.	.
[S_Limb=1.00]	-.027	.0067	-.040	-.013	15.704	1	.000
[S_Limb=2.00]	0[a]	.	.	.	.	.	.
[S_Time=1.00] * [S_Limb=1.00]	.011	.0072	-.003	.025	2.192	1	.139
[S_Time=1.00] * [S_Limb=2.00]	0[a]	.	.	.	.	.	.
[S_Time=2.00] * [S_Limb=1.00]	0[a]	.	.	.	.	.	.
[S_Time=2.00] * [S_Limb=2.00]	0[a]	.	.	.	.	.	.
(Scale)	.000						

Dependent Variable: ScalingLnDdiff
Model: (Intercept), S_Time, S_Limb, S_Time * S_Limb

a. Set to zero because this parameter is redundant.

Estimated Marginal Means 1: Grand Mean

Estimates

Mean	Std. Error	95% Wald Confidence Interval

		Lower	Upper
.0553	.00526	.0450	.0656
Covariates appearing in the model are fixed at the following values: ScalingLnDbase=1.4944			

Estimated Marginal Means 2: S_Time

Estimates

S_Time	Mean	Std. Error	95% Wald Confidence Interval	
			Lower	Upper
Pre	.0492	.00464	.0401	.0583
Post	.0615	.00638	.0490	.0740
Covariates appearing in the model are fixed at the following values: ScalingLnDbase=1.4944				

Estimated Marginal Means 3: S_Limb

Estimates

S_Limb	Mean	Std.	95% Wald

		Error	Confidence Interval	
			Lower	Upper
CON	.0446	.00434	.0361	.0531
EXP	.0660	.00669	.0529	.0791
Covariates appearing in the model are fixed at the following values: ScalingLnDbase=1.4944				

Estimated Marginal Means 4: S_Time* S_Limb

Estimates

S_Time	S_Limb	Mean	Std. Error	95% Wald Confidence Interval	
				Lower	Upper
Pre	CON	.0412	.00496	.0314	.0509
	EXP	.0572	.00504	.0473	.0670
Post	CON	.0481	.00530	.0377	.0585
	EXP	.0748	.00872	.0577	.0919
Covariates appearing in the model are fixed at the following values: ScalingLnDbase=1.4944					